5-2023

Producing Analytical Models of the SPORT Spacecraft for Science Data Processing

Jason L. Powell
Utah State University

PRODUCING ANALYTICAL MODELS OF THE SPORT SPACECRAFT FOR SCIENCE DATA PROCESSING

by

Jason L. Powell

A thesis submitted in partial fulfillment
of the requirements for the degree

of

MASTER OF SCIENCE

in

Electrical Engineering

Approved:

Charles M. Swenson, Ph.D. Major Professor	Todd K. Moon, Ph.D. Committee Member
Reyhan Baktur, Ph.D. Committee Member	D. Richard Cutler, Ph.D. Vice Provost of Graduate Studies

UTAH STATE UNIVERSITY
Logan, Utah

2023

ABSTRACT

Producing Analytical Models of the SPORT Spacecraft for Science Data Processing

by

Jason L. Powell, Master of Science

Utah State University, 2023

Major Professor: Charles M. Swenson, Ph.D.
Department: Electrical and Computer Engineering

Terrestrial weather probes make weather predictions by collecting and analyzing data samples over time, similarly, samples from space weather probes can be used to make important predictions for how conditions in the ionosphere will change in time. These predictions are useful in understanding phenomena such as ionospheric plasma bubbles, which can disrupt radio communications from satellites and their respective ground stations.

Utah State University's Center for Space Engineering has produced a suite of instruments designed to sample and collect space weather data, collectively called Space Weather Probes. Space Weather Probes is flying on the Scintillation Prediction Observation Research Task (SPORT) CubeSat which launched in November 2022. Space Weather Probes instruments work by applying potentials to the space environment and observing response of the space environment. By observing how the space environment interacts with the Space Weather Probes sensors, one can understand the characteristics of the space environment.

This thesis describes the measurements of the Space Weather Probes instruments, how Space Weather Probes data is handled, and the models to demonstrate how Space Weather Probes is expected to respond to the space environment. This thesis discusses how measurements are to be handled to produce meaningful scientific data.

(125 pages)

PUBLIC ABSTRACT

Producing Analytical Models of the SPORT Spacecraft for Science Data Processing

Jason L. Powell

The Scintillation Prediction Observation Research Task (SPORT) is a joint United States of America and Brazil 6U CubeSat mission. The SPORT mission is to understand how the Earth's ionosphere evolves during day and night transitions. Space Weather Probes, a suite of instruments developed by Utah State University, monitors the ionosphere by observing currents and voltages around the SPORT spacecraft body. This thesis presents the data collected by Space Weather Probes and how it is used to measure the ionosphere. Modeling techniques are also presented to demonstrate how the Space Weather Probes instrument is expected to respond to the ionosphere.

To my wife and kids.

ACKNOWLEDGMENTS

I would like to thank a few of the many people who helped me to be where I am today. My major professor, Dr. Charles Swenson, who continually stretches my understanding of what is possible. The other members of my thesis committee, Dr. Todd Moon and Dr. Rehyan Baktur, who have been patient and supportive of me throughout this process. The rest of the ECE department staff, most of whom know me by name, and are always there to offer kind words of encouragement. Most importantly, I would like to thank my family whose support I rely most dependently on.

Jason L. Powell

CONTENTS

LIST OF TABLES

LIST OF FIGURES

ACRONYMS

AC	Alternating Current
ADC	Analog to Digital Converter
CSE	Center for Space Engineering
DC	Direct Current
EFP	Electric Field Probe
FPMU	Floating Potential Measurement Unit
FPP	Floating Potential Probe
GSFC	Goddard Space Flight Center
ILP	Ion Langmuir Probe
ISS	International Space Station
IVM	Ion Velocity Meter
m-NLP	Multi-Needle Langmuir Probe
PIC	Particle in Cell
PICASSO	PICo-satellite for Atmospheric and Space Science Observations
SIP	Sweeping Impedance Probe
SLP	Sweeping Langmuir Probe
SPORT	Scintillation Prediction Observation Research Task
SWP	Space Weather Probes
USU	Utah State University
UTD	The University of Texas at Dallas

CHAPTER 1

Introduction

1.1 The Ionosphere

The ionosphere occupies the approximate region between 80 km to 1000 km above the earth. The existence of the ionosphere was postulated as early as 1839, and was proven to exist when Macaroni received the first transcontinental radio signal, bouncing the transmission off of the ionosphere. It is formed when ultraviolet (EUV) and x-ray photons radiating from the sun separate electrons from molecules, such as oxygen. The result is an ionized gas, or plasma, containing both positively charged ions and free electrons. The density of ionospheric plasma is a function of the density of the neutral gasses, which decreases with altitude and the intensity of solar radiation [1]. The density of the ionosphere is greatest in the altitude range of 400 to 500 km. Free electrons in the ionosphere constitute a conductive body which can reflect radio waves of certain wavelengths.

The properties of the ionosphere vary based on the intensity of solar radiation exposed to the ionosphere. Such fluctuations can occur between day and night, the change of season, and the amount of solar activity on the sun. These parameters constitute a diverse, and changing ionosphere that is difficult to predict. Radio signals passing through such an in-homogeneous environment will reflect in ways that are difficult to predict and often impossible to recover. This effect, referred to as scintillation, can disrupt satellite communication in ways that are not yet well understood.

1.2 Scintillation Prediction Oberservation and Research Task

The Scintillation Prediction Oberservation and Research Task (SPORT) mission is a 6U CubeSat mission (approximately the size of two loaves of bread) representing the collaborative effort between the United States, and Brazil. The United States provided the

instrumentation and launch vehicle, while Brazil handled the spacecraft integration and assembly. SPORT is a science mission designed to understand the preconditions leading to equatorial plasma bubbles and scintillation in the ionosphere. SPORT aims to answer two questions:

1. What is the state of the ionosphere that gives rise to the growth of plasma bubbles that extend into and above the F-peak at different longitudes?

2. How are plasma irregularities at satellite altitudes related to the radio scintillations observed passing through these regions?

The SPORT spacecraft aims to answer these questions by observing the parameters defined by Table 1.1. The instruments associated with these observations, along with the respective range and accuracy requirements of the measurements, are also presented in the table. The spacecraft will be placed in an orbit 400km altitude and 52° inclination to study the low latitude, ±30°, region of the Earth's ionosphere. The expected altitude at the end of two years is 300km.

Table 1.1: Science Objectives of SPORT

Science Objectives to Measurement Requirements Traceability

The Scintillation Prediction Observation Research Task (SPORT)		Instrumentation	Spacecraft
Observational Approach	**Science Measurement Requirements**	**Instrument Approach**	**Space Systems Requirements**
1) What is the state of the ionosphere that gives rise to the growth of plasma irregularities that extend into and above the F-peak?			
Observations in the 1700 to 0100 LT sector over -30° to 30° latitude Height profiles of the plasma density to specify the magnitude and height of the F peak density in the EA Vertical ion drifts at or below the F peak in the EA	**Plasma Density Profile** 1) 140 to 450 km alt 2) 10^4 to 10^7 p/cm^3 range 3) 20% p/cm^3 accuracy 4) 1000 km along track sampling **Ion Drifts (Earth Reference Frame)** 1) ±800 m/s Range 2) 20 m/s precision & accuracy 3) 10 km along track sampling	**GPS Occultation** Observe GPS satellite occultation along and to the sides of the orbit plane to obtain line of site TEC **Ion Velocity Meter** Observe vertical ion drifts by angle of arrival of heavy ions at detector	**Satellite Orbit** 1) ≥1 year mission life 2) 40° to 55° inclination 3) 350 to 450 km altitude 4) ±10 km eccentricity **Spacecraft** 1) ±5° Ram Pointing 1σ 2) ≤1 km position knowledge 3) ≤10 ms timing
2) How are plasma irregularities at satellite altitudes related to the radio scintillations observed passing through these regions?			
Observations in the 2200 to 0200 LT sector over -30° to 30° latitude Observations of irregularities in electron density and E-field power spectral density in slope from 200 km to 200 m	**E-Field (Earth Reference Frame)** 1) ±45 mV/m range 2) 1.1 mV/m precision & accuracy 3) 1 km along track sampling 4) 10 km - 200 m along track waves **Plasma Density** 1) 10^3 to 10^7 p/cm^3 range 2) 10^3 p/cm^3 precision & accuracy 3) 1 km along track sampling 4) 10 km - 200 m along track waves **B-field** 1) ± 56,000 nT range 2) ±100 nT precision and accuracy 3) 1 km along track sampling	**E-Field Double Probe** Observe probe floating potential for AC E-fields from irregularity **GPS Occultation** S4 scintillation index **Langmuir/Impedance** Observe DC and AC probe response for relative and absolute electron density and observe irregularities **Three Axis Magnetometer** Support VxB computation for ion velocity and E-Field measurements	**Spacecraft Mechanisms** 1) ≥0.6 m tip-to-tip booms **Attitude** **(Post Flight Knowledge)** 1) ≤ 0.05° 1σ-uncertainty

The CAD model of the SPORT spacecraft with associated instruments is shown in figure 1.1. The SPORT instruments include an Ion Velocity Meter (IVM) provided by The University of Texas at Dallas (UTD), a Magnetometer, provided by Goddard Space Flight Center (GSFC), a GPS radio occultation receiver provided by The Aerospace Corporation. Specific to this thesis, SPORT also carries a suite of instruments called the Space Weather Probes (SWP) provided by Utah State University (USU). The Space Weather Probes suite of instruments consist of an Electric Field Probe, a Langmuir Probe, a wave spectrometer (electric field probe wave/ Langmuir probe wave), a Magnetometer, and an Impedance probe.

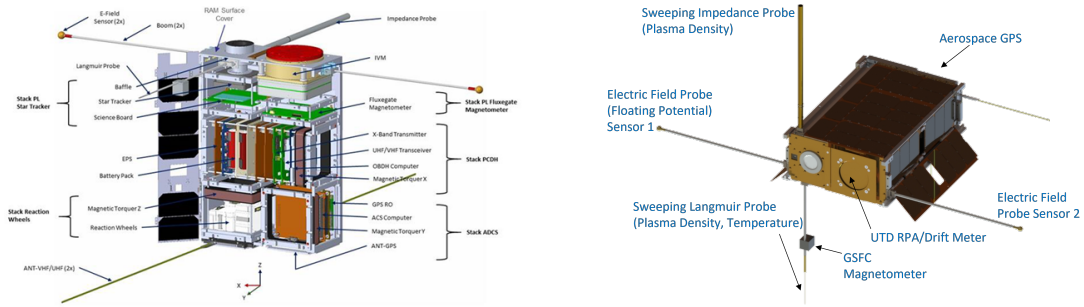

(a) Inside View

(b) Outside View

Fig. 1.1: The SPORT Spacecraft

1.3 Space Weather Probe Measurements

The Utah State University Space Weather Probes instrument suite performs in situ measurements of ionosphere density and temperature, and the electric field. The complete operation and design of this instrument is described in the thesis work done by Nathan Tipton [2], Caleb Young [3] and Jordan Haws [4].

The Langmuir probe and impedance probe both estimate the density of the ambient ionospheric plasma surrounding the SPORT spacecraft. The Langmuir probe has a fixed bias mode, and a sweeping bias mode. In the fixed bias mode, the Langmuir probe applies a fixed bias 3 Volt potential to the probe and monitors the current collected by the probe to observe changes in the plasma density.

Periodically, the Langmuir probe operates in a sweeping bias mode by applying a sweep of 1052 linearly spaced potentials ranging from -2 Volts to 3 Volts, and measures the current collected from the ionosphere at each potential step. The collection current versus voltage data is used to estimate the temperature of the ambient plasma.

The impedance probe measures the dielectric properties of the plasma from the capacitive relationship formed between the probe and spacecraft body at RF frequencies. The plasma density is calculated from the frequency at which resonate conditions occur in the dielectric properties of the ionospheric plasma [2].

The electric field probes consist of two floating potential probes that are mounted opposite from each other on $30cm$ booms. The difference between their potentials across their separation distance provides a 1-dimensional measurement of the electric field. The electric field probe also monitors the spacecraft's potential relative to the surrounding ionosphere during Langmuir probe sweeps.

Table 1.2 summarizes the SPORT data products derived from SWP, and the instrument(s) used to derive them.

Table 1.2: Parameter Returned by the SWP Instrument

Parameter	Primary Instrument	Secondary Instrument(s)
Electron Density	SLP	SIP
Electron Temperature	SLP	-
Electric Fields	EFP	SLP
Ion Number Density	-	SLP

1.4 Space Weather Probes Data Products

Space Weather Probes compiles instrument data into packets defined according to the SWP telemetry dictionary, which is included as part of this thesis in "Command and Telemetry Dictionary.xls". The structure of a generic packet is shown in table 1.3. These packets conform to the structure defined by The Consultative Committee for Space Data Systems (CCSDS) space packet protocol and are referred to as CCSDS packets.

CCSDS packets use a standard header containing the packet's Application Process Identifier (APID) which declares the type of data contained in the packet. A list of Space Weather Probes packet types and their associated telemetry APIDs is shown in table 1.4

Table 1.3: SWP Generic Packet

Address	**15**	**14**	**13**	**12**	**11**	**10**	**9**	**8**	**7**	**6**	**5**	**4**	**3**	**2**	**1**	**0**
0x0000	Packet Version Number			Pac. Type	Sec. Hdr. Flag	Application Process Identifier (See APID sheet)										
0x0002	Sequence Flags		Packet Sequence Count or Packet Name													
0x0004	Packet Data Length															
0x0006	System Clock Milliseconds (32 bits)															
0x0008																
0x000A	Granule 1															
0x000A + (1* granule size)	Granules 2 through N-1															
0x000A + (N - 1 * granule size)	Granule N															
0x000A + (N * granule size)	CheckSum															

Table 1.4: SWP Packet Types

APID	**Mnemonic**	**Description**
0x020	STATUS	Real time clock, GPS clock, voltage, current, and temperature monitors
0x021	SCIENCE	Magnetometer, DC EFP, DC SLP
0x022	SLP_SWEEP	EFP sweep, SLP sweep
0x023	SIP_SWEEP	SIP magnitude, phase, I, Q
0x024	SIP_TRACK	SIP track frequency
0x025	WAVE	Wave power bins, 16 channel real and imaginary for EFP and SLP
0x026	CONFIG	Configuration Echo

Status packets provide a list of auxiliary information related to the current state and health of the Space Weather Probes. **Config** packets report on the current configuration of the electronics board. The **Science**, **SLP_Sweep**, **SIP_Sweep**, **SIP_Track**, and **Wave**

packets contain measurements from the Space Weather Probe instruments. Each packet includes a single system clock, serving as a time stamp, along with science measurements stored in granules. Granule data is produced at a rate specified by the Space Weather Probe instruments. An example of the granule definition for the science packet is shown in table 1.5.

Table 1.5: Science Granule Detail

Word Number	**Bit Number**															
	15	**14**	**13**	**12**	**11**	**10**	**9**	**8**	**7**	**6**	**5**	**4**	**3**	**2**	**1**	**0**
1	Mag Temperature (16 bit)															
2	Mag X-axis (16 bit)															
3	Mag Y-axis (16 bit)															
4	Mag Z-axis (16 bit)															
5	EFP VS1 (MSB 16 bit)															
6	EFP VS2 (MSB 16 bit)															
7	SLP high gain (MSB 16 bit)															
8	SLP low gain (MSB 16 bit)															
9	SLP low gain (LSB 4 bit)				SLP high gain (LSB 4 bit)				EFP VS2 (LSB 4 bit)				EFP VS1 (LSB 4 bit)			

1.5 Langmuir Probe Theory

The work of this thesis primarily discusses methods for interpreting data collected by the SPORT Langmuir probe. As such, a brief history of Langmuir probes, and their theory is presented here.

Langmuir probes have been used since the 1920s to make localized density and temperature parameters of plasma [5]. A Langmuir probe consists of an exposed conductor (the probe) immersed in a plasma environment. The probe is then electrically biased with some voltage, ϕ_b, against the spacecraft to provide a potential difference between the probe and the plasma, called the sheath potential, ϕ_s, as shown in figure 1.2.

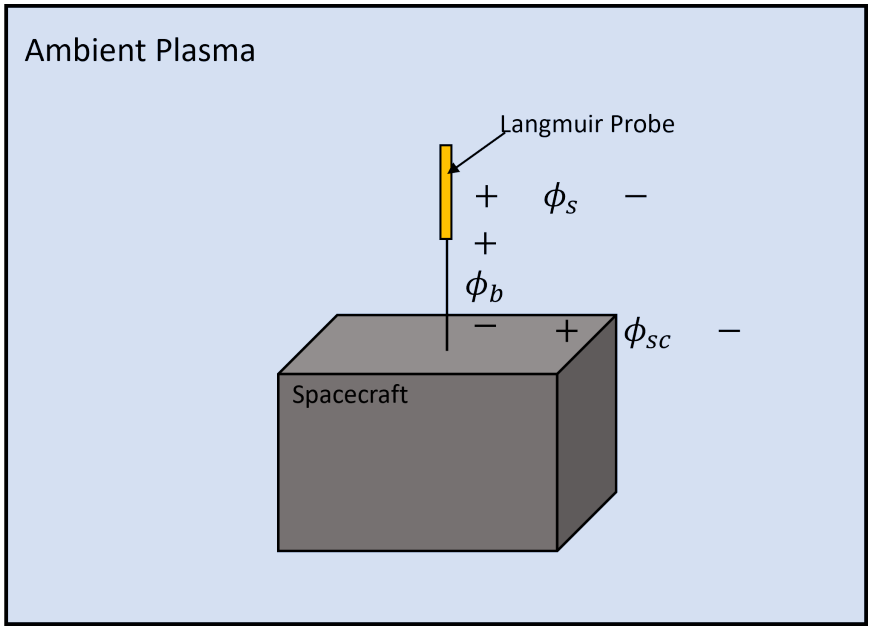

Fig. 1.2: Example Langmuir Probe in Space Environment

Observing the collected current (I) compared to the sheath potential (V) forms a current-voltage (IV) relationship. The temperature and density of the plasma is determined by observing the collected current with multiple sheath potentials, forming an IV curve. It is important to note that the potential applied to the probe by the spacecraft, ϕ_b, and the sheath potential, ϕ_s, have different reference points and are not the same. The relationship between the sheath potential and the bias potential must be determined before IV data can be analyzed.

An example IV data curve is shown in figure 1.3. The x-axis represents the bias potential with corresponding collection current in the y-axis. Typically, the curve is divided into three regions: the ion saturation, electron retardation, and electron saturation region.

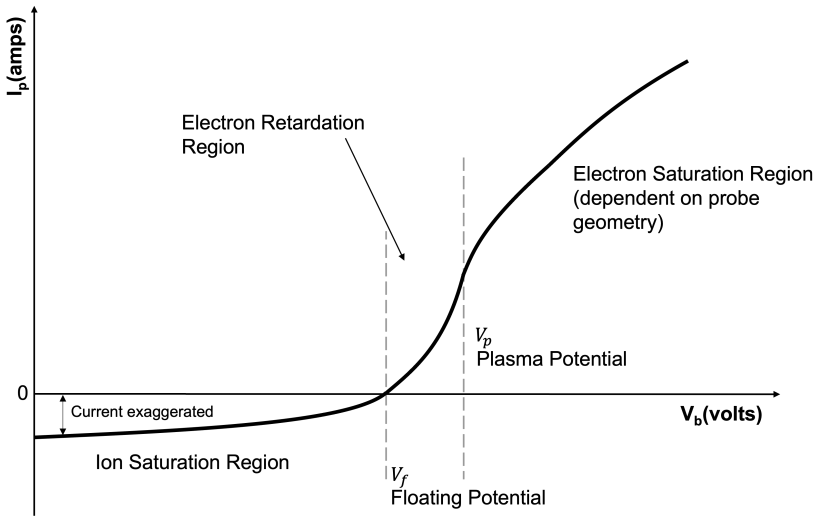

Fig. 1.3: Typical IV Curve for a Langmuir Probe

In the ion saturation region, the probe repels electrons, and attracts ions. In the electron retardation region, both electron and ions are collected. In the electron retardation region electron current collection increases exponentially as a function of temperature with increased bias potential. In the electron saturation region, only electrons are collected, the shape of the region is controlled by the plasma density.

The SPORT Space Weather Probes Langmuir probe operates in both a fixed bias and a swept bias mode as shown in figure 1.4a. The fixed bias mode applies a 3V potential to the probe surface, sampling the plasma in the electron saturation region, as marked by the star in figure 1.4b. The swept bias mode samples all three regions of the IV curve by sweeping the bias potential from -2V to 3V in time, as marked by the red highlighted region in figure 1.4b.

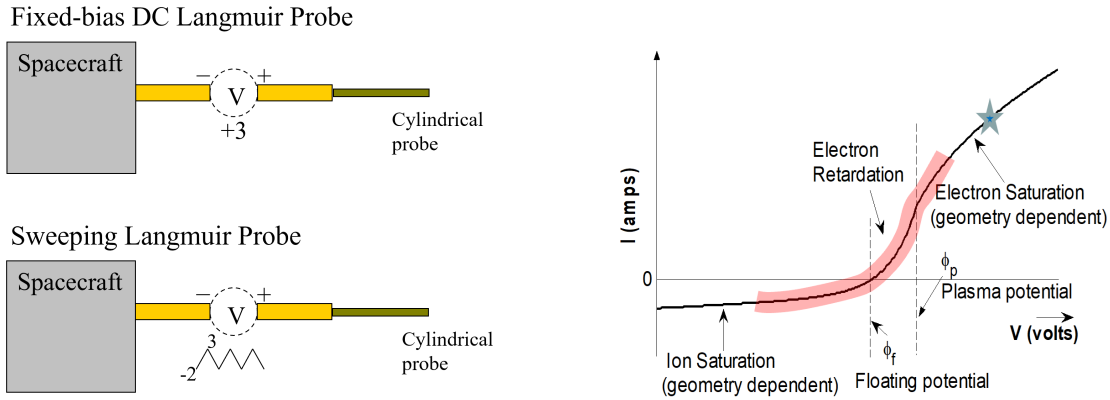

(a) Operation Modes for SPORT SWP Langmuir Probe

(b) Typical IV Curve for a Langmuir Probe

Fig. 1.4: SPORT SWP Langmuir Probe Operation

Although the implementation of a Langmuir probe is simple, the theory underlying the IV curve and how to interpret it is very complicated. Irving Langmuir and H Mott-Smith first developed analytical models for current collected by a conductive body in laboratory plasma, called orbital motion limited (OML) current models [6]. Later work done by Hoegy and Wharton [7], and Brace [8], build on Langmuir's model to more closely model a plasma in a space environment.

1.5.1 Orbital Motion Limited Models

The OML models developed by Langmuir are used to describe the expected current collected by a device. The model considers current collection by species, j, or type of particle that is collected (i.e. electrons or oxygen ions). The total collected current is equal to the sum current from each species j.

A compact form of Langmuir's models are shown in equations 1.1 - 1.3.

$$I = \sum_j = J_{sat_j} A_p F(\Phi_{s_j}) \tag{1.1}$$

$$J_{sat_j} \equiv q n_j \sqrt{\frac{k_b T_j}{2\pi m_j}}, \Phi_{s_j} \equiv \frac{-q_j \phi_{s_j}}{k_b T_j}, \varepsilon \equiv \frac{s}{r_p}, \tilde{\Phi}_{s_j} \equiv \sqrt{\frac{\Phi_{s_j}}{\varepsilon^2 - 1}} \tag{1.2}$$

When the probe potential, ϕ_{probe} is equal to the potential of the ambient plasma, ϕ_p, the current of species j collected by a probe is equal to the number of particles of species j, whose random kinetic motion brings them to the surface of the probe. The saturation current, J_{sat_j}, with units of A/m^2 is used to describe this current as a density per unit area, and is multiplied by the collecting area of the probe, A_p.

When the probe potential is less than the plasma potential, $\phi_{probe} < \phi_p$, an electric force attracts additional positively charged species and repels negatively charged species. When $\phi_{probe} < \phi_p$ the electric force will repel positively charges species and repel negatively charges species. The unit-less collection factor, $F(\Phi_{s_j})$, modulates the equipotential current collection, $J_{sat_j A_p}$, based on the attractive or repulsive electric force cause by the potential difference. The collection factor, $J_{sat_j A_p}$, is dependent on the geometry of the probe. Shown in equation 1.3 is the collection factor for cylindrical probes.

$$F(\Phi_{s_j}) = \begin{cases} exp(\Phi_{s_j}) & \text{for } \Phi_{s_j} \leq 0 \\ \varepsilon \text{erf}(\Phi_{s_j}) + exp(\Phi_{s_j}) \text{erfc}(\varepsilon \tilde{\Phi}_{s_j}) & \text{for } \Phi_{s_j} > 0 \end{cases} \tag{1.3}$$

1.5.2 OML Approximation

OML equations are commonly simplified by the approximation of the collection factor, $F(\Phi_{s_j})$, to equation 1.4

$$F(\Phi_{s_j}) = \begin{cases} exp(\Phi_{s_j}) & \text{for } \Phi_{s_j} < 0 \\ (1+\Phi_{s_j})^{\beta} & \text{for } \Phi_{s_j} > 0 \end{cases} \tag{1.4}$$

The geometrical factor, β, ranges from $0 < \beta \leq 1$, for cylindrical probes, $\beta \approx \frac{1}{2}$.

OML Moving Probe

In a paper by Hoegy and Wharton, Hoegy and Wharton [7] built upon Langmuir's model to define collection factors of moving probes. The expression for a moving cylindrical probe is shown in equation 1.5.

$$F(\Phi_{s_j}) = \begin{cases} exp(\Phi_{s_j})[1 + (\frac{1}{2} - \Phi_{s_j})M_j^2 + (\frac{\Phi_{s_j}^2}{4} + \frac{\Phi_{s_j}}{4} - \frac{1}{16})M_j^4 + ...] & \text{for } \Phi_{s_j} \leq 0 \\ \text{and} M_j << 1 & \\ \frac{2}{\sqrt{\pi}}\sqrt{\Phi_{s_j}} + exp(\Phi_{s_j})erfc(\sqrt{\Phi_{s_j}}) & \\ +\frac{M_j^2}{2}[\frac{2}{\sqrt{\pi}}\sqrt{\Phi_{s_j}} + (1-2\Phi_{s_j})exp(\Phi_{s_j})erfc(\sqrt{\Phi_{s_j}})] & \\ -\frac{M_j^4}{8}[\frac{2}{\sqrt{\pi}}(\Phi_{s_j}+\frac{1}{2})\sqrt{\Phi_{s_j}} + (\frac{1}{2} - 2\Phi_{s_j} - 2\Phi_{s_j}^2)exp(\Phi_{s_j})erfc(\sqrt{\Phi_{s_j}})] + ... & \text{for } \Phi_{s_j} > 0 \\ \text{and } M_j < 4 & \end{cases} \tag{1.5}$$

1.5.3 Complications To Langmuir Probe Theory

Interpreting plasma properties from Langmuir probe measurements is limited to how accurately Langmuir probe theory models plasma interactions to the Langmuir probe. Langmuir probe theory provides an excellent model for how OML currents are collected by the probe. However, the space environment includes more complicated interactions that must also be considered.

Additional Probe Currents

Basic OML Langmuir probe theory defines how free electron, I_E and Ion, I_I currents of a plasma will be collected by a conductive body. Langmuir probe theory does not, however, consider currents due to other phenomenon. Figure 1.5 demonstrates other possible current sources that can be measured by a Langmuir Probe. These currents include electron loss from the photoelectric effect, back scatter and secondary electron emission from energetic particle collisions, and ion ram current in mesothermal cases.

Additionally, Langmuir probe theory does not account for particle gyrations due to the magnetic field, or the presence of particle collisions with the neutral atmosphere.

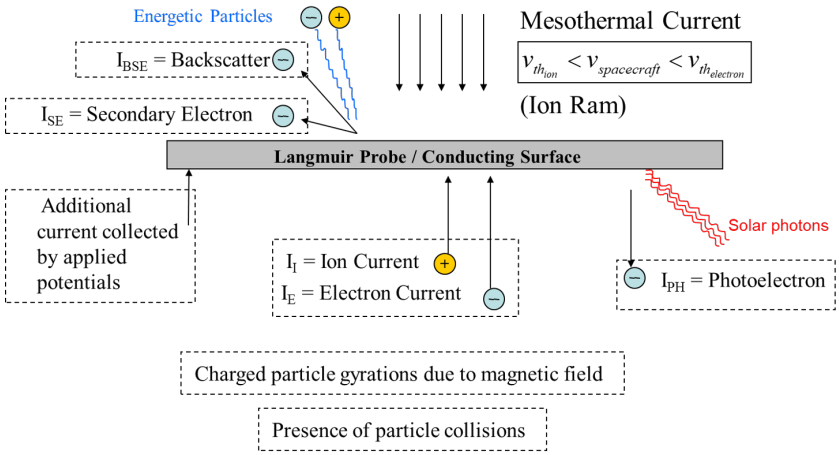

Fig. 1.5: Complications to Basic Langmuir Probe Theory

Additional current effects of these phenomenon are small compared to the collected OML currents in the 400km altitude range. Space Weather Probes is interested in understanding how these effects will impact Langmuir probe measurements, specifically currents due to ion ram collection and the photoelectric effect.

Spacecraft Wake

When a high-speed spacecraft moves through a plasma two main regions form: a compression region in the ram, and a rarefaction "wake" region behind the body. The

structure of the wake depends on a variety of factors including the spacecraft's velocity, the potential of the spacecraft, and the ambient magnetic field.

The SPORT mission has a velocity of approximately $7.4 km/s$. This velocity is about seven times greater than the local thermal speed of $O+$ ions, but less than the electron thermal speed. As a result, a wake of low density ions will form behind the spacecraft. This wake reduces the effective collection area a Langmuir probe can collect current over.

Spacecraft Charghing

It is important to define the potentials on the SPORT spacecraft and how they are related to Space Weather Probes. Table 1.6 defines relevant potentials on the SPORT spacecraft. Corresponding potentials are shown in figure 1.6.

Table 1.6: SPORT SWP Potential Definitions

Potential	**Symbol**	**Positive Reference**	**Negative Reference**
Spacecraft Potential	ϕ_{sc}	Spacecraft Body	Ambient Plasma
Bias Potential	ϕ_b	Langmuir Probe	Spacecraft Body
Sheath Potential	ϕ_s	Langmuir Probe	Ambient Plasma
Electric Field Probe Potential	ϕ_{efp}	Floating Potential Probe (1)	Spacecraft Body
Electric Field Floating Potential	ϕ_f	Floating Potential Probe (1)	Ambient Plasma

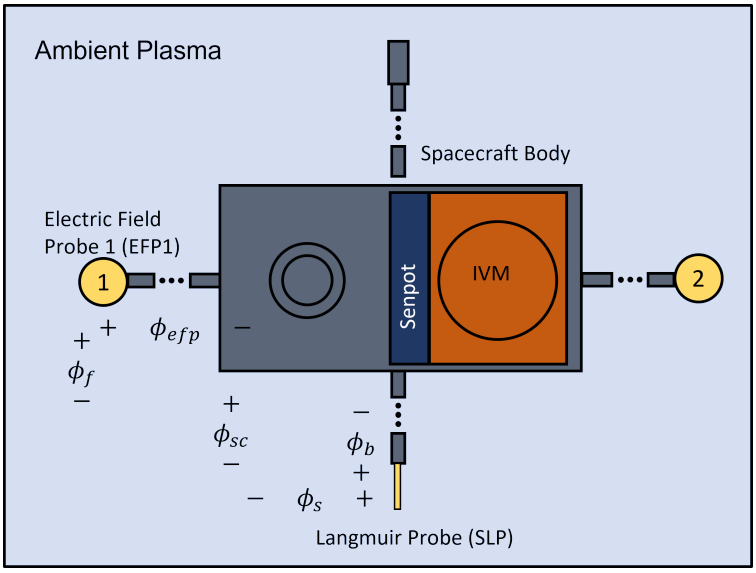

Fig. 1.6: Sport Potentials

As shown in figure 1.6, the sheath potential, ϕ_s, is not equivalent to the bias potential on the probe, ϕ_b. These potentials are related to each other with the spacecraft potential, ϕ_{sc}. ϕ_{sc} is the potential of the spacecraft with reference to the ambient plasma, or spacecraft charge.

The collection current, I_j, is inversely proportional to the mass, m_j of the species. Because electrons are much lighter compared to ions, in a quasi-neutral environment the electron collection current is typically much greater than the ion saturation current. Left floating, a spacecraft body will charge negative until the electron current, I_e, is balanced with the ion current I_i, typically around $-1V$.

Collected currents from the driven potential of a Langmuir probe must be balanced by return currents from the spacecraft chassis ground. Because a conductor is able to collect many more electrons than ions when applying potentials of equal magnitude (either positive or negative) the current collection area of the spacecraft must be much larger than the biased probe in order to collect a comparable amount of ions when the probe is operating in the electron saturation region.

Due to the limited surface area of CubeSats a positive potential on a Langmuir probe

often results in more current from electrons than can be returned through the surface of spacecraft by ion collection. As a result, the whole spacecraft charges negative relative to the space environment to force a balance between the current collected on the probe and the current returned by the spacecraft surface.

Understanding how the probe/spacecraft surface area ratios affect Langmuir probe operation on CubeSats has been the subject of multiple studies [9] [10]. The charge of the SPORT spacecraft, relative to the ambient ionosphere, must be well understood to properly make temperature and density estimates for the Space Weather Probes Langmuir probe. Space Weather Probes uses the floating potential probes of the electric field probe to measure the spacecraft potential relative to the ambient plasma, as shown in figure 1.6.

1.6 Langmuir Probe Modeling Techniques

Many techniques for modeling the effects of Langmuir probes on small spacecraft exist. The SPORT satellite is modeled using two software packages: LTspice, and NASCAP-2k. A brief description of these software packages is discussed here.

1.6.1 LTspice

SPICE ("Simulation Program with Integrated Circuit Emphasis") is a general-purpose analog electronic circuit simulator. It is a program used in integrated circuit and board-level design to predict circuit behavior and verify circuit designs [11]. USU previously used SPICE models for sounding rocket probes in ionospheric plasma [12] and has revisited this approach for the SPORT CubeSat mission.

The SPICE models consist of SPICE macro circuits implemented using voltage controlled current sources. The models are encapsulated in LTspice's schematic capture front end as graphical elements, like a standard electronic part. Figure 1.7 shows circuit models of devices encapsulated in LTspice. The models shown in 1.7 describe both spheres and cylinders as they interact with various conditions within the ionosphere. The device is used by applying a voltage potential between the ionosphere (top node) and the collecting surface

(bottom node) and measuring the current through the device. The symbol used is similar to that of a diode.

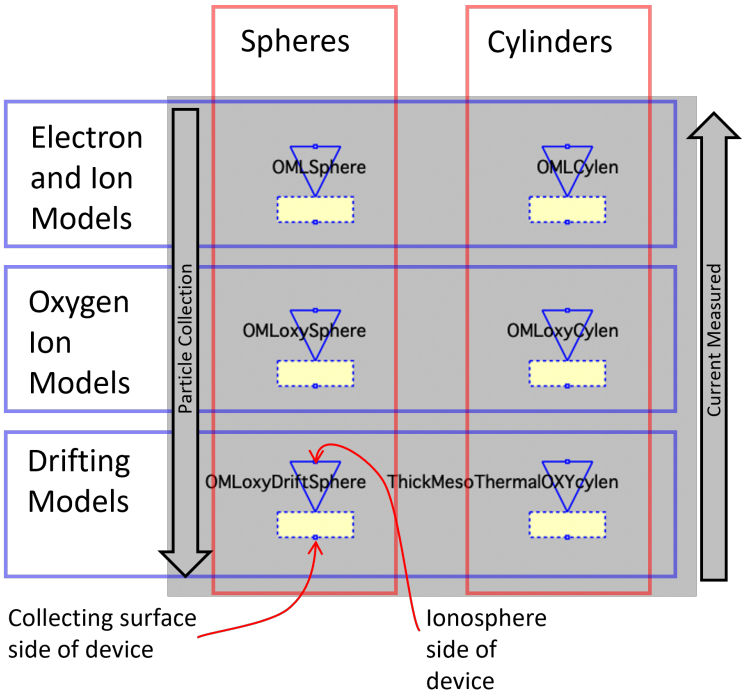

Fig. 1.7: LTspice Models

LTspice is capable of modeling the effects of spacecraft charging and the spacecraft wake, but does not include effects due to additional currents. LTspice models allow users to easily and quickly model spacecraft interactions.

1.6.2 NASCAP-2k

Nascap-2k is an interactive toolkit for studying plasma interaction with realistic spacecraft models in three dimensions. Nascap-2k enables plasma-interactions specialists to perform realistic analyses with direct application to engineering problems. The software allows users to define spacecraft surfaces, geometries, and the structure of the computational space surrounding a spacecraft. Users can then solve for time-dependent potentials on spacecraft surfaces, solve for the electrostatic potential around the object, generate, track and other-

wise process particles of various species. Nascap-2k's built in plotting tools allow users to view surface potentials, space potentials, particle trajectories and time-dependent potentials and currents [13]. Figure 1.8 outlines the structure for using Nascap-2k.

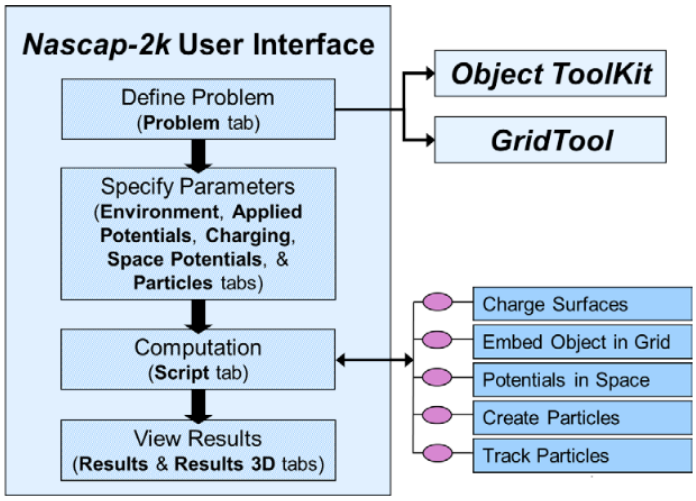

Fig. 1.8: Nascap-2k Structure

Nascap-2k, like LTspice, is capable of modeling the effects of spacecraft charging, and the spacecraft wake. Nascap-2k is also capable of including the effects of additional current sources.

1.7 Other Space Weather Probe Instruments

In addition to making measurements with a Langmuir probe, Space Weather Probes also makes measurements with an electric field probe, and an impedance probe. The theories governing these probes are discussed here.

1.7.1 Electric Field Probe Theory

The electric field probe, or electric field double probe, is constructed from two identical floating potential probes immersed in a plasma. The floating potential probes measure the potential difference between the probe surface and the spacecraft body. The floating

potential probes are separated by a distance, d. This distance can be represented as a vector pointing from sensor 1 to sensor 2 using the notation $\vec{d}_{1,2}$. The potential difference between these probes, $\phi_{1,2}$ is given by

$$\phi_{1,2} = \vec{E} \cdot \vec{d}_{1,2} \tag{1.6}$$

Where $\vec{E}$ is the ambient electric field to be observed. The measured voltage divided by the separation distance, d, gives the component of the electric field projected in the direction of the vector $\vec{d}_{1,2}$.

1.7.2 Impedance Probe Theory

An impedance probe forms a capacitive relationship between the probe surface and some other point (typically the spacecraft body). The plasma that lies between the probe surface and the spacecraft body constitutes the dielectric material of the capacitor. The capacitance between the probe and spacecraft body is measured by inserting a sweep of high frequency signals into the probe and measuring the return current.

1.8 Thesis Outline

Chapter 2 discusses the techniques for relating Space Weather Probe measurements, in digital counts, to real world quantities such as voltages and currents. Chapter 3 discusses SPORT modeling results from LTspice and Nascap-2k. Chapter 4 discusses the methods for processing Space Weather Probe data collected by SPORT, and producing ionospheric measurements. Chapter 5 discusses future work and lessons learned.

CHAPTER 2

Space Weather Probe Measurement Models

Space Weather Probes is a collection of measurement techniques for sensing the fundamental parameters of the ionosphere. These parameters consist of plasma density, temperature, and electric fields, along with a supporting measurement of the ambient magnetic field. The techniques ultimately rely on measurements of both DC and AC voltages and currents in response to both natural environmental stimulus and applied voltage stimulus. Table 2.1 summarizes the measurements made by each SWP instrument.

Table 2.1: SWP Instrument SI Units

Instrument	**Packet**	**Measurement**	**Unit**
Electric Field Probes	Science, SLP	Spacecraft Potential	Volts
Magnetometer	Science	Magnetic Field Strength	Tesla
Langmuir Probe	Science, SLP	Probe Return Current	Amperes
Electric Field Wave	Wave	Power Spectral Density	Volts per root Hertz
Langmuir Wave	Wave	Power Spectral Density	Amperes per root Hertz
Impedance Probe	SIP	Impedance	Ohms
Impedance Probe Track	SIP Track	Track Frequency	Hertz

In addition to science observations, Space Weather Probes monitors the health and status of the electronics board. Space Weather Probes tracks the voltage supply level and current draw of power regulators, and board temperature. These measurements are included in the status packet and are collectively referred to as housekeeping measurements.

The fundamental requirements in terms of range and sensitivity for currents and voltage are determined for each instrument based on the expected ranges of the ionospheric parameters to guarantee sufficient performance over all ionospheric conditions.

The Space Weather Probe instruments minimally process the measurements in analog circuitry and then quantize signal data using analog to digital converters (ADCs). The measurements are over-sampled in time and final processing of the data is achieved using an FPGA where the digital signal processing occurs without adding external noise. The FPGA also functions to control the instrument and packages the resulting data for transmission.

The measured and quantized data exists in digital words or counts that are related to the physical units of voltage, current, impedance, or frequency with a mathematical relationship. This section presents a brief overview of the functional requirements for each of the SWP measurements and describes the mathematical models used to relate instrument counts to physical units.

2.1 Mathematical Models of Space Weather Probes

This section details Space Weather Probe instrument measurements, their requirements, and the mathematical models used to convert measurements to physical units.

2.1.1 Housekeeping

The housekeeping section of Space Weather Probes monitors the health and status of the electronics by monitoring the power supply voltage levels, current draws, and temperatures at various locations. The housekeeping data primarily originates from four ADC chips, which also provide temperature measurements. Housekeeping measurements fall into three categories: voltage, current, and temperature. Table 2.2 summarizes the housekeeping measurements that are made.

Table 2.2: Housekeeping Monitors

Measurement	**Sensors**	**Unit**
Voltage	+5 +1V8A +1V8D +4V5A -1V8A +3V3D -4V5	Volts
Current	+5V +1V8A +1V8D +4V5A -4V5A -1V8A +3V3D	Amperes
Temperature	U60 U55 U48 U49	Degrees Cesius

Voltage Monitors

The Space Weather Probes electronics makes use of a variety of different voltage supplies that are generated from a single voltage input to the electronics. The housekeeping section monitors each of the voltage supply levels which are produced by several different power and voltage regulator chips. The voltage supply levels are quantized on Space Weather Probes using a 16-bit ADC to quantize voltage measurements. The ADS 1118 ADC chips require the monitored voltage to be in the range specified by equation 2.1.

$$0 < V_{in} < 4.5 \tag{2.1}$$

Supply voltages outside of the specified range are moved into the range by gaining the monitored voltage level using inverting op-amp drivers and voltage dividers. The gain term, G_s, is specific to the monitored voltage supply, s.

The supply voltage of each supply measured in ADC counts, C_s, is converted to voltage, V, using a linear mathematical model. The linear model consists of two parameters: the gain and offset. The gain parameter, G, specifies the number of counts to one Volt (or line slope), and offset parameter, O, specifies the number of counts equal to zero Volts (or line offset), as shown in equation 2.2.

$$V = C_s * G + O \tag{2.2}$$

Figure 2.1 shows a generic version of the linear model used here. In this case, counts are related to the physical unit of Volts.

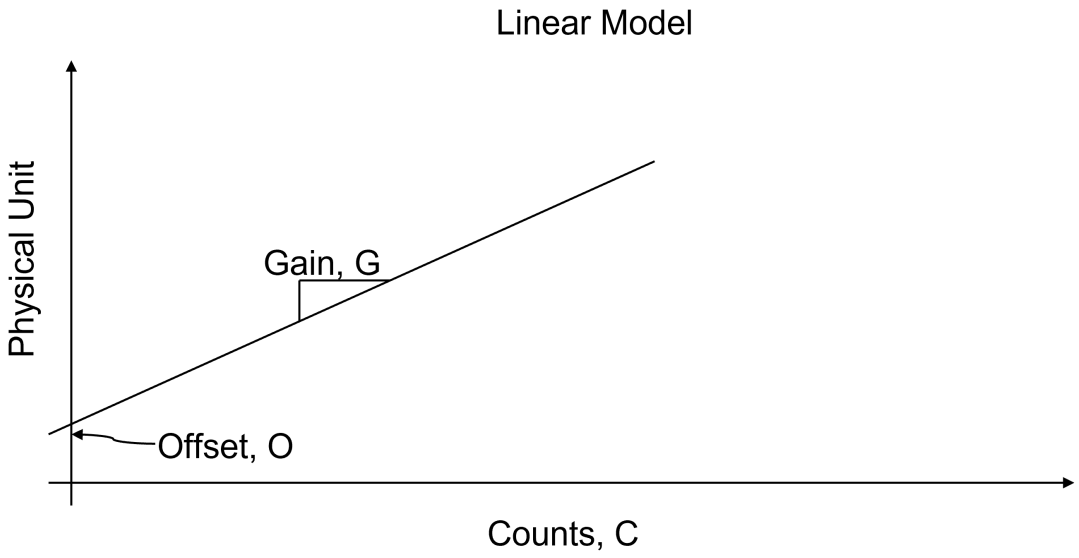

Fig. 2.1: Generic Linear Model

The supply voltage, V_s, is calculated by dividing the voltage gain, G_s, specific to the voltage supply.

$$V_s = \frac{V}{G_s} \tag{2.3}$$

Current Monitors

SWP uses the LT6105 current monitoring chip and a small 0.01 Ohm resister to convert the current supplied by each voltage regulator to a voltage level. The voltage to current conversion, in V/A, is specified by the transimpedance gain, G_{TIA}, of the current monitor chips. The voltage level is quantized with the same ADC used for monitoring voltage levels.

$$V_S = I_S * G_{TIA} \tag{2.4}$$

The current draw of each supply measured in ADC counts, C_s, is converted to voltage, V_s using a linear model. The gain parameter, G, specifies the number of counts to one

Volt. The offset parameter, O, specifies the number of counts equal to zero Volts. The transimpedance gain is divided from the measurement to calculate the actual current draw as shown in equations 2.5 and 2.6.

$$V_S = C_S * G_S + O_S \tag{2.5}$$

$$I_S = \frac{V_S}{G_{TIA}} \tag{2.6}$$

Temperature Monitors

Temperature sensors are built into the four voltage and current monitoring ADS 1118 ADC chips. The temperature sensors are based on a linear model that relates quantized temperature measurements of each sensor, C_i, to temperature, T_i, in degrees Celsius. The gain parameter, G, specifies the temperature counts to one degree Celsius, and offset parameter, O, specifies the counts equal to zero degrees Celsius.

$$T_i = C_i * G_i + O_i \tag{2.7}$$

$$i = 1, 2, 3, 4 \tag{2.8}$$

2.1.2 Electric Field Probe

The electric field probe (EFP) consists of two floating potential probes (FPPs) which are differenced to produce the EFP measurement. The floating potential probes serve as voltage measurement devices with high input resistance to monitor the voltage between the spacecraft body and a spherical probe that is deployed away from the spacecraft. Measurements from the electric field probe are included in both the science packet at a $100Hz$ sampling rate, and in the sweeping Langmuir probe packet at a $20kHz$ sampling rate. The measurement requirements for the floating potential probes and the range they are to be tested over are shown in table 2.3.

Table 2.3: Electric Field Probe Requirements

Parameter	**Units**	**Requirement**	**Test Range**
Input Voltage Range	Volts	-1.7 to +1.7	-1.9 to +1.9
Measurement Precision	uV	<360	TBD
Measurement Bandwidth	Hz	40	50
Input Resistance	Ohms	R>10^10	R >10^11

Floating potential probe voltage is quantized to counts with an ADC. The mathematical model used to relate measurements between measured counts, C, and voltage, V, consists of two parameters: the gain, G, and offset, O. The gain term specifies the number of counts to one Volt, and the offset term specifies the number of counts equal to zero Volts.

$$V = C * G + O \tag{2.9}$$

The model assumes a linear relationship between voltages and counts. This assumption works well while the temperature of instrument electronics is constant. The SWP instrumentation is expected to work over a range of temperatures, therefore the model for the electric field probe is expanded to consider the required temperature range.

The temperature is included in the model by assuming a linear relationship between fluctuations in gain and offset parameters with temperature. Four terms are specified to define the gain and offset for floating potential measurement conversion based on temperature: two for the gain as a function of temperature, G_1,O_1, and two for the offset as a function of temperature, G_2,O_2 The temperature model can be seen in figure 2.2.

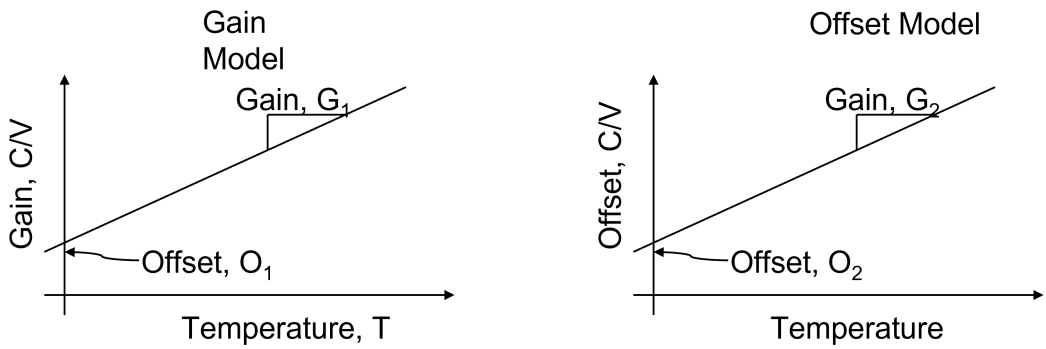

Fig. 2.2: Temperature Model

The final formula for converting FPP measurements to voltages can be seen in equation 2.10.

$$V = C * (G_1 * T + O_1) + (G_2 * T + O_2) \tag{2.10}$$

2.1.3 Langmuir Probe

The Sweeping Langmuir Probe (SLP) has functional similarities to an Ohm meter where the ratio of the applied voltage to the measured current is converted to Ohms. Instead, the SLP reports the measured current collected from the surrounding plasma as the probe surface is placed at various potentials over a range of positive and negative values.

The SLP operates in one of two modes for applying potentials to the plasma, sweeping or fixed bias as shown in figure 2.27b. The potential applied to the probe is controlled by a digital to analog converter (DAC). The SLP then measures the current collected by the probe surface using a transimpedance amplifier. The voltage output of this amplifier is converted to digital counts using an analog to digital converter. Two gain channels are used for the SLP current measurements called “High” and “Low”. The SLP requirements specified by space weather probes is shown in table 2.4.

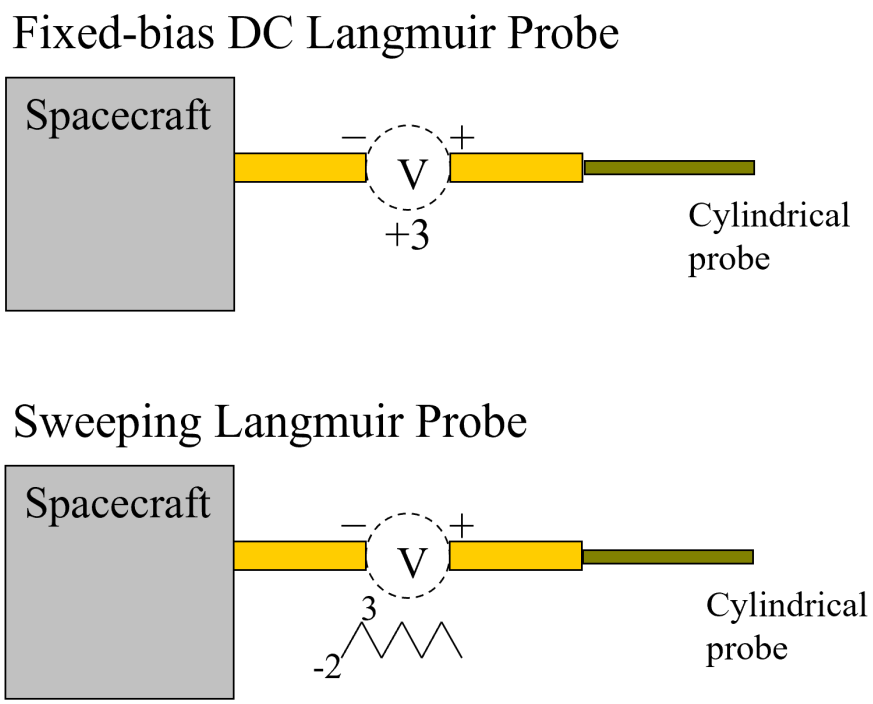

Fig. 2.3: Langmuir Probe Operation Modes

Table 2.4: Langmuir Probe Requirements

Parameter	**Units**	**Requirement**	**Test Range**
Output Voltage Range	Volts	-2 to +3	-2 to +3
High Gain Current Range	nA	-50 to +50	-55 to 55
Low Gain Current Range	uA	-50 to +50	-55 to 55
DC Measurement Bandwidth	Hz	40	50
DC Sample Rate	Hz	100 Hz	NA
Sweep Measurement Bandwidth	kHz	10	0.01 to 100
Sweep Step Sample Rate	kHz	2	20

Mathematical models are used to describe the instrument's output voltage, the output current in fixed bias mode, and the output current in sweeping bias mode.

Langmuir Probe Output Voltage

Understanding the voltage applied by the probe, relative to the current collected, is critical to the function of a Langmuir probe. To ensure the high fidelity of the output voltage the Langmuir probe DAC is supplied by a high precision voltage reference chip (LTC6655). The supply value of $4.096V$ is specifically chosen to allow for simple division and precise programming of voltage steps in $10mV$ units.

The output of the DAC voltage was tested and measured at multiple intervals of the Langmuir probe sweep to verify the output voltage conformed to the required programmed voltage.

The linear model is used to relate the output voltage, V_{OUT}, of all the DACs to the expected voltage, V_{EXP}, consists of two parameters: the gain, G, and offset, O. The gain term specifies the relationship between expected Volts to output Volts, and the offset term specifies the number of expected volts equal to zero output volts as shown in equation 2.11.

$$V_{OUT} = V_{EXP} * G + O \tag{2.11}$$

Fixed Bias Langmuir Current Measurement

The current measured by the DC Langmuir probe uses two AD4003 18bit ADCs to quantify the collected current for separate analog high- and low-gain channels. Separate calibration models are needed for the high- and low-gain channels.

The linear model used to relate the high gain channel measured counts, C_{HG}, and current, I_{HG}, consists of two parameters: the gain, G_{HG}, and offset, O_{HG}. The gain term specifies the number of counts to one Ampere, and the offset term specifies the number of counts equal to zero Amperes. The high gain linear model is shown in equation 2.12

$$I_{HG} = C_{HG} * G_{HG} + O_{HG} \tag{2.12}$$

The linear model was also used for the low gain channel; however, it will be shown that

the Langmuir probe does not operate linearly over part of the required sensitivity range. The non-linearity is resolved by modeling the non-linear region with a cubic model. The linear region of the low gain channel still employs a linear model. Parameters a, b, c, and d, are used to define the third order terms of the non-linear model. The low gain linear model is shown in equation 2.13

$$I_{LG} = \begin{cases} C_{LG} * G_{LG+} O_{LG} & \text{Linear Region} \\ aC_{LG}^3 + bC_{LG}^2 + cC_{LG} + d & \text{Non-Linear Region} \end{cases} \tag{2.13}$$

As with the electric field probe, these models assume the temperature of the instrument electronics is constant. The model for the fixed bias Langmuir probe is expanded to consider the required temperature range. The temperature is included in the model by assuming a linear relationship between fluctuations in linear and non-linear parameters with temperature, and fitting terms to individual models.

Sweeping Langmuir Current Measurement

The current measured by the sweeping Langmuir probe uses the same AD4003 18bit ADC as the fixed bias channel to quantify the collected current in digital counts for the high and low gain channels. It was originally expected that the same calibration model could be used for both the swept bias and fixed bias operation modes. This did not turn out to be the case due to different digital processing of the signals in the FPGA.

In addition to different digital processing chains, an unintended design error related to the supply rails of a differencing operational amplifier in the analog signal processing chain caused the output of the swept bias current to behave differently when higher output voltages were applied by the bias probe. High signal levels of the input voltage exceeded the common mode range of the circuit resulting in non-linear behavior. As a result, the current collected in the sweeping bias mode is dependent on the bias voltage.

The sweeping Langmuir probe is correctly converted by creating a separate calibration

model for swept current measurements. Since the voltage steps applied to the Langmuir probe are finite, a gain, G, and offset, O, conversion term are specified for each DAC step, s, as shown in equation 2.14.

$$I_{HG} = C_{HG} * G_{HG}[s] + O_{HG}[s] \tag{2.14}$$

$$I_{LG} = C_{LG} * G_{LG}[s] + O_{LG}[s] \tag{2.15}$$

The nature of the designed test procedures does not allow step parameters to be compared to temperature.

2.1.4 Electric Field and Langmuir Wave Probes

The electric field wave probe measures the power spectral density of the electric field by differencing FPP signals and computing a Fast Fourier Transform (FFT) on the signal. Power spectral density is divided into 16 bins, or frequency channels, and is measured in Volts per root Hertz, $V/\sqrt{Hz}$. The frequency sensitivity for each EFP channel is specified in table 2.5.

Table 2.5: Wave Probe Channel Sensitivity

ID	**Start Hz**	**Stop Hz**
Ch01	49	98
Ch02	98	146
Ch03	146	195
Ch04	195	293
Ch05	293	391
Ch06	391	537
Ch07	537	781
Ch08	781	1172
Ch09	1172	1660
Ch10	1660	2441
Ch11	2441	3613
Ch12	3613	5273
Ch13	5273	7813
Ch14	7813	11475
Ch15	11475	16943
Ch16	16943	25000

The Langmuir wave probe measures the power spectral density of the current measured by the fixed bias Langmuir probe and is calculated using a FFT and dividing power into 16 bins. Power spectral density is divided into 16 bins, or frequency channels, and is measured in Amperes per root Hertz, $A/\sqrt{Hz}$. The frequency sensitive for each SLP frequency channel is the same as the EFP wave probe.

The measurement requirements for the electric field, and langmuir probe wave channels are shown in table

Table 2.6: Electric Field and Langmuir Wave Probe Requirements

Parameter	**Units**	**Requirement**	**Test Range**
EFP Wave Channels	Channels	16	16
SLP Wave Channels	Channels	16	16
Frequency Range	Hz	30 to 20,000	1 to 30,000

The power measured by the EFP Wave bins, b, are quantified in units of counts. A unique linear model is used to relate measured counts, C_{EFP_b}, the power spectral density of each bin. The linear model consists of two parameters: the gain, G_{EFP_b}, and offset, O_{EFP_b}.The gain term specifies the number of counts to one Volt per root Hertz, and the offset term specifies the number of counts equal to zero Volts per root Hertz as shown in equation 2.16.

$$\frac{V}{\sqrt{Hz}} = C_{EFP_b} * G_{EFP_b} + O_{EFP_b} \tag{2.16}$$

The power measured by the Langmuir Wave bins, b, are quantified in units of counts. A unique linear model is used to relate measured counts, C_{LP_b}, to the power spectral density of each bin. The linear model consists of two parameters: the gain, G_{LP_b}, and offset, O_{LP_b}.The gain term specifies the number of counts to one Ampere per root Hertz, and the offset term specifies the number of counts equal to zero Amperes per root Hertz as shown in equation 2.17.

$$\frac{A}{\sqrt{Hz}} = C_{LP_b} * G_{LP_b} + O_{LP_b} \tag{2.17}$$

2.1.5 Impedance Probe

The Sweeping Impedance Probe (SIP) operates as a RF network analyzer that operates

in the 1 to $30MHz$ range. Sinusoidal voltages are applied to the probe and the resulting current is measured in quadrature. The magnitude and the phase of the current relative to the applied voltage can be determined from the quadrature samples.

The Sweeping Impedance Probe uses a high-speed DAC to create the RF voltage signal which is applied to the probe surface relative to the spacecraft body. The RF current, having traversed through the space plasma of some equivalent impedance, is measured using a high-speed ADC. Quadrature, I, and Q, samples of the current are computed digitally and aggregated to the final sampling rate. The SIP requirements are shown in the table 2.7.

Table 2.7: Sweeping Impedance Probe Requirements

Parameter	**Units**	**Requirement**	**Test Range**
Output Voltage amplitude	mV	100	5 to 1000
Frequency Range	MHz	2 to 30	1 to 30
Minimum Impedance Magnitude	k Ohm	1.33	0.25
Maximum Impedance Magnitude	K Ohm	30	100
Impedance Phase	deg	-90 to 90	-90 to 90

Separate mathematical models are used to describe the SIP output signal, and the return current measured by the SIP.

Impedance Probe Output Signal

The impedance probe's high-speed DAC is set by a numerically controlled oscillator generated within the FPGA fabric. The output digital cosine wave is fed directly to the high-speed DAC at an 80 MHz rate producing stepped sinusoidal waveforms in the 1 to $30Mhz$ range. These waveforms are then processed using a low-pass filter.

The amplitude of the voltage signal is controlled by a second DAC which is fed from an interpolating lookup table within the FPGA. The output amplitude had a target value of $200mV$ peak to peak and was continually adjusted across the operating frequency range

using the table. This corrected for amplitude reductions at high frequency due to the direct digital synthesis (DDS) technique and some pass band variations in the reconstruction filter. The output signal amplitude table is presented in figure 2.4 at 512 discrete points in terms of the DDS control word.

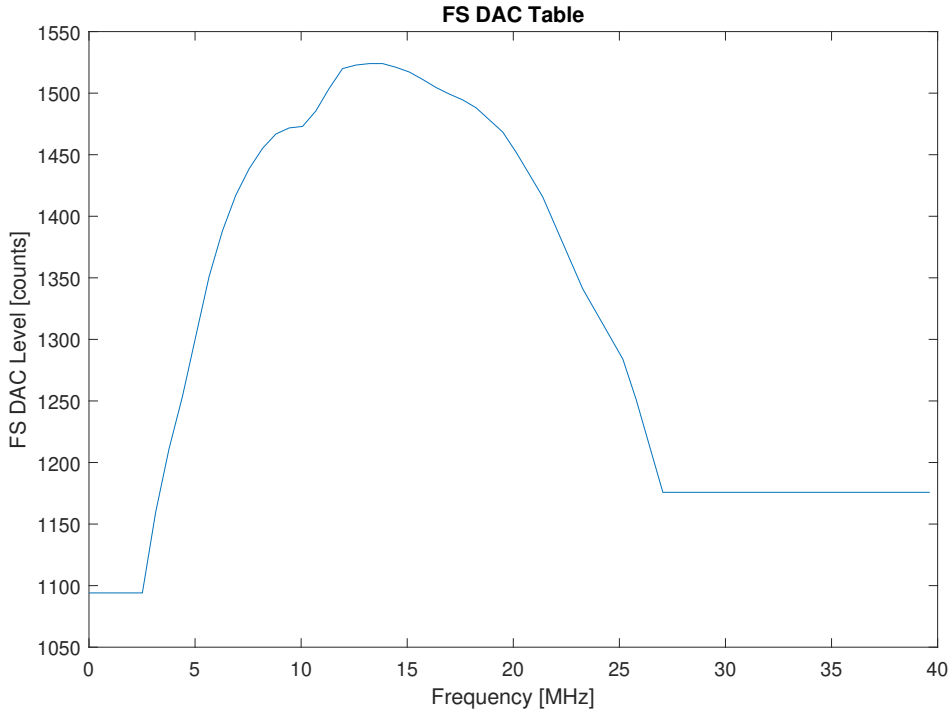

Fig. 2.4: FS DAC Correction Table

Impedance Probe Return Signal

The impedance probe uses a current transformer, burden resistor, and amplifier to determine to convert the RF current flowing to the probe into a voltage. A high-speed ADC is used to digitally sample the resulting current signal. The signal is then digitally mixed within the FPGA to produce in-phase, I, and quadrature, Q, components of the current signal. Separate linear models are used to relate I and Q samples of current to the real and complex components of an equivalent impedance applied between the probe and spacecraft. In this fashion both the output voltage and measured current are combined into

one calibration for the impedance probe.

The linear model used to relate in-phase samples, I, and resistance, R, shown in equation 2.18, consists of two parameters: the gain, G_I, and offset, O_I. The gain term specifies the number of counts to one ohm, and the offset term specifies the number of counts equal to zero ohms.

$$R = C_I * G_I + O_I \tag{2.18}$$

The linear model used to relate quadrature phase samples, Q, and reactance, X, shown in equation 2.19, consists of two parameters: the gain, G_Q, and offset, O_Q. The gain term specifies the number of counts to one ohm, and the offset term specifies the number of counts equal to zero ohms.

$$X = C_Q * G_Q + O_Q \tag{2.19}$$

A procedure to relate measurement samples to temperature is not defined.

2.1.6 Magnetometer

The magnetometer provides a 3-axis measurement of the ambient magnetic field strength and temperature of the chip. The magnetometer is a stand-alone chip that reports the field strength of each axis as counts. The requirements for the SWP magnetometer are shown in table 2.8.

Table 2.8: Magnetometer Requirements

Parameter	**Units**	**Requirement**	**Test Range**
Magnetic Field	nT	>57,000	66,000
Sample Rate	Hz	100	1 to 5000
Sensitivity	nT	1000	NA

Quantized magnetometer counts, C_x, C_y, C_z, are converted to magnetic field strength, B_x, B_y, B_z, in Tesla, using a linear model. The gain parameter, G, specifies the number of counts to one Tesla, and offset parameter, O, specifies the number of counts equal to zero Tesla, as shown in the equations 2.20 - 2.22.

$$B_x = C_x * G_z + O_x \tag{2.20}$$

$$B_y = C_y * G_y + O_y \tag{2.21}$$

$$B_z = C_z * G_z + O_z \tag{2.22}$$

Temperature samples measured by the magnetometer thermal sensor are likewise converted from temperature counts, C, to the temperature, T, in degrees Celsius. The gain parameter, G, specifies temperature counts per one degree Celsius, and the offset term, O, specifies the number of counts relating to zero degrees Celsius, as shown in formula. The magnetometer was not tested during thermal testing, and variation due to temperature is not considered directly with temperature.

2.2 Test Procedures

The Space Weather Probes team developed a set of test procedures designed to verify that SWP met the design requirements. Test procedures were also developed to provide calibration data for mathematical models of the SWP instruments. The test procedures are documented in PowerPoint presentation “SPORT USU Space Weather Probes Test and

Calibration Rev 24.pptx". A summary of the test procedures is presented in table 2.9.

Table 2.9: Space Weather Probes Test Procedures

Test #	Name	Associated Instruments	Short Description	Function
1	EFP Gain and Offset	EFP	Determine the gain and offset of the EFP	Calibration
2	EFP Frequency Response	EFP/ EFP Wave	Determine the frequency response of the DC EFP	Calibration
3	EFP Input Resistance and Guarding	EFP	Demonstrate the DC input resistance of the EFP	Verification
4	SLP DC Gain and Offset	SLP	Determine the gain and offset current of the DC LP	Verification/ Calibration
5	SLP Gain and Offset	SLP	Determine the gain and offset of the SLP	Calibration
6	SLP Frequency Response	SLP/ SLP Wave	Determine the frequency response of the SLP	Calibration
7	SLP Sweep Output and Linearity	SLP	Determine the output voltage of the SLP	Calibration
8	Spectrometer White Noise	EFP Wave	Determine the gain and offset of theEFP Wave	Verification
9	Frequency Output	SIP	Determine the frequency output of the SIP	Calibration
10	Precision Gain and Linearity	SIP	Determine the gain and offset of the SIP	Calibration
11	Frequency Lock	SIP	Verify track functionality of the SIP	Verification
12	Frequency Response	Magnetometer	Determine the input frequency response of the SIP	Calibration
13	Gain and Offset	Magnetometer	Determine the gain and offset magnetic field of the magnetometer	Calibration
14	Frequency Response	Magnetometer	determine the frequency response of the magnetometer	Calibration

2.2.1 Automated Testing

The calibration and verification tests can each be run individually but are designed to be configured together and run in an automated testing environment. The SWP team implemented the test procedures in LabVIEW to enable automation. LabVIEW directly controlled a National Instruments Virtual bench and controlled a Keithley 6221 DC and AC current source via externally called MATLAB scripts.

A LabVIEW Graphical User Interface (GUI) was created to control the automated tests. The GUI allowed the team to select which tests would be run and how long the automated testing would run for. LabVIEW used the network time protocol to timestamp the start and end of each test to synchronize data collected by the SWP electronics board. The LabVIEW setup is shown in figure 2.5.

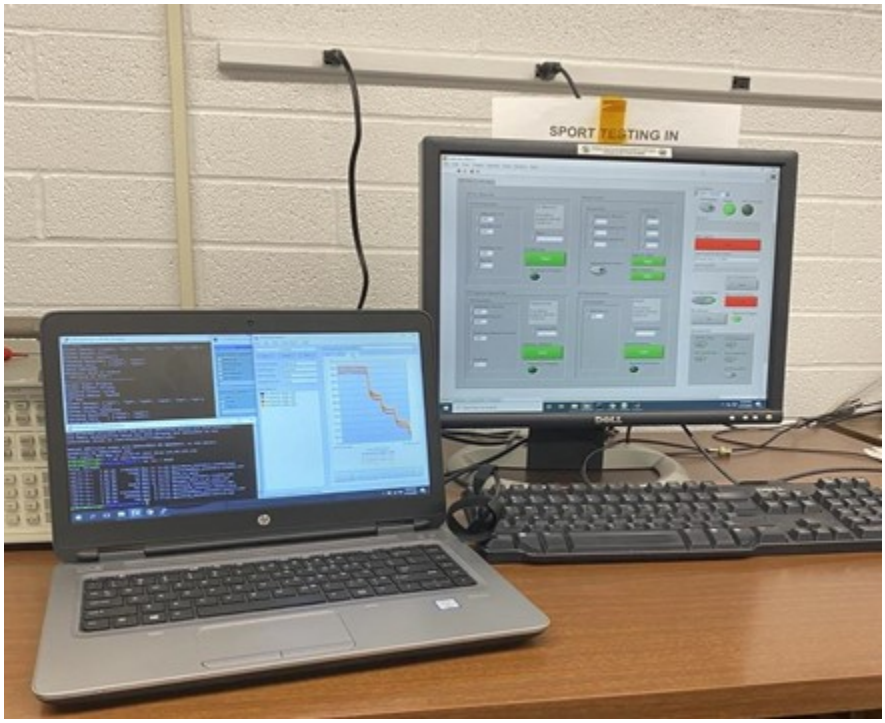

Fig. 2.5: Automated Test Setup

The automated testing environment defines two test configurations, A and B, that are set up in a thermal chamber to test SWP electronics over the specified temperature range.

Test Configuration A

Test Configuration A performs tests 1,2,4,6, and 10. The floating potential inputs connect to the Virtual Bench signal generator to supply DC voltages for the EFP Gain and offset test (Test 1), and AC signals for the EFP Frequency Response Test (Test 2).

The Langmuir probe input connects to the Keithley current source to supply DC currents for the SLP DC Gain and Offset test (Test 4), and AC currents for the SLP Frequency Response Test (Test 6). The Virtual Bench, Keithley current source, and SWP electronics board share a common ground.

An impedance probe calibrator is connected across the SIP for the Precision Gain and Linearity test (Test 10). The value of the SIP Calibrator is fixed during testing, providing only one data point. Test configuration A is shown in figure 2.6.

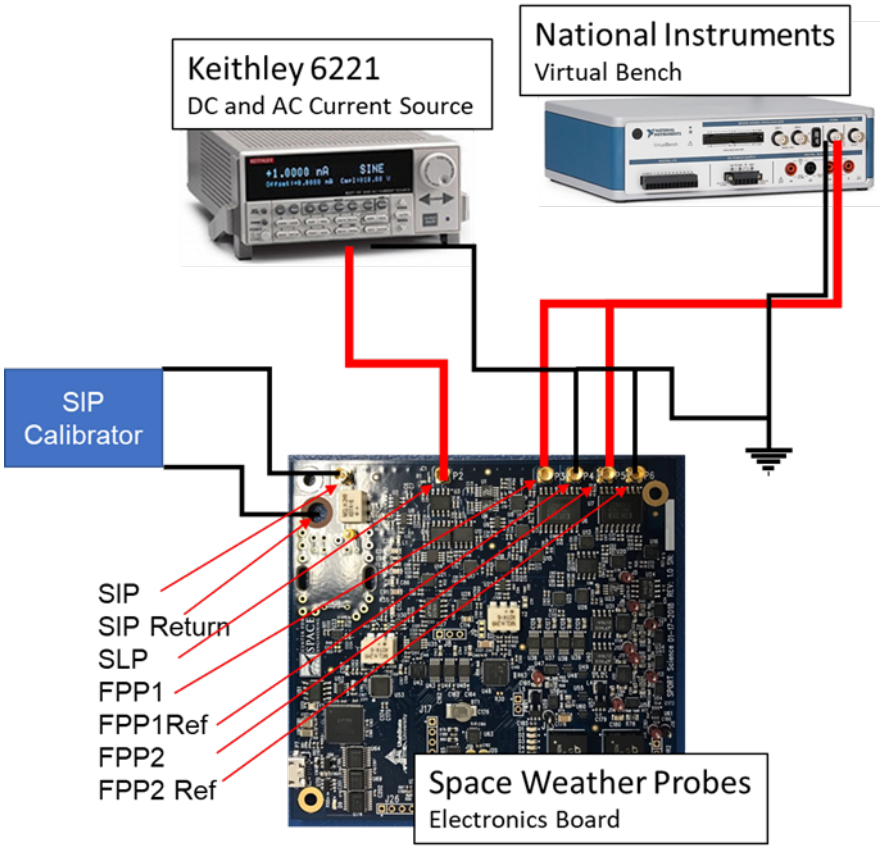

Fig. 2.6: Test Configuration A

Test Configuration B

Test Configuration B performs tests 4,6,7, and 10. The Langmuir probe input connects to ground through a calibrator resistor, providing one data point for the SLP DC Gain and Offset test (test 4). The Langmuir probe input additionally connects to the input of floating potential probe one for the SLP Sweep Output Gain and Linearity Test (Test 7). The input of floating potential probe 2 connects to the Virtual Bench with the same configuration as A. Test configuration B is shown in figure 2.7.

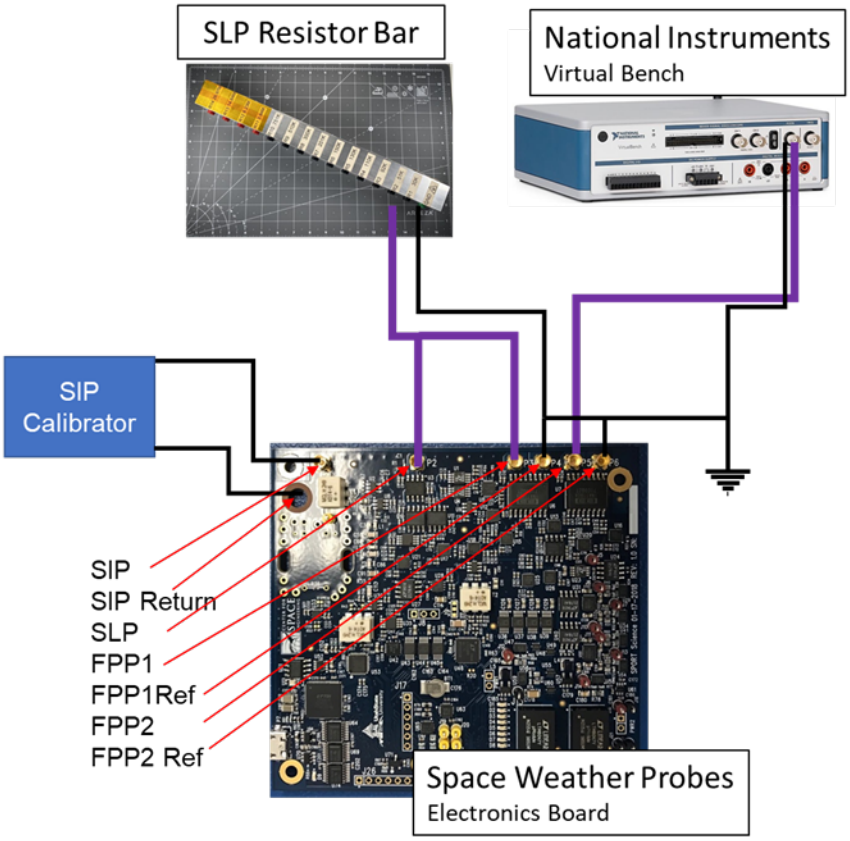

Fig. 2.7: Test Configuration B

2.2.2 Thermal Testing

Space weather probes verified thermal operational requirements with the thermal profile shown in figure 2.8. The thermal profile is achieved by placing the SWP electronics board in an insulated chamber. A Cole-Palmer pipes temperature-controlled coolant through the chamber to set chamber temperature. The board temperature is independently monitored with a multimeter. To achieve the coldest possible temperature, dry ice is added to the thermal chamber at the end of the cold profile. Connections to SWP test equipment are routed outside of the thermal chamber as shown in figure 2.9.

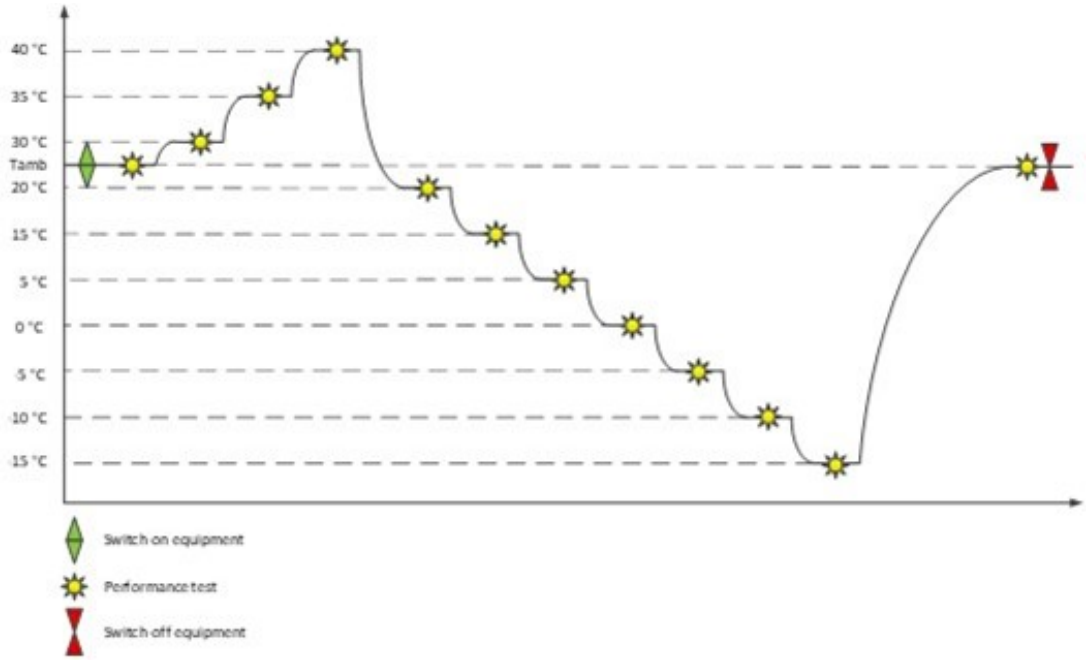

Fig. 2.8: Thermal Profile

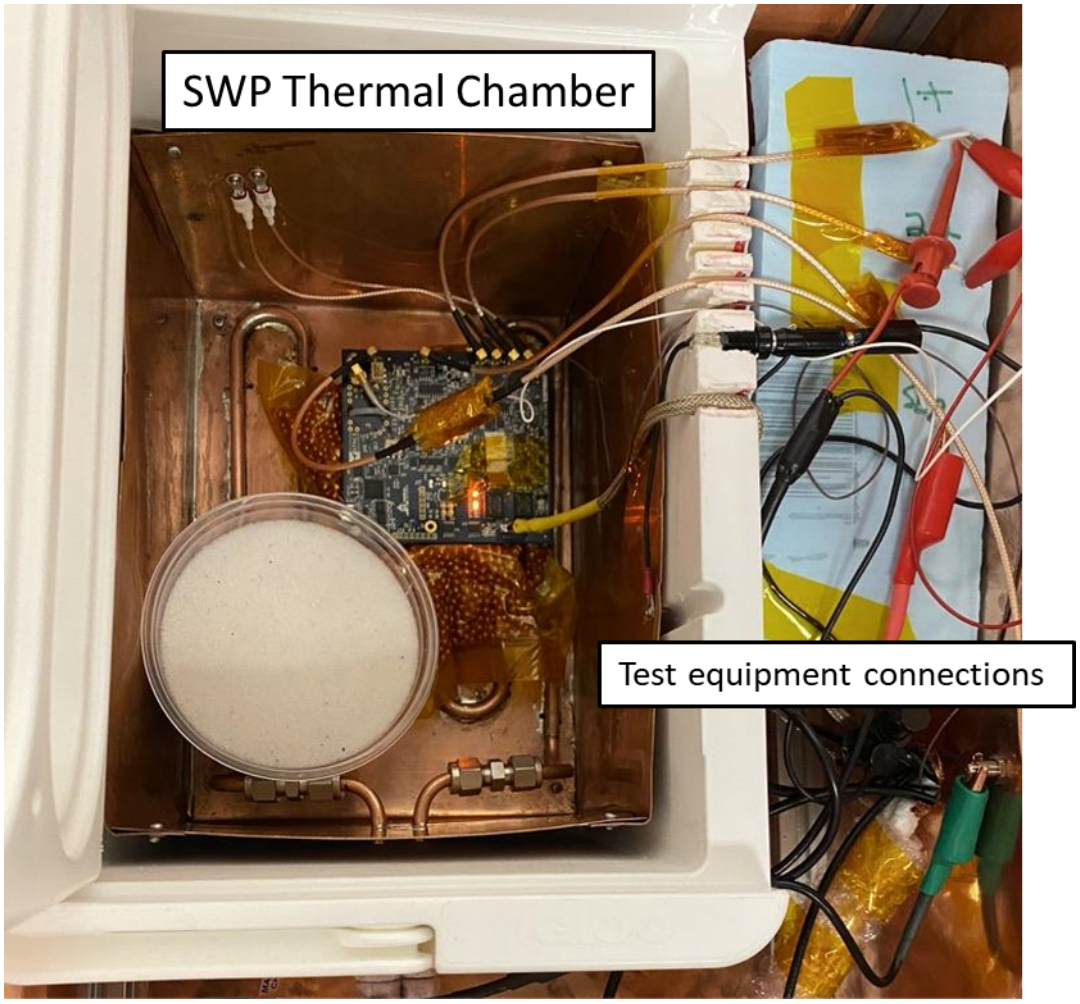

Fig. 2.9: SWP Thermal Chamber

A summary of thermal calibration test procedures is shown in table 2.10.

Table 2.10: Thermal Test Summary

Test Date	**SN**	**Configuration**	**Data File**
5/4/2020	4	#A	sportData_20200504-170641.bin
5/7/2020	3	#A	sportData_20200507-082217.bin
5/11/2020	3	#B	sportData_20200511-104334.bin
6/24/2020	4	#B	sportData_20200624-142806.bin
7/6/2020	4	#B	sportData_20200706-192333.bin
7/15/2020	3	#B	sportData_20200715-114220.bin
7/17/2020	3	#A	sportData_20200717-085758.bin
8/5/2020	3	#A	sportData_20200805-155449.bin
8/7/2020	3	#B	sportData_20200807-104928.bin

Space weather probes initially selected serial number 4 as the flight unit because SN4 instruments fit the defined linear models best. However, an accident in the thermal temperature chamber caused a coolant leak and damaged SN4. SN3 took SN4s place as the flight unit. SN3 was in the final flight configuration for the August 5th and August 8th thermal tests. Data sets from these tests are used to perform calibration.

2.3 Instrument Calibration

Conversion factors for instrument models are calculated from the instrument calibration testing. This section describes the relevant test data for each instrument calibration, and how they are used to produce conversion factors of digital words back to voltages, currents, etc.

2.3.1 Housekeeping Calibration

Calibration tests for SWP voltage, current, and temperature monitors are described here.

Voltage Supply Monitors

The only calibration possible for the housekeeping voltage monitors is to compare the voltage measured by the DAC in counts to the voltage independently measured by an external digital voltage meter. A single data sample taken in this fashion does not allow for a linear calibration of data, therefore, the manufacturer supplied conversion factors are used. The manufacture specifies a gain of, $G_M = 62.5\mu V/\text{Count}$, and no offset. Conversion factors supplied by the manufacturer, in conjunction with specified supply gains are consistent with observations. The conversion formula used for voltage supply monitors is shown in equation 2.23.

$$V_s = \frac{C_s * G_M}{G_S} \tag{2.23}$$

The gains, G_s, for each supply voltage, S, is shown in table 2.11.

Table 2.11: Voltage Supply Gain

Voltage Supply, S	**Gain,** G_s
5V	0.3509
1V8A	1
1V8D	1
4V5A	0.3509
-1V8A	-0.5862
3V3D	0.5
-4V5A	-0.3509

Current Supply Monitors

The SWP test procedure does not define any method to calibrate SLP current monitors. The manufacturer supplied conversions are used instead. The manufacturer specifies a gain of $G_M = 62.5\mu V/\text{Count}$, and no offset. The conversion formula used for current supply

monitors is shown in equation 2.24

$$I_s = \frac{C_s * G_M}{G_{TIA}} \tag{2.24}$$

The transimpedance gain, G_{TIA}, of these current monitors chips is configured using resistors on the SWP board and set to:

$$G_{TIA} = 2.004 \frac{V}{A} \tag{2.25}$$

Temperature Monitors

The temperatures measured by ADC sensors are calibrated using the thermal chamber. The thermal chamber controls the known board temperature over the required temperature range. The known board temperature is compared to the temperature made by ADC temperature sensors.

The temperature measured by each ADC sensor in counts is compared to the controlled board temperature. Calibration data is fit to the linear model to produce conversion factors of gain, G, and offset, O, for each ADC thermal sensor. The conversion factors for each temperature sensor are shown in equations 2.26 - 2.29.

$$T_{U60} = C_{U60} * 0.0077 - 4.0781 \tag{2.26}$$

$$T_{U55} = C_{U5}5 * 0.0077 - 3.2172 \tag{2.27}$$

$$T_{U48} = C_{U48} * 0.0077 - 1.5723 \tag{2.28}$$

$$T_{U49} = C_{U49} * 0.0077 - 1.9177 \tag{2.29}$$

2.3.2 Electric Field Probe Calibration

The DC voltage potential measured by both electric field probes are calibrated using

the electric field gain and offset test. The electric field gain and offset test injects a stair step voltage sweep into the inputs of both floating potential probes. The voltage steps range from -2 to 2 Volts, with 0.1 Volts per step and one second dwells at each step as shown in the figure 2.10.

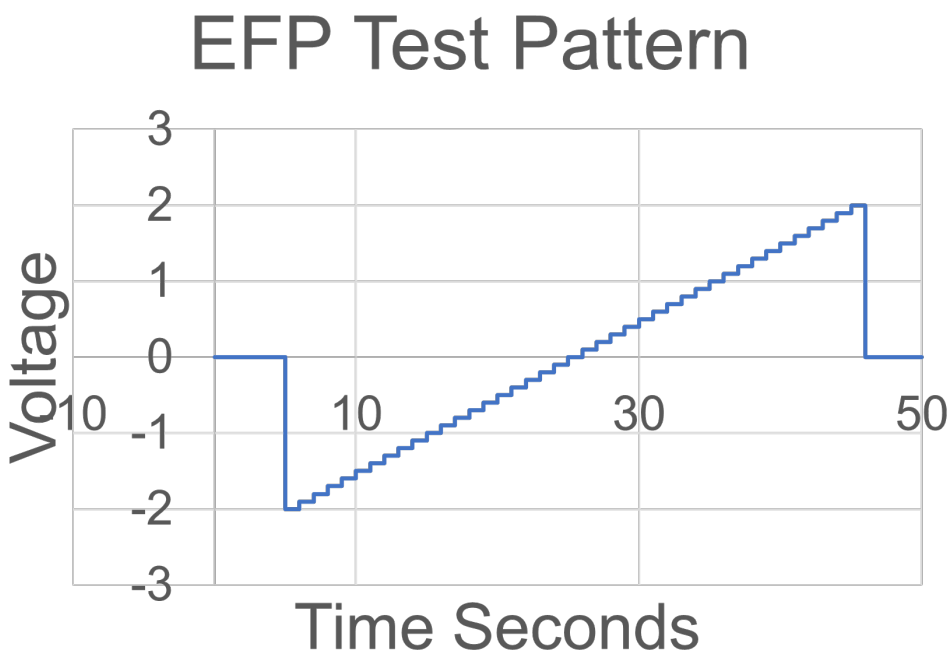

Fig. 2.10: Electric Field Probe Calibration Steps

The voltage potential measured by each floating potential probe in counts is compared to the supplied voltage level. Calibration data is fit to the linear model to produce conversion factors of gain, G, and offset, O.

Figure 2.11 shows the calibration for sample data taken during an electric field gain and offset test. Superimposed on calibration data is the line of best fit for each probe. Residual data, indicating the difference between the linear model, and actual calibration data is also shown.

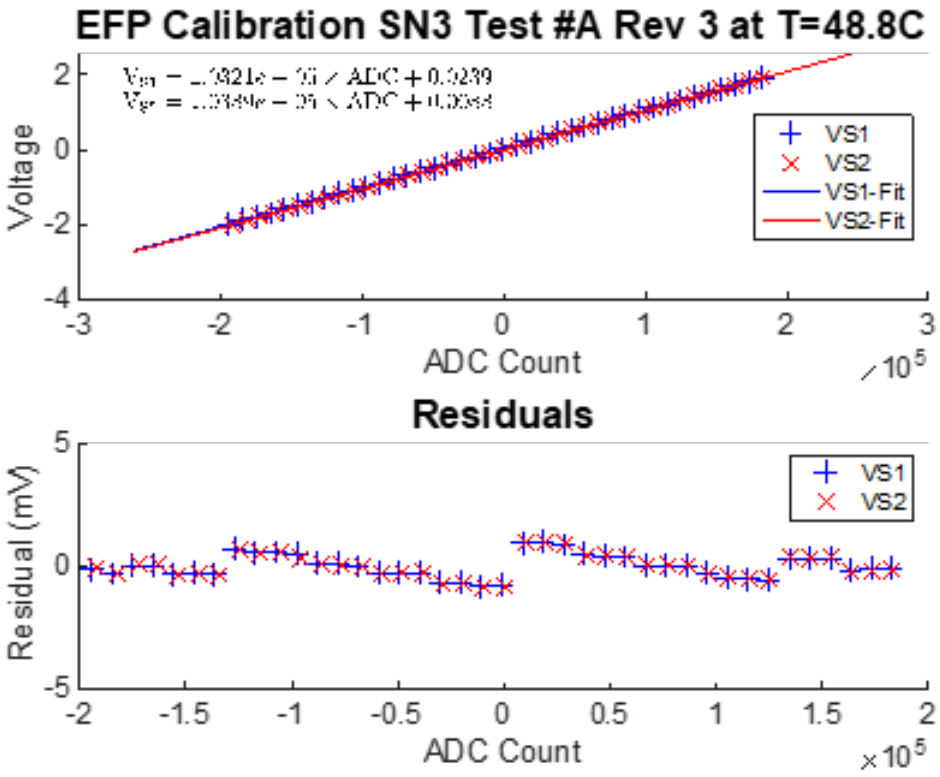

Fig. 2.11: Electric Field Probe Calibration

The electric field gain and offset test is completed multiple times at each step in the temperature profile. Conversion factors of gain and offset are calculated for each fixed temperature test. The temperature measured on the SWP board in degrees Celsius is compared to the fixed temperature gain and offset values produced at those temperatures. A line is fit to the comparison to produce conversion factors for the gain, G_1, O_1, and offset, G_2, O_2. Figure 2.12 shows the calibration for all test 1 data taken during thermal test configuration A.

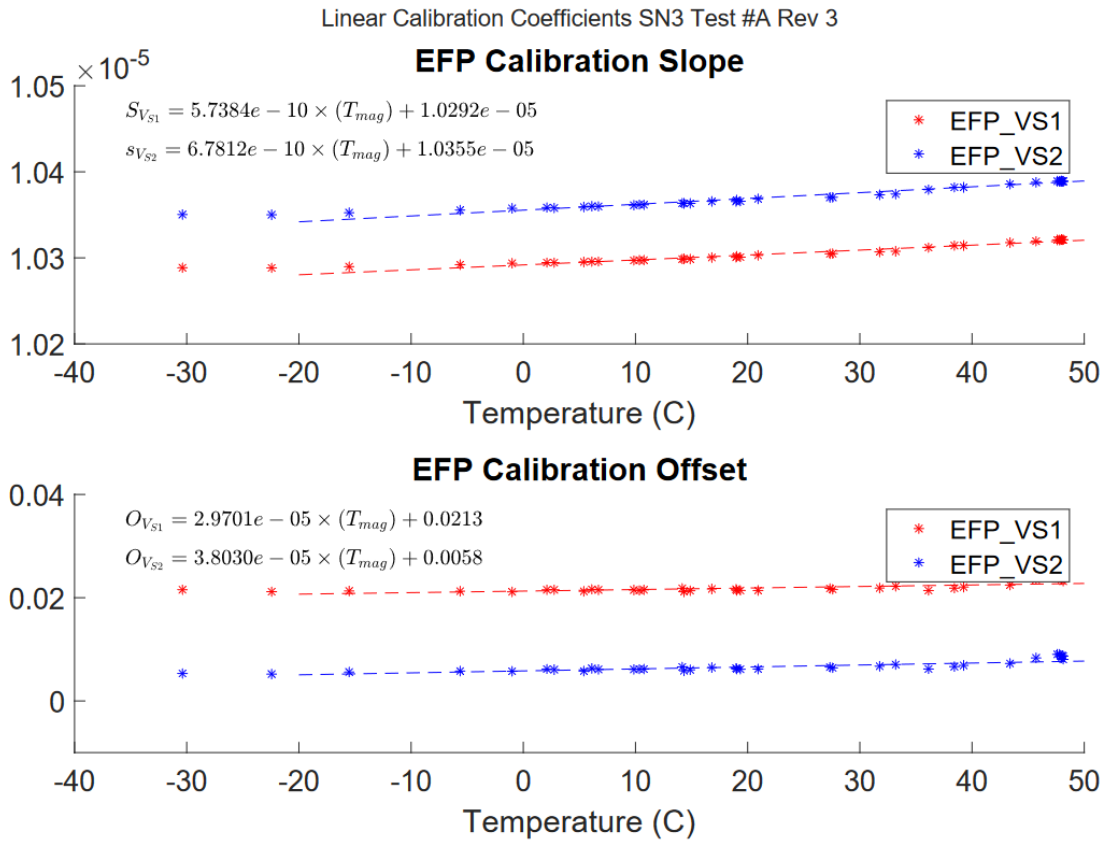

Fig. 2.12: Electric Field Probe Thermal Calibration

The calibration process reveals the conversion factors specified by the linear mathematical model designed. The conversion factors are used to interpret collected EFP data in counts to voltages during post-processing.

SWP test and calibration procedures calibrate electric field probe data collected from the science packet. SWP calibration procedures assumed that the conversion factors for electric field probe samples would be the same for the science and sweeping Langmuir probe packets. However, a review of calibration data sets revealed unexpected differences between electric field probe data sampled from these packets. Additional considerations required for converting EFP data measured in the SLP packet will be discussed later.

2.3.3 Langmuir Probe Calibration

The Langmuir probe fixed bias probe and sweeping bias current measurements are separately calibrated. The DAC output voltage is also calibrated.

Langmuir Probe DC Gain and Offset

The Langmuir probe DC gain and offset test injects a stair step current sweep into the inputs of the Langmuir Probe. The current sweep ranges from -55 to $55\mu A$, with $2.75\mu A$ per step and one second dwells at each step for the low gain channel as shown in the left axis of figure 2.13. The current sweep is repeated with the same pattern with adjusted current range of -55 to $55nA$, with $2.75nA$ per step and one second dwells at each step for the high gain channel as shown in the right axis of figure 2.13.

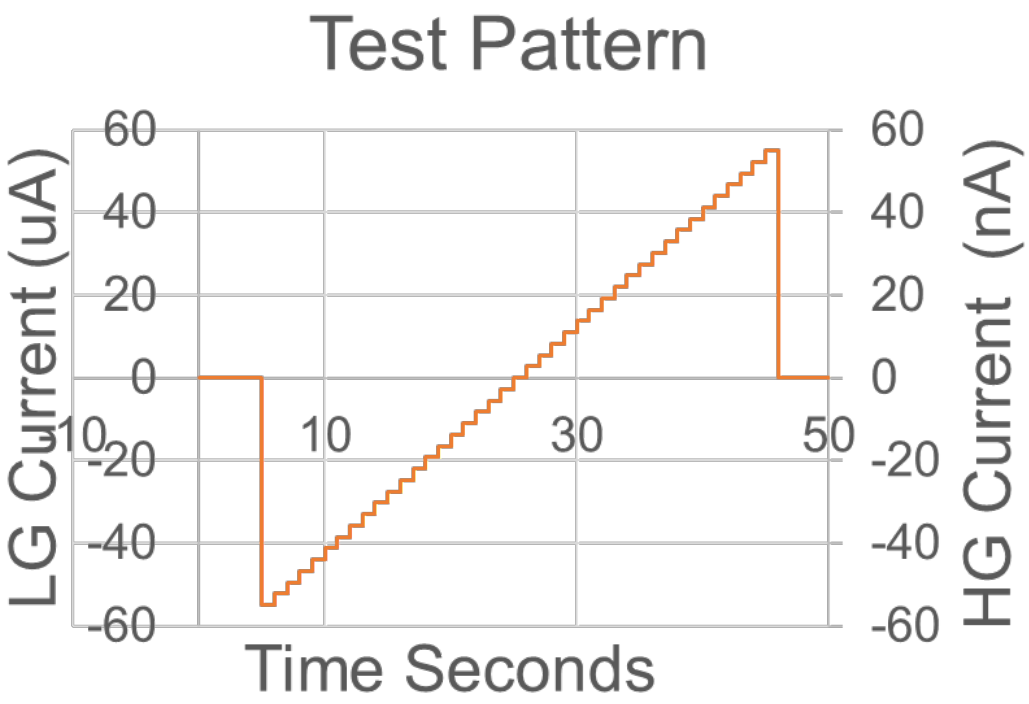

Fig. 2.13: Electric Field Probe Thermal Calibration

The results of a Langmuir probe DC gain and offset test are shown in figure 2.14.

The data demonstrates that the low gain channel does not have a linear response over the specified sensitivity range. Test data also shows that the high gain channel does not properly gain the current signal. High gain channel counts are saturated over the required sensitivity range.

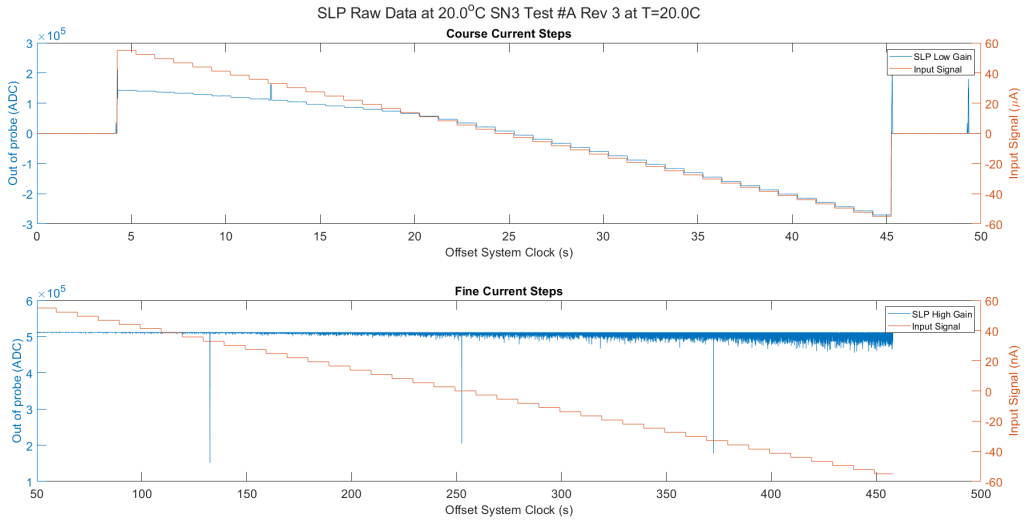

Fig. 2.14: Electric Field Probe Thermal Calibration

The current measured by the low gain fixed bias probe in counts is compared to the supplied current level. The non-linear current region is resolved by modeling the region with a cubic model, parameters $a, b, c,$ and d are used to define the third order terms of the non-linear model. Calibration data in the linear region is fit to the linear model to produce conversion factors of gain, G, and offset, O.

Figure 2.15 shows the calibration for sample data taken during a SLP DC Gain and Offset test. Superimposed on calibration data is the linear line of best fit for the current in the linear region, and a cubic line of best fit for the current in the non-linear region. Residual data, indicating the difference between the model, and actual calibration data is also shown.

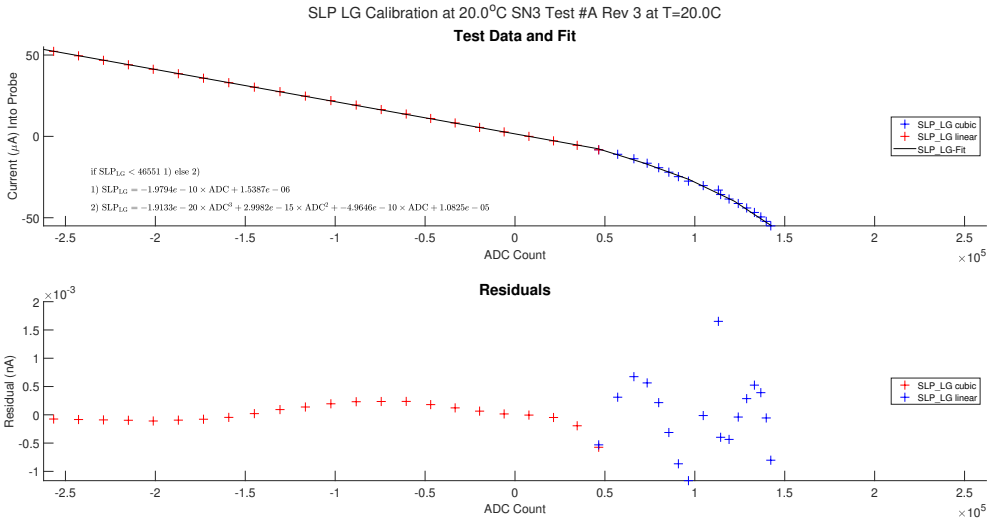

Fig. 2.15: Electric Field Probe Thermal Calibration

The current measured by the high gain fixed bias probe in counts is compared to the supplied current level. Because the channel is saturated, no meaningful conversion factors can be defined.

The temperature measured on the SWP board in degrees Celsius is compared to the fixed temperature gain and offset values of the linear fit produced at those temperatures. A line is fit to the comparison to produce conversion factors for the gain, G_1, and offset, O_1. Temperature calibration showed that the offset current did not behave linearly with temperature. A cubic model is used to interpret the offset current over the specified temperature range. Figure 2.16 shows the calibration data taken over the thermal range. Superimposed on the figure is the linear and cubic line fits used for thermal calibration of the linear region.

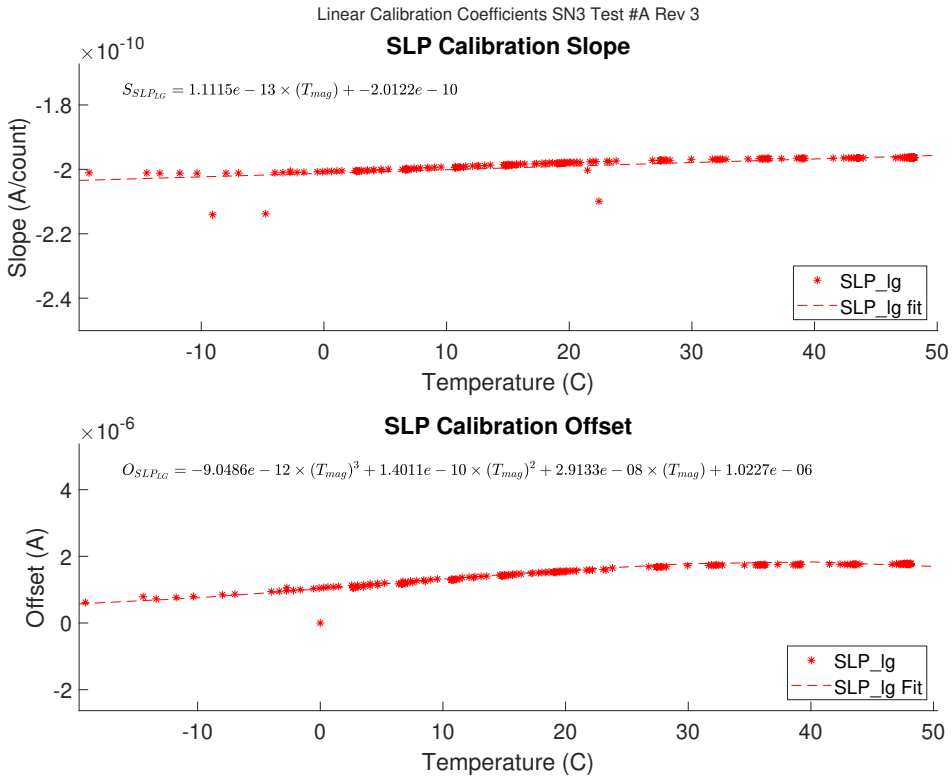

Fig. 2.16: Electric Field Probe Thermal Calibration

The temperature measured on the SWP board in degrees Celsius is compared to the fixed temperature cubic values of the cubic fit produced at those temperatures. A line is fit to the comparison to produce conversion factors for each of the cubic terms. Figure 2.17 shows the calibration data taken over the thermal range. Superimposed on the figure is the linear and cubic line fits used for thermal calibration of the linear region.

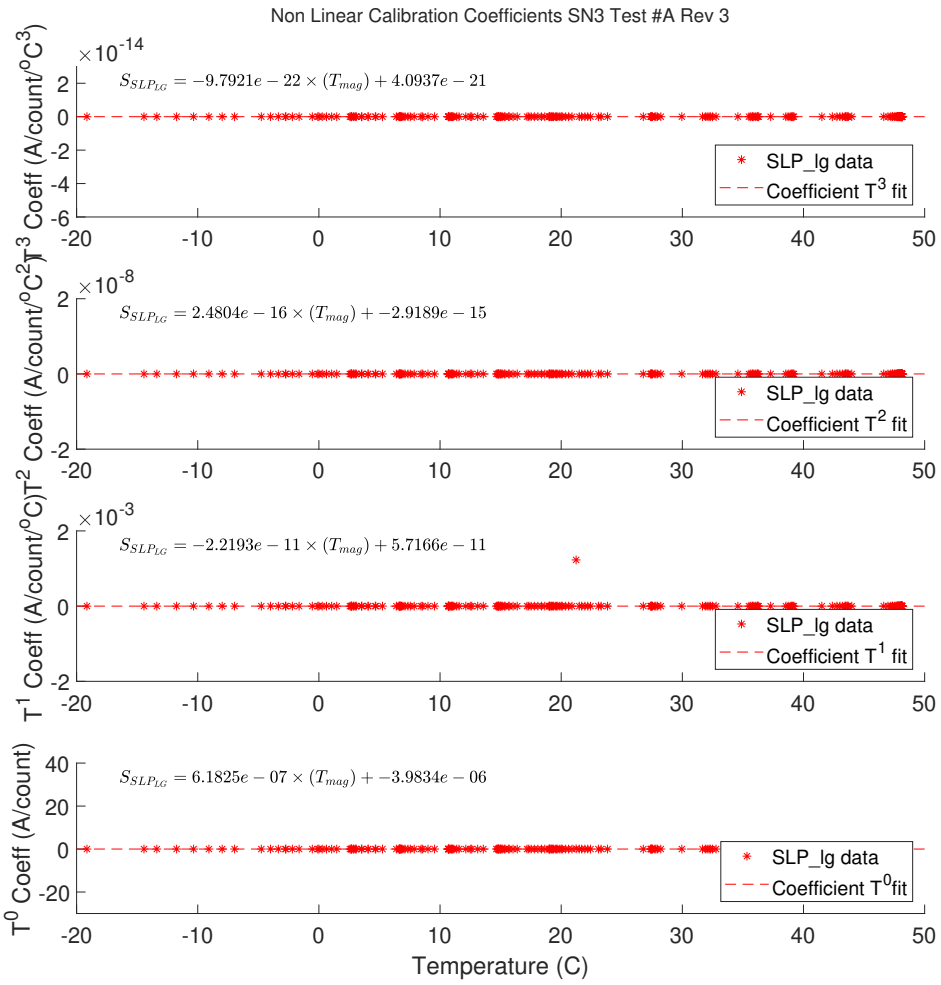

Fig. 2.17: Electric Field Probe Thermal Calibration

Langmuir Probe Sweep Gain and Offset

The Langmuir probe gain and offset test uses a set of fourteen resistor calibrators to supply a known current source into the Langmuir probe. The Langmuir probe output is connected to ground through resistor values ranging from $30k\Omega - 27M\Omega$. The current, I, measured by the Langmuir probe is equal to the voltage, V, supplied by the DAC at step, s, divided by the resistance of the calibrator, R_i as shown in equation 2.30.

$$I = \frac{V[s]}{R_i} \tag{2.30}$$

The resistance of each calibration resistor can be seen in table 2.12.

Table 2.12: Calibration Resitors

Resistor	**Value** ($k\Omega$)
R1	30
R2	51
R3	92
R4	110
R5	130
R6	150
R7	201
R8	300
R9	510
R10	751
R11	3945
R12	8237
R13	14843
R14	26971

The current measured by the Langmuir probe in counts is compared to the expected current for each DAC voltage step for each resistor calibrator. Calibration data is fit to the linear model to produce conversion factors of gain, G, and offset, O. Figure 2.18 shows the calibration of Langmuir probe data at selected steps taken at room temperature. Residual data, indicating the error between the linear model, and actual calibration data is also shown.

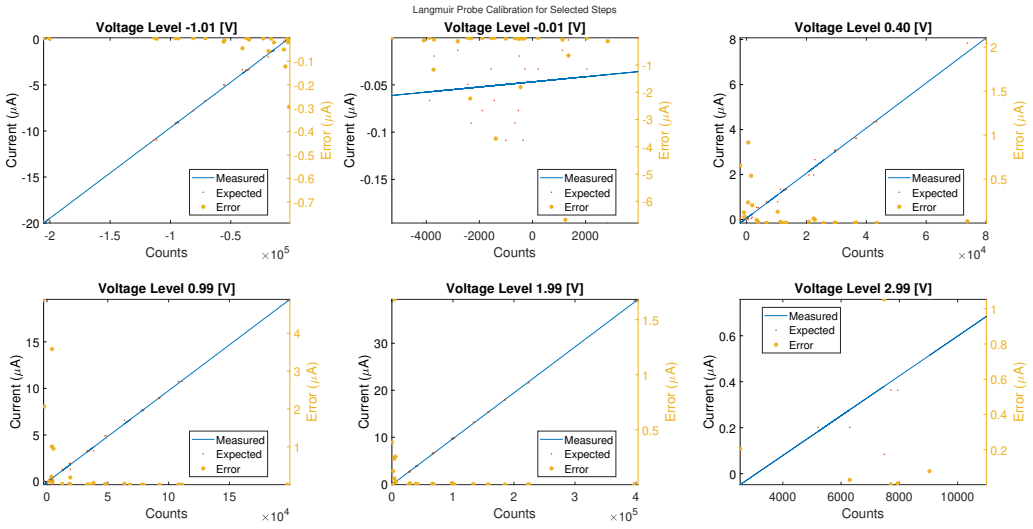

Fig. 2.18: Langmuir Probe Sweep Calibration Selected Steps

Figure 2.19 shows the conversion parameters of gain, G, and offset, O, for unique DAC voltage steps in the Sweep. Residual data, indicating the difference between the linear model, and actual calibration data is also shown for each step.

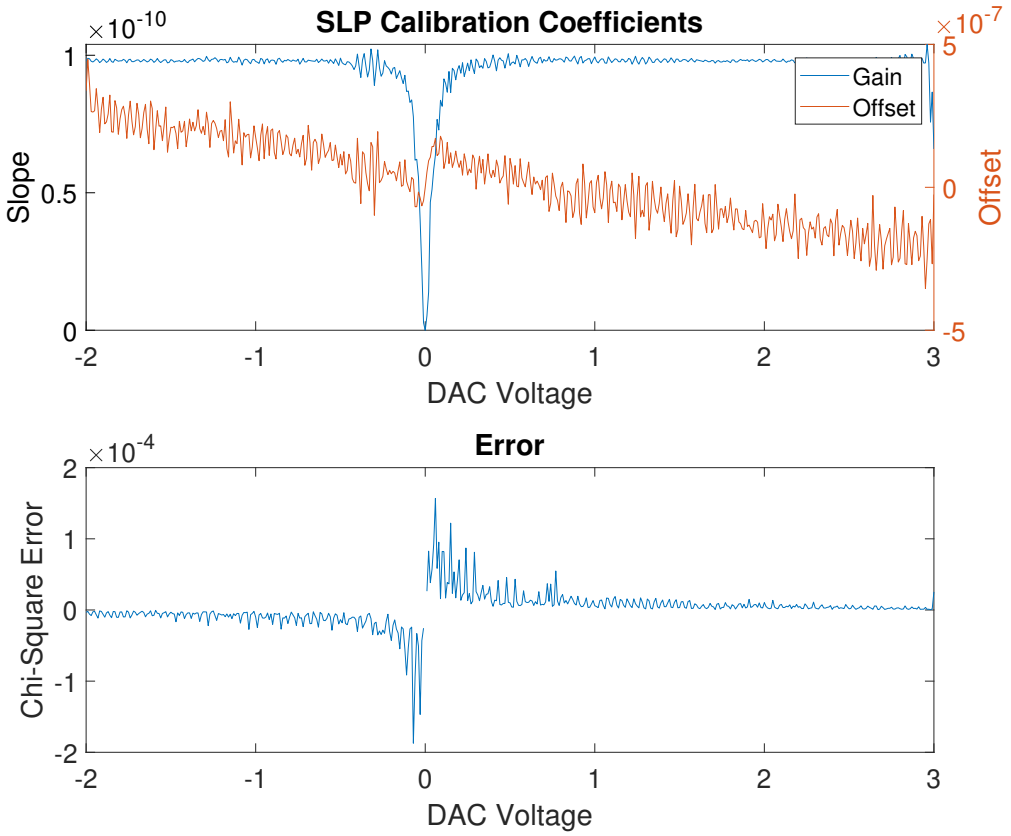

Fig. 2.19: Langmuir Probe Sweep Calibration

The calibration process reveals the conversion factors specified by the linear mathematical model designed. The conversion factors are used to interpret collected SLP data in counts to currents during post-processing. The data set used to produce this calibration, and figures is saved in 'LP_Sweep_Cal_Data_Set.mat', collected on August 18th, 2020.

The Langmuir offset gain and linearity test is completed during thermal testing with a fixed resistor calibrator. Conversion factors cannot be thermally calculated with only a single data point.

Langmuir Probe Output Voltage

The SLP Sweep Output and Linearity test was designed to calibrate the output voltage of the Langmuir probe sweep with the electric field probe. Because the voltage sweep

consists of voltages outside of the required sensitivity range of the electric field probe, this test did not work as intended.

The SLP Sweep Output and Linearity Test instead used a digital voltage meter to measure the output voltage supplied by the SLP sweep at specified voltage steps. Every 20th step of the sweep is measured with error less than 0.04 Volts, as shown in figure 2.20.

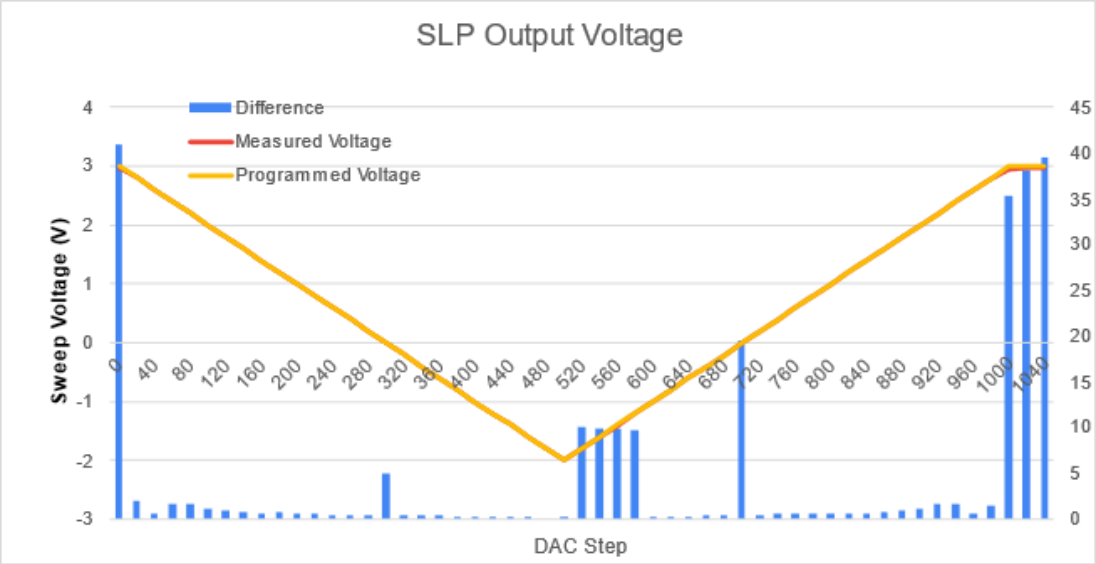

Fig. 2.20: Langmuir Probe Sweep Calibration

The high precision on the DAC is due to the precision reference source that is used to source the DAC voltage. The high precision of DAC voltage steps negates the need for further conversion. The output voltage is set to the programmed voltage level.

2.3.4 Electric Field and Langmuir Wave Probe

The Electric field and Langmuir wave probes are calibrated using data from the EFP Frequency Response test, and the SLP Frequency Response test. Calibrations from these tests are discussed in this section.

Electric Field Wave

Power spectral density from the electric field wave probe is calibrated using data from

the EFP frequency response test. The EFP frequency response test injects AC voltage signals into both channels of the electric field probe. The frequency of the signal is adjusted to apply logarithmically spaced frequencies to the probe. The range of frequencies applied to the probe is from $5Hz \leq f \leq 30kHz$. The specific frequencies applied to the probe, as well as the duration of the signals are shown in table 2.13.

Table 2.13: Frequency Sweep

Frequency Table Part A		
Point	**Hz**	**s**
1	5	20
2	6	17
3	7	15
4	8	13
5	10	10
6	11	10
7	13	8
8	15	7
9	17	6
10	19	6
11	22	5
12	26	4
13	30	4
14	34	3
15	40	3
16	46	3
17	53	2
18	62	2
19	72	2
20	83	2

Frequency Table Part B		
Point	**Hz**	**s**
31	417	1
32	484	1
33	560	1
34	649	1
35	752	1
36	872	1
37	1010	1
38	1171	1
39	1357	1
40	1572	1
41	1822	1
42	2111	1
43	2447	1
44	2835	1
45	3286	1
46	3808	1
47	4413	1
48	5114	1
49	5926	1
50	6867	1

21	96	2	51	7958	1
22	111	1	52	9223	1
23	129	1	53	10688	1
24	149	1	54	12386	1
25	173	1	55	14353	1
26	200	1	56	16634	1
27	232	1	57	19276	1
28	268	1	58	22339	1
29	311	1	59	25888	1
30	360	1	60	30000	1

The EFP wave probe channels will be sensitive to the input signal only when the input frequency of the signal is in the specified sensitivity range of the channel. The power measured by each EFP wave channel in counts is compared to the supplied power. During the times when the signal is in the channel sensitivity range, the passband, the power is expected to be equal to the amplitude squared. When the signal is not in the channel sensitivity range, the stopband, the power is expected to be equal to zero.

The amplitude of the EFP frequency sweep is fixed. The signal is either in the pass band, or in the stop band. Samples collected during the pass or stop bands are collectively averaged together to create two Calibration data points, one for the stop, and one for the pass band. Calibration data points are fit to the linear model to produce conversion factors of gain, G, and offset, O, for each EFP wave channel.

Figure 2.21 shows the calibration for sample data taken during an EFP frequency response test for EFP wave channel 13. Superimposed on calibration data is the line of best fit for channel 13.

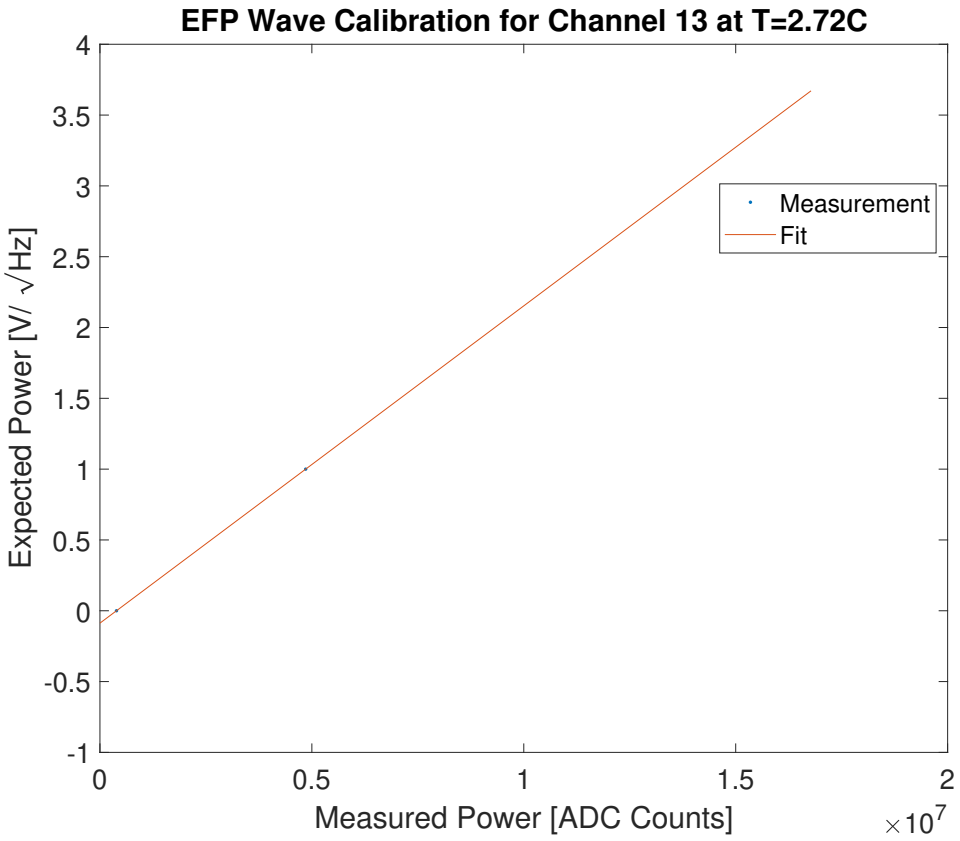

Fig. 2.21: Langmuir Probe Sweep Calibration

The EFP frequency response test is completed multiple times at each step in the temperature profile. Conversion factors of gain and offset are calculated for each fixed temperature test. The temperature measured on the SWP board in degrees Celsius is compared to the fixed temperature gain and offset values produced at those temperatures. A line is fit to the comparison to produce conversion factors for the gain, G_1, O_1, and offset, G_2, O_2. Figure 2.22 shows the calibration for all test 1 data taken during thermal test configuration A for EFP wave channel 13.

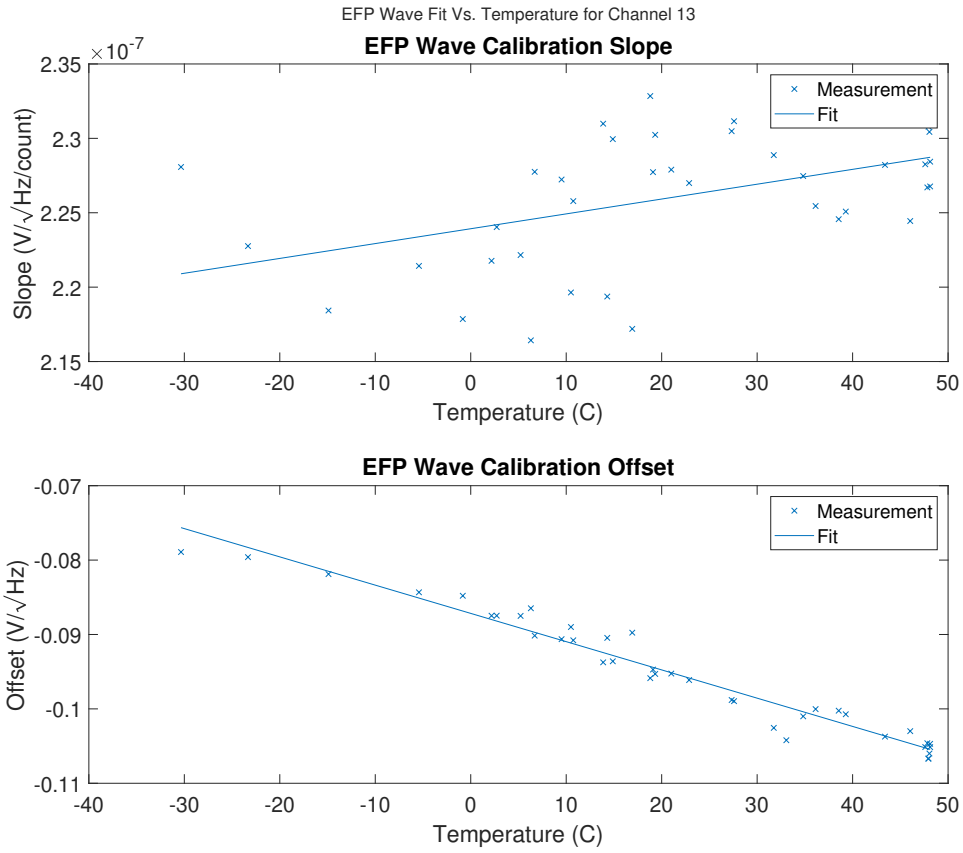

Fig. 2.22: Langmuir Probe Sweep Calibration

The calibration process reveals the conversion factors specified by the linear mathematical model designed. The conversion factors are used to interpret collected EFP wave data in counts to power during post-processing.

Langmuir Wave Probe

Power spectral density from the Langmuir wave probe is calibrated using data from the SLP frequency response test. The SLP frequency response test injects AC current signals into the Langmuir probe. The frequency of the signal is adjusted to apply logarithmically spaced frequencies to the probe. The range of frequencies applied to the probe is from $5Hz \leq f \leq 30kHz$. The specific frequencies applied to the probe, as well as the duration of the signals match the electric field probe frequency sweep table shown in table 2.13.

Preliminary data from the SLP frequency response test suggested the Langmuir Wave probe operated as expected. However, later tests, reviewed after the delivery of Space Weather Probes, showed that the Langmuir wave probe does not perform the intended function. The issue is believed to be introduced during a firmware update sometime late in development. Because no meaningful Langmuir wave data can be produced, the calibration procedure does not produce conversion factors for the Langmuir wave probe.

2.3.5 Sweeping Impedance Probe

The sweeping impedance probe output signal, and return current measurements are seperately calibrated.

The RF return signal measured by both sweeping impedance probe is calibrated using the precision gain and linearity test. The precision gain and linearity test connect the output SIP signal to the return signal path with calibrator loads of known impedance. The calibrator loads, with their associated impedances used for calibration, is shown in table 2.14.

Table 2.14: SIP Calibrators

Calibrator Name	**Load**
R2	502Ω
R3	999Ω
R4	$2.01k\Omega$
R5	$5k\Omega$
R6	$10k\Omega$
R7	$15.1k\Omega$
R8	$25k\Omega$
R9	$49.9k\Omega$
R10	$101k\Omega$
C3	15pF
C4	8.2pF
C5	3.6pF
C6	2.0pF
C7	1.0pF

The in-phase current, I, measured by the impedance probe in counts is compared to the expected current level for each of the resistive loads. The quadrature phase current, Q, measured by the impedance probe in counts is compared to the expected current level for each of the capacitive load.

The signal response is expected to vary as a function of the input signal frequency, and the calibration is done for each step, S, of the SIP frequency sweep. Calibration data is fit to the linear model to produce conversion factors of gain, $G_I[S], G_Q[S]$, and offset, $O_I[S], O_Q[S]$.

Figure shows I and Q calibration sample data for selected frequencies taken during a precision gain and linearity test. Superimposed on calibration data is the line of best fit for each frequency.

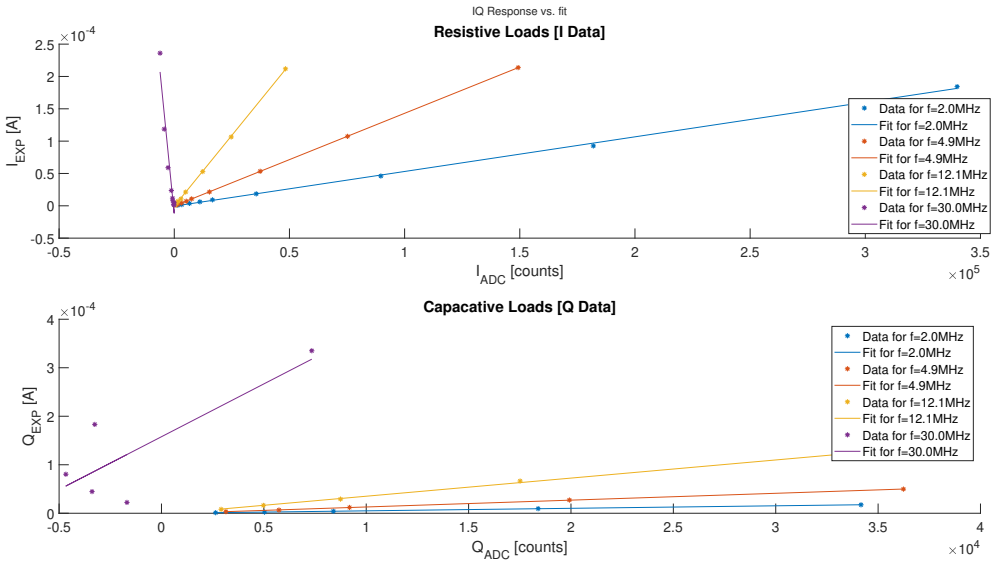

Fig. 2.23: Sweeping Impedance Probe Calibration

The calibration process reveals the conversion factors specified by the linear mathematical model designed. The conversion factors are used to interpret collected SIP return current data in counts to current during post-processing.

2.3.6 Magnetometer

The calibrations for the magnetometer and magnetometer temperature sensor are discussed here.

Magnetometer Sensor

The magnetometer is calibrated using data from the magnetometer gain and offset test. The magnetometer gain and offset test applies a current source to a Helmholtz coil, inducing magnetic fields of known strength. The currents applied to the magnetometer, along with the resulting induced magnetic field are shown in table 2.15.

Table 2.15: Magnetometer Calibration

Current mA	**Field Strength** nT
80	66,588
70	58,265
60	49,941
50	41,618
40	33,294
30	24,971
20	16,647
10	8,324
0	0
-10	-8,324
-20	-16,647
-30	-24,971
-40	-33,294
-50	-41,618
-60	-49,941
-70	-58,265
-80	-66,588

The three axes of SWP magnetometer are positively and negatively aligned with the Helmholtz coil, and ADC samples from the relevant axis is sampled. The ambient magnetic field during testing is assumed to be constant and subtracted from data by comparing positively and negatively aligned data samples. The SWP electronics board is shown during magnetometer testing in figure 2.24.

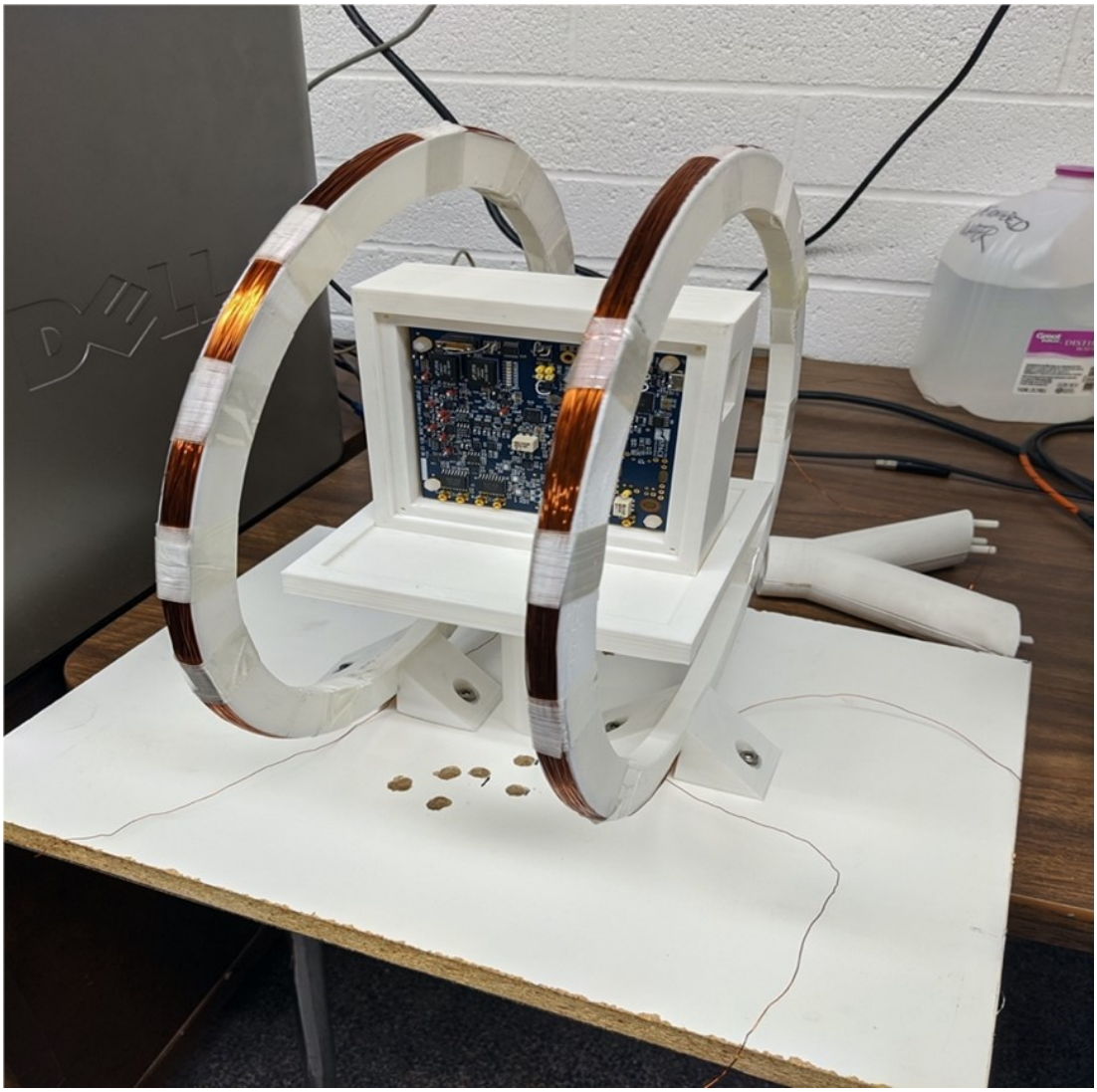

Fig. 2.24: Magnetometer Testing

The magnetic field strength of each axis, B_x, B_y, B_z, in counts is compared to the induced magnetic field in Tesla. A line is fit to the comparison to produce conversion factors for the gain, G_x, G_y, G_z and offset, O_x, O_y, O_z. Figure 2.25 shows the calibration data taken during a magnetometer gain and offset test.

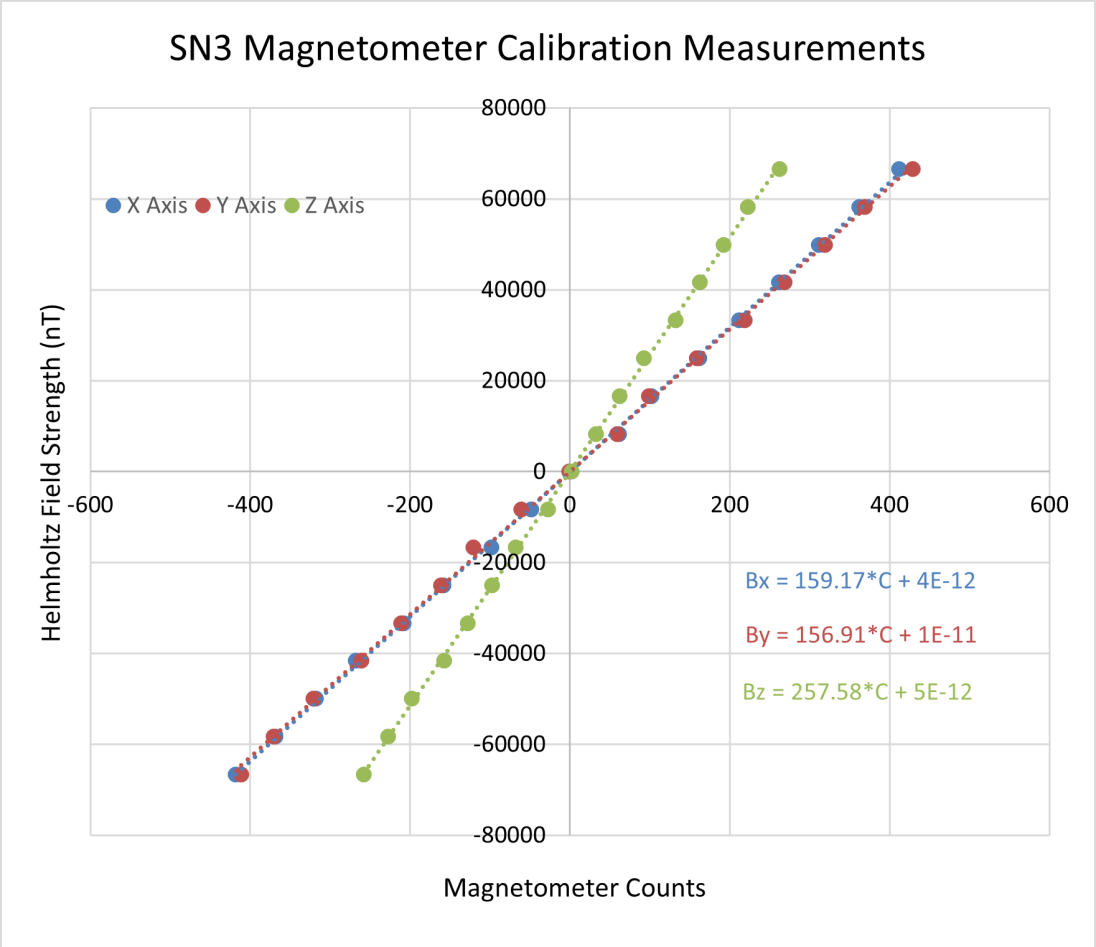

Fig. 2.25: Magnetometer Calibration

Magnetometer Temperature Sensor

The magnetometer temperature sensor is calibrated using the same method that was employed for the ADC temperature sensors. The conversion factors from the magnetometer temperature calibration is shown in equation 2.31.

$$T_{Mag} = C_{Mag} * 0.0224 + 453.2 \tag{2.31}$$

2.4 Conversion Process

Conversion data from each SWP instrument is collated together and saved as MATLAB

data structures. These data structures are used in the data conversion process to provide physical measurements of data sampled by SWP. This section describes how conversion data is stored for each instrument.

2.5 Additional Considerations

This section discusses additional procedures used to correctly interpret SWP data.

2.5.1 Electric Field Probe Measurements

SWP calibration procedures assumed that the conversion factors for electric field probe samples would be the same for the science and sweeping Langmuir probe packets. However, a review of calibration data sets revealed unexpected differences between electric field probe data sampled from these packets. These differences are the result of how the electric field probe signal is measured and digitally sampled.

Figure 2.26 shows a simplified block diagram of how the electric field probe signal is measured and digitally sampled on SWP. Shown in the signal chain are unique digital down sample blocks for the science packet and SLP packet, and an analog low pass filter.

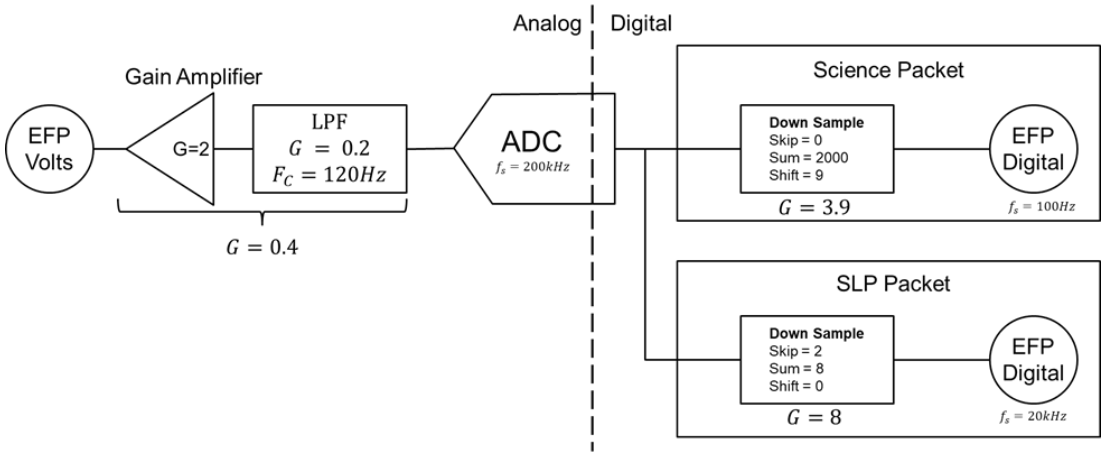

Fig. 2.26: EFP Signal Chain

Down Sampling

The digital down sample blocks increase sample resolution by combining multiple sample measurements. The combination also reduces the sample rate to the rates specified by the SWP telemetry dictionary. The down sample block defines parameters Skip, Sum, and Shift. The Skip parameter is used to omit samples taken during transient sample periods that should be ignored. The Sum parameter specifies the number of data samples to add together. The Shift parameter specifies a binary shift that serves as a binary division operation. Table 2.16 summarizes the skip, sum and shift parameters for electric field probe measurements.

Table 2.16: EFP Down Sample Parameters

Packet	**Skip**	**Sum**	**Shift**	**Sample Rate**	**Gain**
Science	0	2000	9	100Hz	3.90625
Sweeping Langmuir	2	8	0	20kHz	8

The science packet operates on 2000 ADC samples (reducing the sample rate to $100Hz$), by summing all 2000 samples together and bit-shifting by nine (or dividing by 512). The SLP packet operates on 10 ADC samples (reducing the sample rate to $20kHz$), by skipping 2 samples, and summing the remaining 8. SLP samples are not bit-shifted (no division). The down sample operation introduces a gain factor into data samples, s, recorded in the science and SLP packets. The gain factor is equal to the number of samples summed together, divided by the division factor as shown in equations 2.32 - 2.34.

$$Science_{EFP} = \frac{2000}{512} \cdot s \tag{2.32}$$

$$SLP_{EFP} = 8 \cdot s \tag{2.33}$$

$$G_{science} = 3.9, G_{SLP} = 8 \tag{2.34}$$

Calibration data from the science packet is used to produce conversion factors for electric field probe samples and includes the science packet gain factor. To use these conversion factors, electric field probe measurements from the SLP packet must properly account for the relative gain between the science and SLP down sample blocks. The relative gain, G_{rel}, is shown in equation 2.35.

$$G_{rel} = \frac{G_{SLP}}{G_{science}} = 2.048 \tag{2.35}$$

Electric field probe measurements sampled by the SLP packet are divided by the gain factor to convert measurements as shown in equation 2.36.

$$EFP_V = ScienceConversion(EFP_{SLP})/G_{rel} \tag{2.36}$$

Low Pass Filter

The low pass filter in the electric field probe analog chain was designed to meet requirements for the electric field probe samples made in the science packet. The required bandwidth of electric field probe samples from the science packet is $0 - 40Hz$. The magnitude and phase response of the low pass filter in this region is approximately constant.

The required bandwidth of electric field probe samples made by the SLP packet, however, is $0 - 10kHz$. The magnitude and phase response of the low pass filter is not constant over the required bandwidth and is not ideal for samples made by the SLP packet. The analog electric filter is shown in figure 2.27a. The transfer function for the low pass filter is shown in equation 2.37. The filter's magnitude and frequency response and transfer function is shown in figure 2.27.

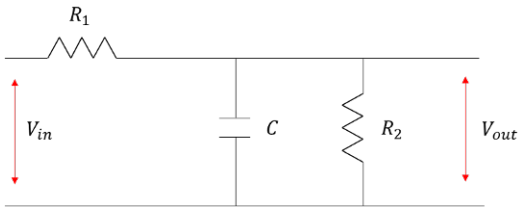

(a) LPF Circuit Diagram

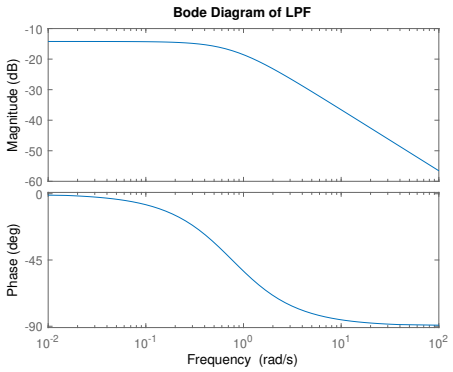

(b) Magnitude/ Phase Response

Fig. 2.27: Electric Field Probe Low Pass Filter

$$H(s) = \frac{\frac{1}{R_1 C}}{s + (1 + \frac{R_1}{R_2})\frac{1}{R_1 c}} \tag{2.37}$$

A digital inverse filter is designed to undo the effects of the analog filter in post processing. The filter is designed in MATLAB by creating a continuous time transfer function model of the LPF, $H(s)$, converting the model from continuous to discrete time, $H(z)$, and inverting the digital filter, $H^{-1}(z)$.

The low pass filter has a DC gain of G= 0.2. The effects of the low pass filter DC gain are accounted for with the science conversion. The inverse filter undoes the effects of the low pass filter magnitude response, including the DC gain factor. Since both operations account for the DC gain, an additional gain correction factor must be included to undo the effects of one of the magnitude corrections.

Sweeping Langmuir Probe Packet Conversion

Figure 2.28 shows a block diagram for SLP electric field probe measurement conversion. The EFP signal is first converted to volts using the science conversion. Gain correction terms are applied to the voltage signal to correct for the relative gain of the SLP packet, and to account for the low pass filter DC gain. The voltage signal is inverse filtered to undo the

phase response of the low pass filter.

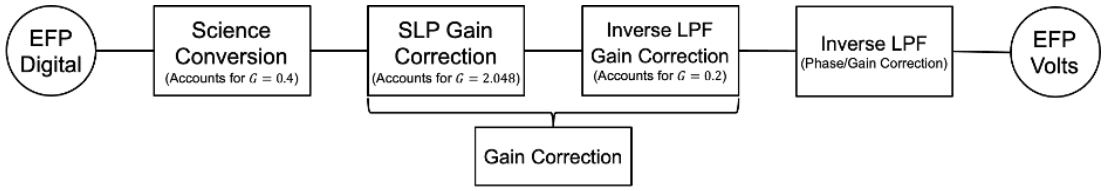

Fig. 2.28: SLP EFP Processing Chain

Low Pass Filter Calibration

The inverse filter is defined by the passive components $R1, R2$, and C of the low pass filter. The inverse filter is only effective when the passive component values are well known. While the low pass filter specifies passive component values, the components used have specific tolerances specified by the part manufacturer. Additionally, properties of passive components vary based on temperature.

Test configuration B connects the output of the Langmuir probe DAC to the input of electric field probe sensor 1. The original intention of this configuration was to use electric field probe data to observe the variation in the Langmuir probe DAC voltage from the expected curve. Because the Langmuir probe output voltage is separately shown to provide a high-fidelity signal, the output signal is instead used to calibrate parameters of the electric field probe low pass filter.

The SLP electric field probe measurements, converted to voltages with the science conversion, and appropriately gained are fit to the expected output voltage of the Langmuir probe using a non-linear curve fitting algorithm [14]. The curve fitting algorithm adjusts filter values of $R1, R2,$ and C to find parameters with the least square error.

Figure 2.29 demonstrates the process of the curve fitting algorithm. The measured electric field probe signal (shown in blue) is filtered according to parameters $R1, R2$, and C (shown in red). The filtered signal is then compared to the programmed output voltage set by the Langmuir probe DAC (yellow signal). The applied voltage signal of the Langmuir probe DAC is greater than the sensitivity range of the electric field probe, only the linear

regions (highlighted in red) are considered in the curve fitting algorithm.

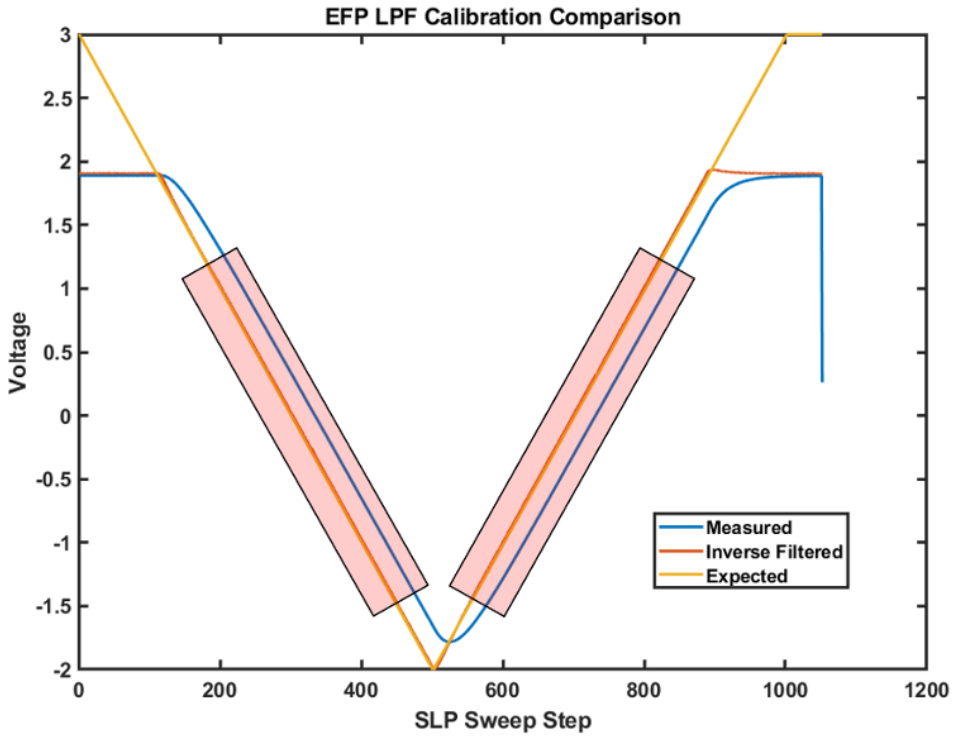

Fig. 2.29: Low Pass Filter Calibration Process

A fit is produced for every single SLP packet during test configuration B. Figure 2.30 shows the results of the fitting process. Figure 2.30a compares the filtered EFP signal to the applied voltage measurement for an individual sweep. The first tile overlays the expected voltage measurement with the filtered electric field probe signal. The second tile calculates the residual difference (Measured - Expected) of the two signals. The signals closely match in the linear regions of the electric field probe measurement.

Figure 2.30b shows the calculated parameters $R1, R2$, and C for each sweep during test configuration B. The temperature dependence of component values can be seen clearly by comparing component variation to the temperature profile of the sweep, shown in the fourth tile.

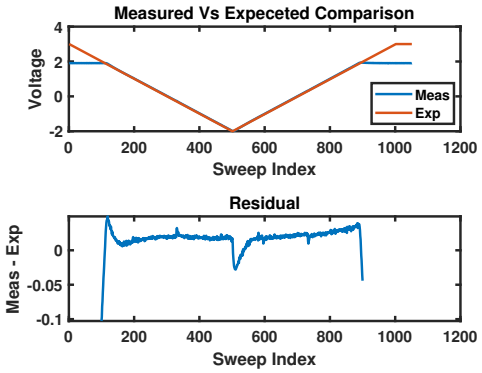

(a) Inverse Low Pass Filter Example

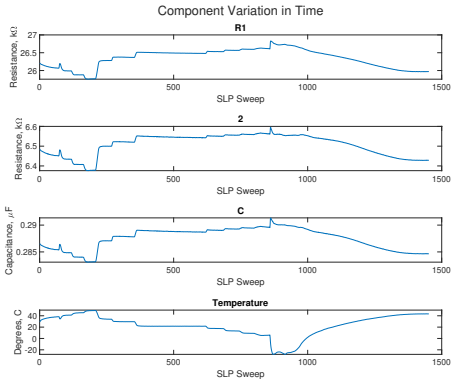

(b) Temperature Variation of LPF Components

Fig. 2.30: Results of Low Pass Filter Fitting

Figure 2.31 shows the temperature fit that is used to calculate low pass filter component values. Figure 2.31a plots component values against temperature. Overlayed on the plots, is a cubic line fit relating temperature to component value. Figure 2.31b plots the mean square error between the expected voltage and electric field probe measurements filtered with component values defined by the fitted temperature curve.

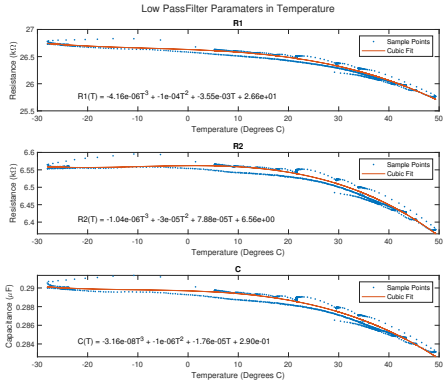

(a) Temperature Fit for LPF Components

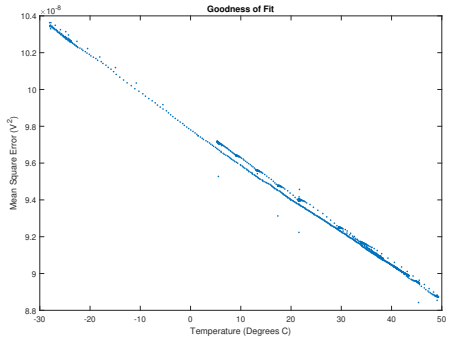

(b) Calculated Error

Fig. 2.31: Temperature Calibration of LPF

Electric Field Probe 2

No calibration data exists for the low pass filter in the second electric field probe channel, FPP2. Space Weather Probes assumes that both channels will have similar responses. Additionally, electric field probe measurements made during an SLP are used to monitor the potential of the spacecraft. This measurement requires a single floating potential probe, when significant differences between FPP measurements are found, FPP channel one measurements are favored.

Time Shift

Care was taken to ensure that measurements made during an SLP sweep step were time aligned with the Langmuir probe output voltage of that step. The electric field probe low pass filter introduced a specific, frequency dependent delay that is removed with an inverse low pass filter. The low pass filter does not completely account for all the delay. SWP assumes the remainder of the analog signal delay is approximately constant in frequency.

The approximate signal delay is calculated by measuring the time difference between the linear regions of the electric field probe voltage measurement, and Langmuir probe current measurement with the expected output voltage. Figure 2.32 shows the results of the time alignment calculation for each Langmuir probe sweep of test configuration B. The X axis shows the sweeps in time, and the Y axis shows the approximated delay time (in sweep samples).

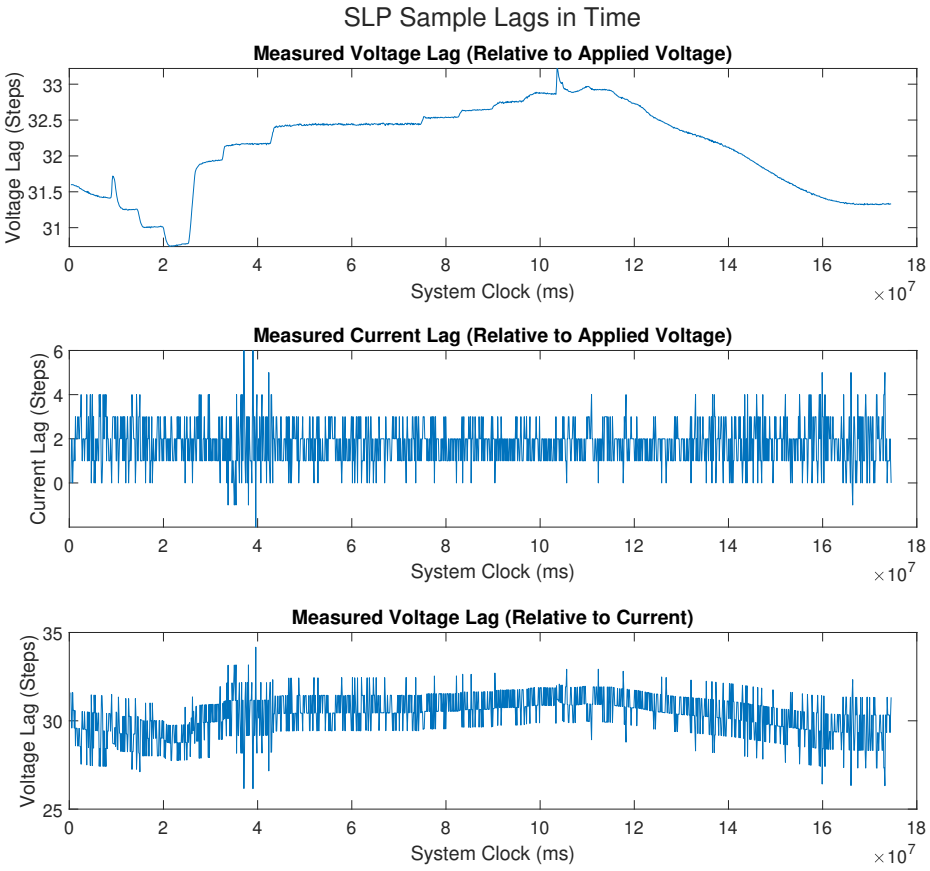

Fig. 2.32: SLP Lag in time

The electric field probe voltage lag contains the temperature profile, which is believed to be residual from the low pass filter approximation. A rounded average time delay of 2 samples is selected to best represent the time delay of all data samples. All data samples from the Langmuir probe, and electric field probe measurements are time shifted by 2 samples.

CHAPTER 3

SPORT Modeling

Langmuir probe theory provides an analytical model to define interaction of a charged body with a plasma due to collisions. The SPORT spacecraft consists of multiple conductive bodies, increasing the complexity of analytically modeling the SPORT interactions with a space plasma. Additionally, the reality of the space environment provides additional current sources who interact with the spacecraft that cannot be analytically modeled.

This section discusses two methods for modeling the additional complexities incumbent of SPORT. LTspice, and NASCAP2K.

3.1 LTspice

LTspice is used to model plasma interactions with the SPORT spacecraft by modeling the SPORT spacecraft using circuit element and implementing the circuit design in LTspice. Once the SPORT model is implemented in LTspice, a problem scenario is generated by specifying parameters of the in-situ plasma, as well as setting the bias potential of SPORT instruments. The scenario can then be run in LTspice to observe how the SPORT spacecraft will interact with the in-situ plasma environment.

3.1.1 SPORT Circuit Model

A circuit model of the SPORT spacecraft is created by considering the conducting bodies of the SPORT spacecraft that will interact with the in-situ plasma. This includes the body of the spacecraft, the Langmuir and electric field probes from USU's Space weather probe, as well as the Ion velocity meter produced by UTD. Figure 3.1 shows these elements included in the circuit model. The USU sweeping impedance probe applies low amplitude frequency signals relative to the spacecraft body, and is therefore modeled as part of the spacecraft body in the circuit.

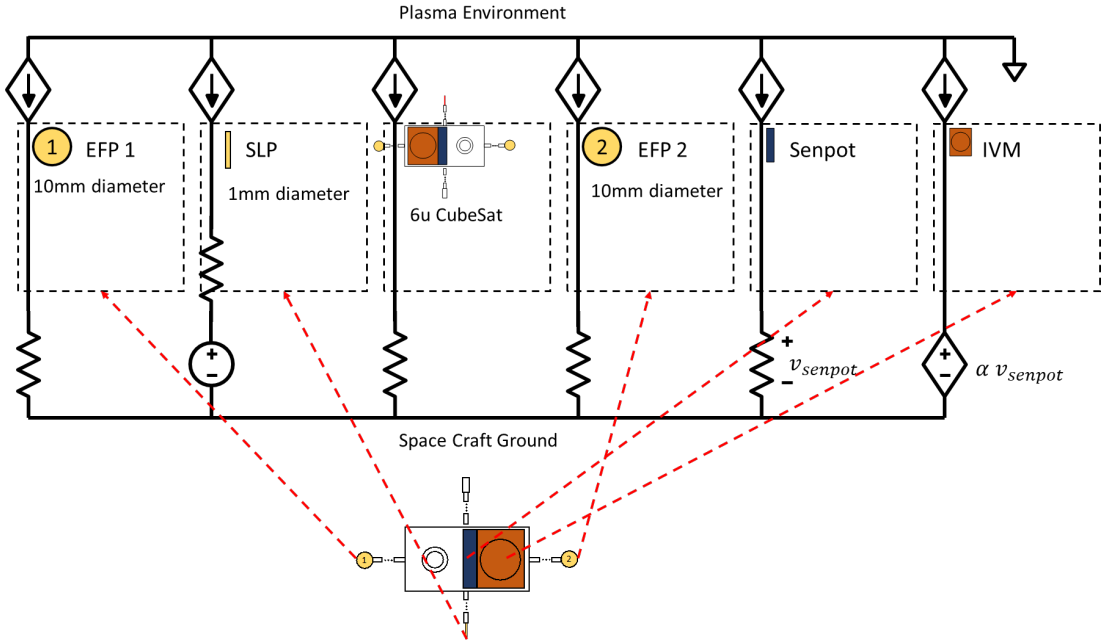

Fig. 3.1: SPORT Circuit Model

The electrical model defines the ambient plasma environment as the reference, or ground node. The spacecraft chassis, which is the ground reference for SPORT instrumentation, is drawn at the bottom of the circuit. Defining the circuit model in this way clearly specifies the probe's electrical relationship to the spacecraft, while still maintaining continuity with typical plasma physics models, which consider the ambient plasma as reference.

The probe-plasma interaction of the spacecraft sensors are modeled as voltage dependant current sources. The electric field probes are electrically isolated from the spacecraft ground, modeled by high impedance resistors R_{EFP_1} and R_{EFP_2}. The Langmuir probe sensor is biased relative to spacecraft ground with bias potential, V_{Bias}. The spacecraft body also interacts with the plasma and is modeled with a separate voltage dependant current source.

A portion of the ion velocity meter aperture plane, the SenPot reference surface, is isolated from the reference ground. The SenPot amplifier generates a potential with respect to spacecraft ground to maintain the IVM reference ground at the floating potential with

respect to the plasma. This amplifier is modeled as a voltage dependant voltage source. While the effects of the SenPot amplifier are included in the circuit model, the actual configuration of SPORT shorts the IVM to ground.

3.1.2 Model Implementation in LTspice

The circuit model is implemented in LTspice as shown in figure 3.2. The voltage dependant current sources are implemented with the developed SPICE macro circuits that model current collection. The spice macro circuits are selected to best match the geometrical shape of the conducting bodies, and the velocity of the spacecraft, relative to the plasma. The spice macro models accept the geometrical size of the conductors as an input.

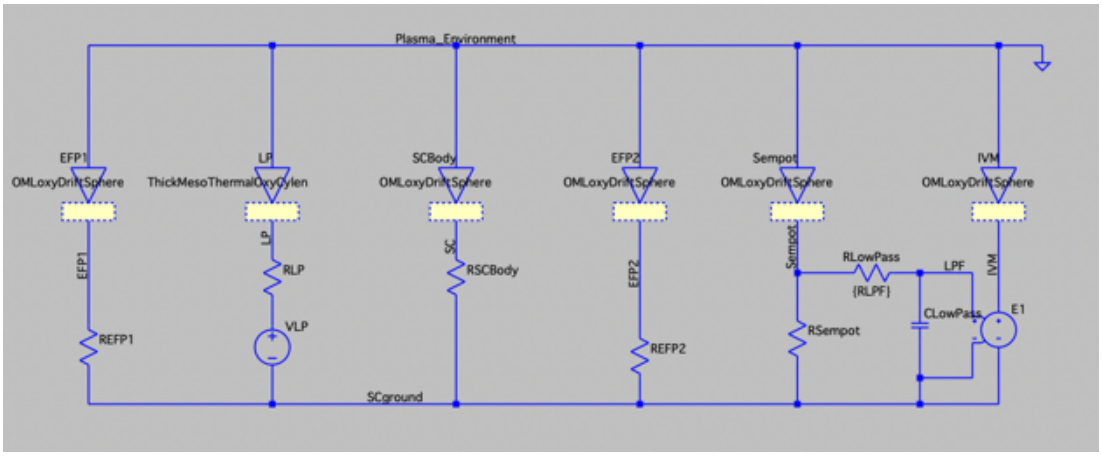

Fig. 3.2: SPORT Spice Circuit Model

3.1.3 Problem Scenarios

The problem scenario is created in LTspice by defining the plasma environment to interact with the spice macro models and the bias potential of the Langmuir Probe. The plasma environment is defined by setting the In addition to defining geometrical parameters, the spice plasma models also accept parameters to define the density and temperature to model. The

The spacecraft wake is not directly modeled using LTspice. However, the effects can be indirectly modeled by adjusting the collection area of the spacecraft, and observing the

effects of current collection and spacecraft charging as a result. Table 3.1 specifies the configurable LTspice parameters, and the range of interest for modeling SPORT.

Table 3.1: LTspice Scenario Parameters

Parameter	**Range**
LP Bias Voltage	-2 to 3 V
Plasma Density	10^9 to $10^{13}m^{-3}$
Plasma Temperature	300 to 2500 K
Spacecraft Collection Area	0.2 to $0.22m^2$

3.1.4 LTspice Scenario Results

Figure 3.3 shows the results of LTspice simulations. The simulation limits the collection area of the spacecraft to model the wake of the spacecraft. In this simulation, the spacecraft to Langmuir probe collection area ratio of 235. Simulations for other collection ratios are shown in appendix B.

The first column of figure 3.3 plots the sheath potential versus the current collected by the Langmuir probe at $500K$, $1500K$, and $2500K$. Column 2 shows how the relationship of the sheath potential to the bias potential applied by the spacecraft. Theoretically, the sheath potential should be the consistent with the bias potential, but as shown in column 3, the spacecraft potential begins to charge negatively when the Langmuir probe is biased with larger potentials.

The simulation results suggest that the SPORT spacecraft will experience spacecraft charging during Langmuir probe sweeps for most plasma observed. Floating potential measurements from the Space Weather Probes electric field probe are used to monitor the spacecraft charging during a sweep.

3.2 Nascap-2K

SPORT modeled in Nascap-2k by first describing the physical properties of the SPORT

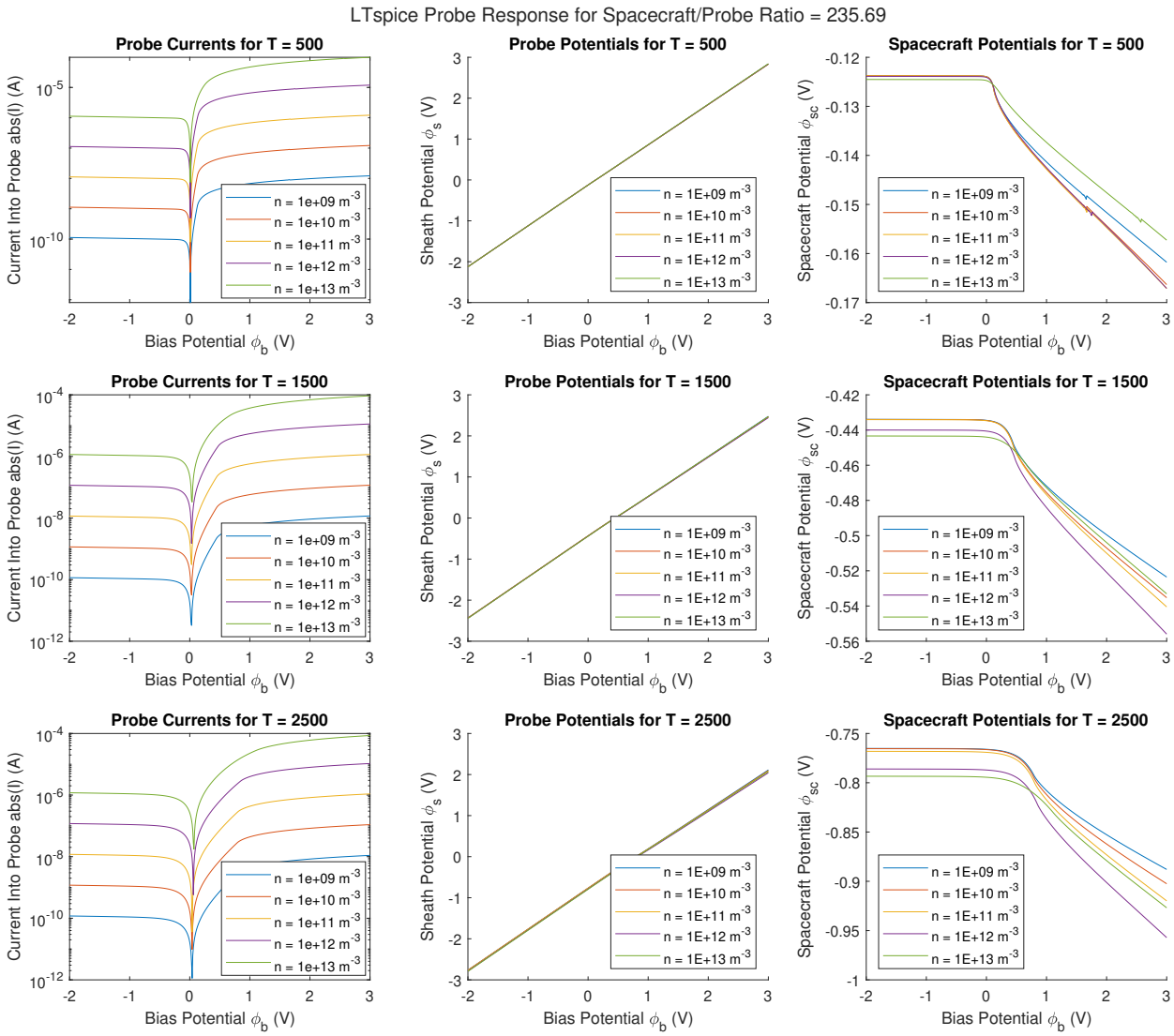

Fig. 3.3: LTspice Simulation Results

spacecraft using Nascap-2k's Object Tool Kit. A mesh grid is defined around the modeled SPORT spacecraft to define the boundaries of the modeled plasma environment using Nascap-2k's grid tool. A problem scenario is then designed in Nascap-2k, and simulated.

3.2.1 Object Tool Kit

The SPORT spacecraft is modeled in Nascap-2k's Object Tool Kit (OTK). Figure 3.4 shows the SPORT spacecraft modeled in Object Tool Kit. The model approximates the spherical electric field probes and cylindrical langmuir probe as boxes, but otherwise is built to scale. The dimensions used in the SPORT model are shown in table 3.2.

The spacecraft body is divided into cubes approximately 1.8cm in length. The Langmuir probe, and booms are divided into cubes based on their smallest dimension.

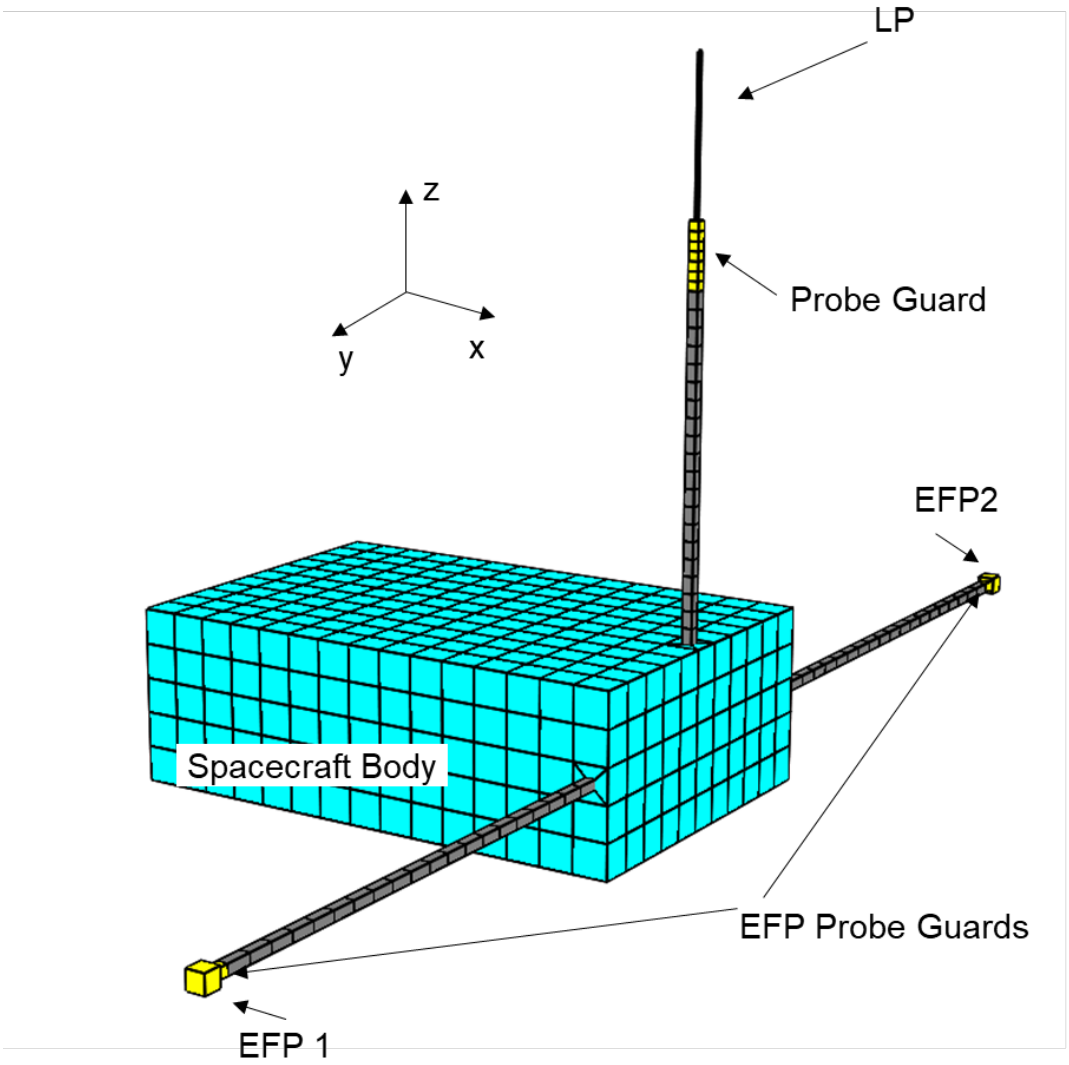

Fig. 3.4: SPORT Nascap-2k Model

Table 3.2: Nascap-2k SPORT Model Dimensions

Element	Dimensions (x,y,z), mm	Material
Spacecraft Body	300,200,100	Aluminum
EFP1, EFP2	9.7,9.7,9.7	Gold
EFP Guards	5,7.7,5	Gold
EFP Booms	5,294,5	Graphite
LP	1,1,85.2	Gold
LP Guard	5,5,35.8	Gold
LP Boom	5,5,188	Graphite

The spacecraft body and probe booms are defined as a single conductive body. The electric field probes, the Langmuir probe, and their respective booms are all electrically isolated as unique conductive bodies.

3.2.2 Mesh Grids

A system of arbitrarily nested cubic grids is used to calculate electrostatic potentials and fields, store charge densities, and track charged particles in the space external to the spacecraft. Electrostatic potential and electric field are defined at each grid point, leading to strictly continuous electric fields. GridTool is used to construct a grid system about an object. GridTool is then used to add nested child grids to achieve adequate resolution near the object and in other regions of interest. [13].

SWP is primarily interested in modeling the effects of biasing the Langmuir probe relative to the spacecraft body. The primary grid used by sport has dimensions of 50x50x30 cells, each with dimensions of 1.81cm, to match the size of cells in the SPORT spacecraft. The parent grid is subdivided (by a factor of 2 each time) into several child grids to increase resolution around the Langmuir Probe. Figure 3.6 depicts the defined grids for the SPORT spacecraft simulation.

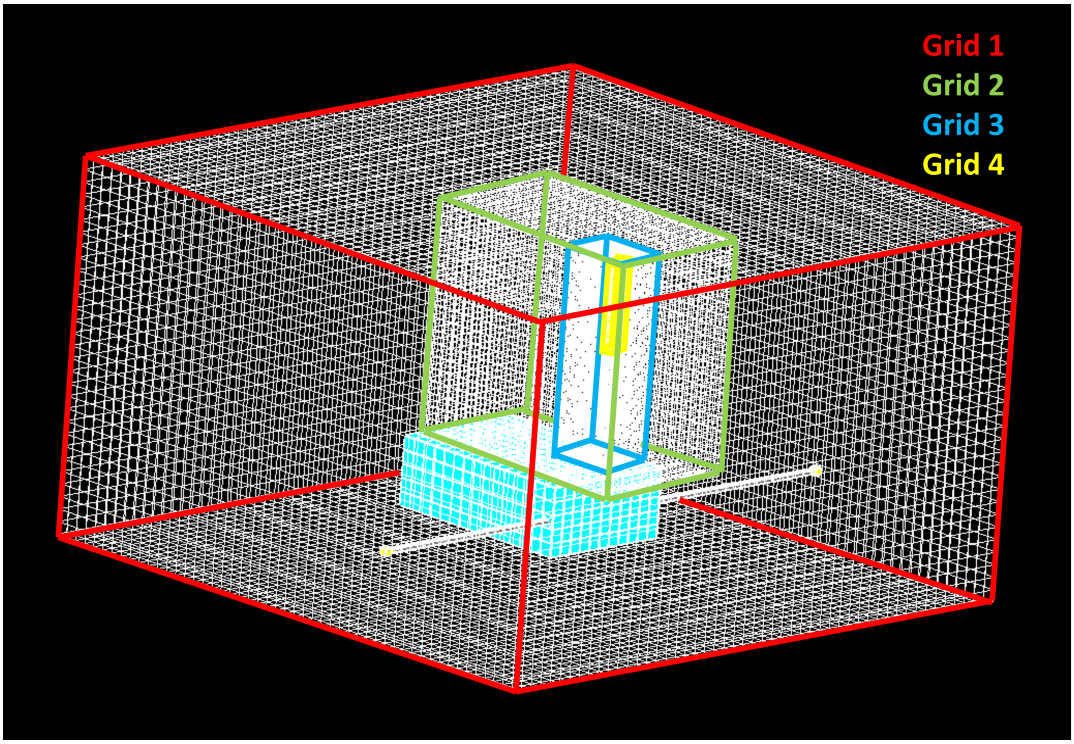

Fig. 3.5: SPORT Grid Definition

3.2.3 Nascap-2k Problem Definition

Nascap-2k supports geosynchronous, low Earth orbit (LEO) or plume, auroral, and interplanetary environments. Common to all four are the options to specify the local magnetic field vector, the direction toward the sun, the (relative) sun intensity at the location of the spacecraft, and mass, charge, and percent of plasma density for up to one-hundred species of particles.

For the SPORT simulation, a LEO orbit is specified. The environment parameters are configured to specify an oxygen ion plasma, with a spacecraft velocity of 7.4km/s, consistent with the expected conditions for the SPORT orbit. The sun intensity and magnetic field of the orbit can have non-zero values, the simulation is simplified by omitting these factors.

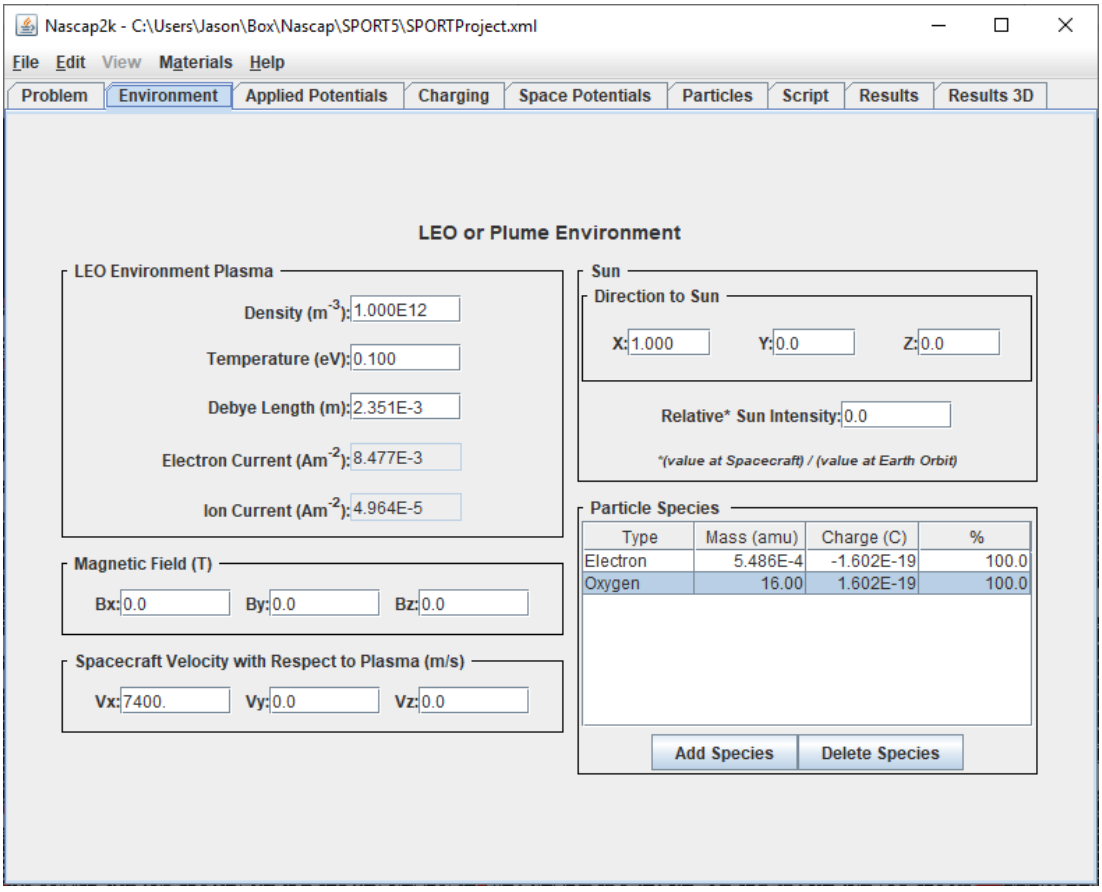

Fig. 3.6: SPORT Grid Definition

Table 3.3 summarizes the parameters specified for the SPORT simulation.

Table 3.3: Nascap-2k Environment Parameters Considered

Parameter	**Definition**	**SPORT Simulation Range**
LEO Environment Plasma		
Density	Number density of the ambient plasma (m^{-3}).	$1x10^{9} to 1x10^{13}$
Temperature	Temperature of the ambient plasma (eV)	0.0259 to 0.1293 (300 to 1500 K)
Debye Length	Debye length of the ambient plasma (m)	-
Electron Current Electron thermal current (Am-2).	Electron thermal current (Am^{-2})	-
Ion Current Ion thermal current (Am-2).	Ion thermal current (Am^{-2})	-
Magnetic Field		
Bx, By, Bz	Components of the ambient magnetic field vector (tesla) in the spacecraft frame of reference	0,0,0
Spacecraft Velocity		
Vx, Vy, Vz	Components of the spacecraft velocity vector (m/s). (Used for computing ram ion and wake effects)	7.4x10^{3},0,0
Sun		
Direction to Sun (X,Y,Z)	Direction toward the sun in the spacecraft frame of reference	-
Relative Sun Intensity	Ratio of sun intensity at the spacecraft over the 1 AU value	0 to 1
Particle Species	Specification of particle species through their mass, charge, and percentage of the total plasma density	Oxygen Ion Plasma

The applied potentials tab allows the user to specify how the potentials of the spacecraft body should be set relative to each other. For the SPORT simulation, the spacecraft body is allowed to float relative to the plasma environment, with the exception of the Langmuir probe, and Langmuir probe guard, which are both biased, relative to the spacecraft potential. The bias voltage applied to the Langmuir probe are configured to sweep over the potential sweep with a custom script.

3.2.4 Nascap-2k Results

Figure 3.7 shows the results of Nascap-2k simulations. Similar to LTspice, the simulation results suggest that the SPORT spacecraft will experience spacecraft charging during Langmuir probe sweeps for most plasma observed.

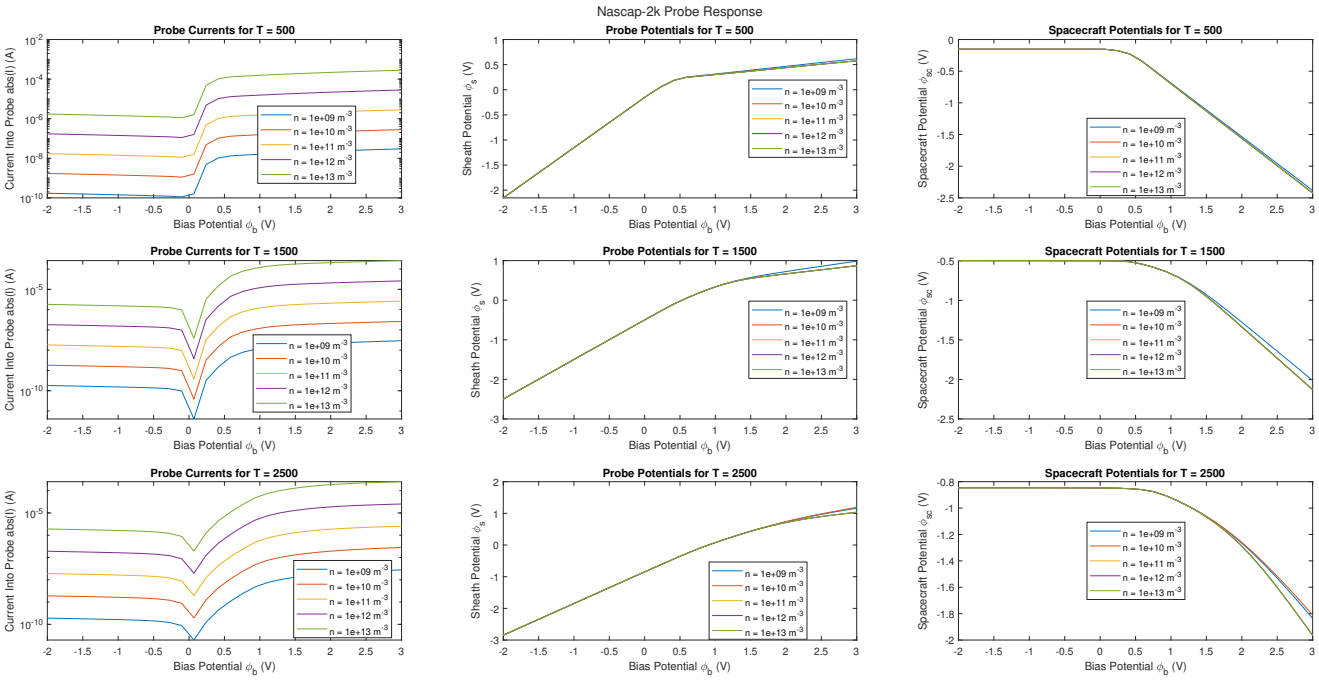

Fig. 3.7: Nascap-2k Simulation Results

The LTspice simulation adjusted the effective collection area of the spacecraft to model the spacecraft wake. Nascap-2k builds the spacecraft wake into the simulation. Figure 3.8

shows the wake of the spacecraft for a plasma with particle density $1x10^{12} particles/m^3$, and temperature $1500K$. Figure 3.9 shows the spacecraft wake for the same plasma. The body of the spacecraft, produces a significant wake in the plasma. The low density region behind the spacecraft cannot be used for ion current collection. The comparatively small Langmuir probe, however, has a much smaller wake footprint.

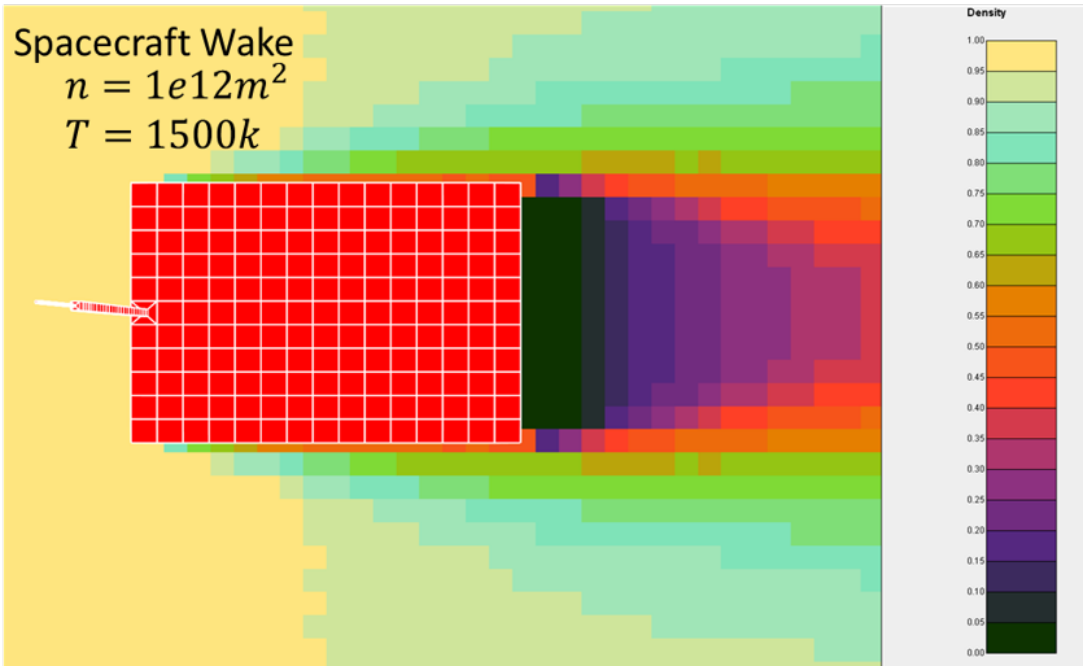

Fig. 3.8: Nascap-2k Model of SPORT Wake

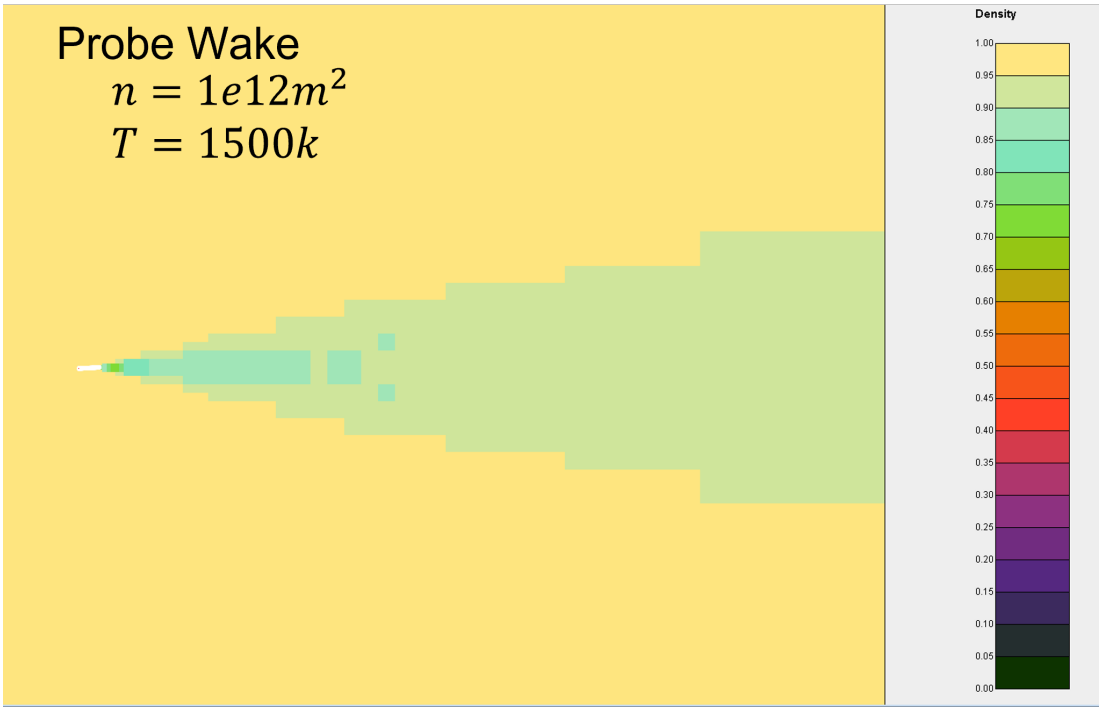

Fig. 3.9: Nascap-2k Model of SPORT Wake

3.3 Model and Data Comparisons

The LTspice simulation results are compared to the results of Nascap-2k. Figure 3.10 the results of both simulations together. The first column plots the expected current collected by the Langmuir probes in both simulations. Columns 2 and 3 plot the probe and spacecraft potential, relative to the ambient plasma. In each row, the Nascap-2k current is the same, while the LTspice simulation compares results for various current collection areas possibly observed.

The results match best in the electron retardation region. The differences in current collection in the ion saturation and electron saturation regions are believed to be a result of improper modeling of the Langmuir probe collection region in LTspice. As stated earlier, the probe collection area will be a function of the effective area of the probe that is not in the wake. Additionally, slight differences in the defined collection area of the Nascap-2k vs. LTspice probe collection area exist, these differences are a result of limitations in Nascap-2k object tool kit.

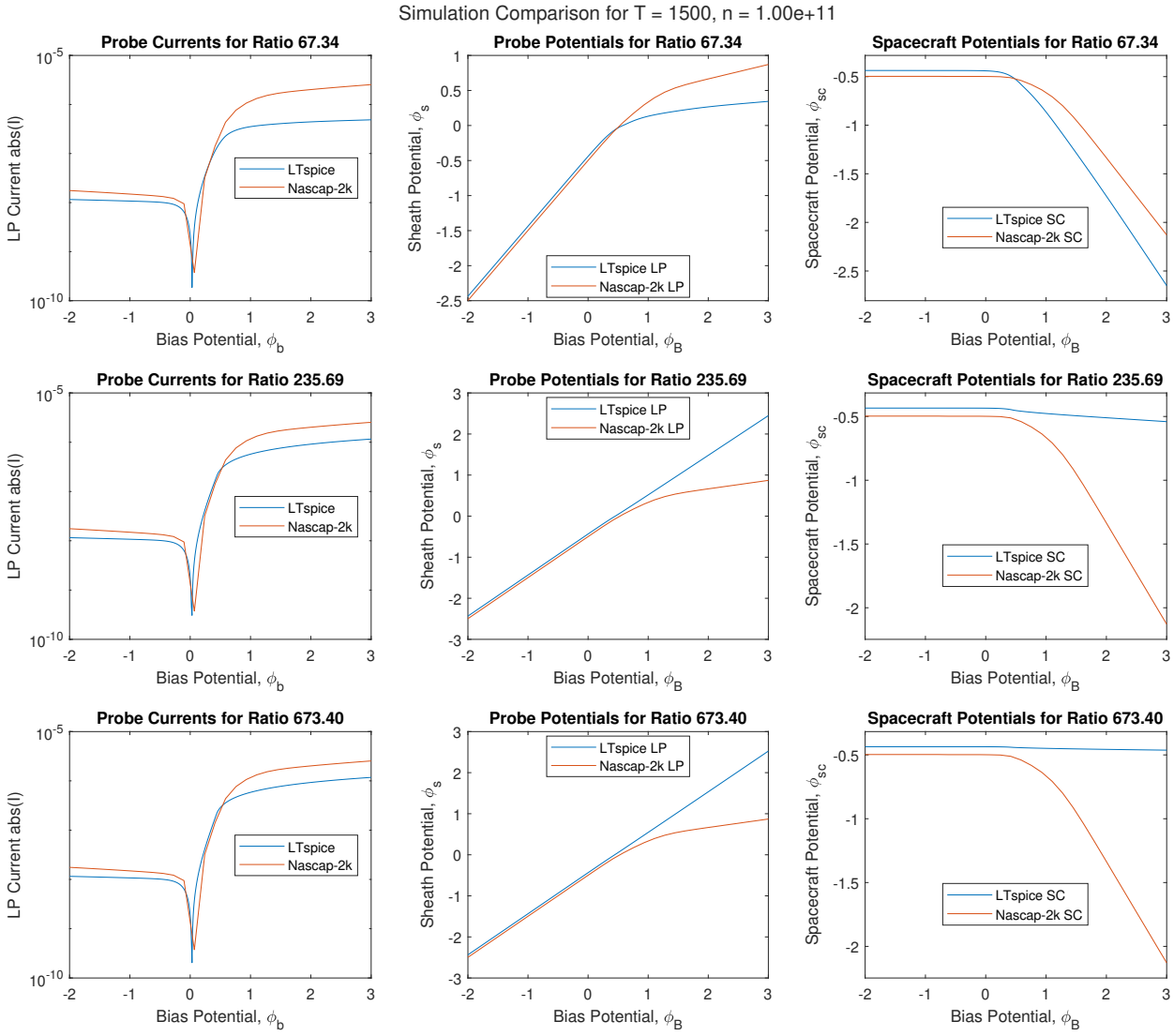

Fig. 3.10: Simulation Comparison

3.4 Model Conclusions

Nascap-2k has significant modeling advantages over LTspice simulation, specifically, Nascap-2k has the ability to model more complicated interactions of the space environment. While Nascap-2k may be computationally superior to LTspice, LTspice is advantageous for quickly modeling the interactions of multiple probes together. LTspice can be used as a tool to quickly get a general idea of how a spacecraft should respond to various plasma environments. When more specific interactions need to be modeled, tools such as Nascap-2k should be used.

CHAPTER 4

Data Processing

Scientific measurements made by the SPORT spacecraft must undergo processing before the measurements can be used by the scientific community. The SPORT mission categorizes science data according to the definitions given in table 4.1. In general, Level 0 and Level 2 data are handled by the entire SPORT team, whereas Level 1 data are handled exclusively by the instrument provider.

Table 4.1: Science Data Level Descriptions

Data Level Descriptions	
Level 0	Data that are telemetered from the SPORT science instruments to the FlightComputure, packaged into CCSDS packets, downlinked from the observatory to the ground station. Also called "Raw Data"
Level 1	Instrument-specific data products that are calculated as intermediate steps in the process of converting Level 0 (i.e., Raw Data) to Level 2 data, the latter of which represents a physically meaningful measurement of the space environment. Also called "Intermediate Data Products"
Level 2	Physically meaningful data products that represent a physical parameter of the space environment. Level 2 Data are represented as a time series of vector and/or scalar parameters, usually with calibration factors applied, depending on the instrument. "Bad" data must be replaced with a (TBR) numeric value. Also called "Physical Data Products"
Level 3	Physically meaningful data further processed to enhance functionality of Level 2 data (e.g. electron density profiles). Also called "Enhanced Data Products"

Figure 4.1 illustrates the end-to-end data flow from initial acquisition of the SPORT data. This section discusses the algorithms operated on Level 0 data by Utah State University to produce Level 2 data.

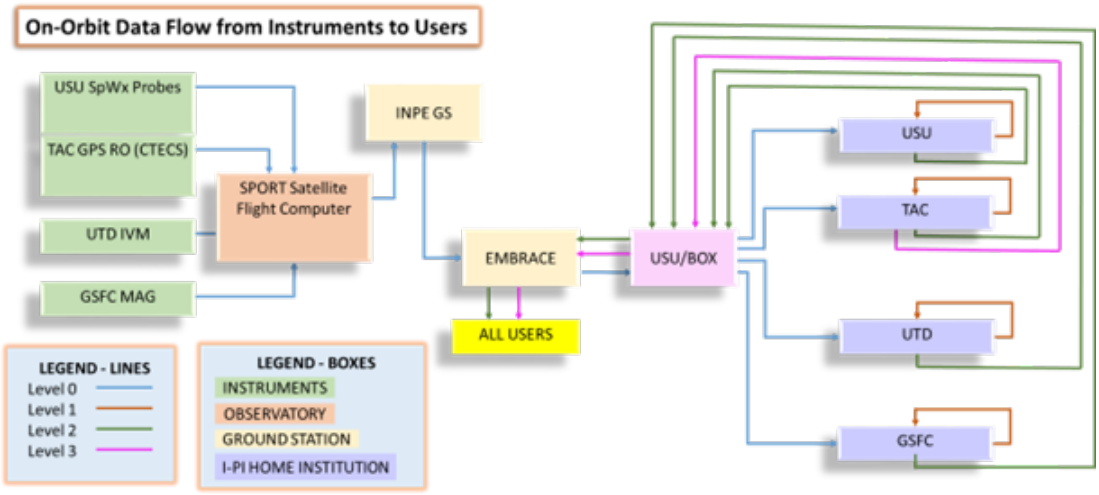

Fig. 4.1: SPORT Science Data Flow Diagram

4.1 Level 0 to Level 1 Data Processing

USU receives SWP data as binary files designated as L0. The process for elevating data from L0 to L1 includes unpacking data, registering packets in time, and converting ADC counts into physical units. Figure 4.2 illustrates the process of elevating SWP data products from L0 to L1 data.

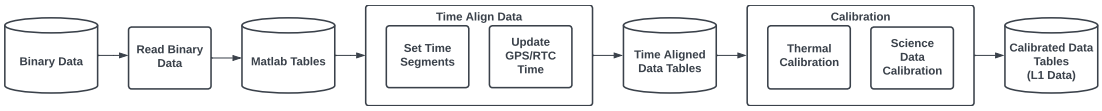

Fig. 4.2: SPORT Data Processing Chain

4.1.1 Unpacking Data

SWP CCSDS packets are sent to the ground as a binary stream and stored as a binary file. Packet headers are parsed from the data to identify the type, and location of each packet within the file. Packet data is extracted from each packet according to the defined packet and granule structure. Each packet is written to a unique MATLAB table. The items in a science granule make up the columns of the MATLAB table, with each granule saved as a single line in the table. The system clock is extrapolated to each science measurement based on the defined sample rate. Table 4.2 shows the example structure of a MATLAB

table for the science packet.

Table 4.2: Science Table Detail

Table Element	Description
PacketCount_A	Packet Count
PacketCount_B	Granule Count
System_Clock	System Clock Time Stamp
Mag_Temperature	Magnetometer Temperature
Mag_X_axis	Magnetometer X field measurement
Mag_Y_axis	Magnetometer Y field measurement
Mag_Z_axis	Magnetometer Z field measurement
EFP_VS1	EFP Floating Potential 1
EFP_VS2	EFP Floating Potential 2
SLP_high_gain	SLP high gain current
SLP_low_gain	SLP low gain current

4.1.2 Packet Registration

In addition to the system clock, SWP also uses a GPS clock, and a real-time clock (RTC) chip. The system clock is contained as a 32 bit number and is the smallest clock value to telemeter. SWP minimizes the telemetry budget by time stamping science instrument packets with only the system clock. The GPS, and RTC clock values are sent periodically with the SWP Status packet.

Received science packets are registered relative to each other by time-aligning their system clock stamps with the GPS time stamp of the Status packets. Additionally, packets are time-aligned to the RTC time-stamp. While the RTC is less accurate than GPS time, the RTC clock is more reliable and used as a backup when GPS data is not available to SWP.

4.1.3 Conversion

SWP instruments measure current, voltages, impedances, and power spectral density data. Measurements are quantized by SWP using ADCs, producing measurements in units of counts. Science measurements must be converted from ADC counts to appropriate SI units before they can be used for science analysis.

SWP first interpolates the board temperature from the science packet to all other packet types, and converts the interpolated temperature into degrees Celsius. Temperature interpolation is based on GPS time, and RTC time when GPS time-stamps are not available.

The conversion process uses temperature dependent conversion factors developed from calibration data and the mathematical models of the Space Weather Probes instrumentation. The calibration process happens in MATLAB script "doconversion.m", where developed conversion functions relate ADC counts to SI units for the instruments of SWP.

Converted data is stored in Matlab tables alongside raw ADC counts.

4.2 Level 1 to Level 2 Data Processing

L1 data provides time aligned, calibrated data as measured by the SWP suite. Data is further processed into L2 data by applying measurements to analytical models of probe plasma interactions. Instruments are analyzed to produce measurements of density, temperature, and electric field data according to table 1.2.

4.2.1 Density Data Product

The Space Weather Probes sweeping impedance probe and sweeping Langmuir probes are used to measure the density of the atmosphere as shown in figure 4.3. The distinct measurement techniques between instruments allow for further calibration and adjustment of measurements to ensure agreement between measurement tecniques.

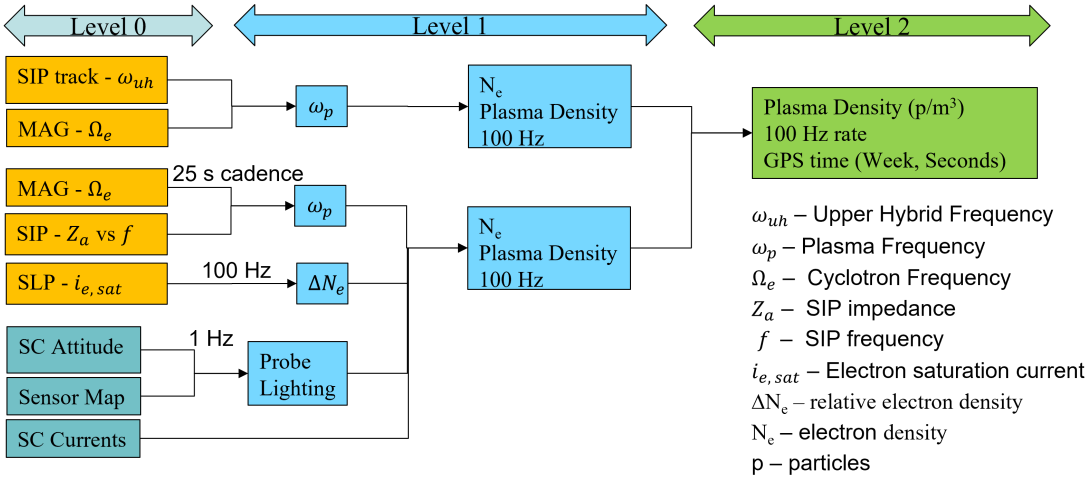

Fig. 4.3: Density Data Product

4.2.2 Temperature Data Product

The Space Weather Probes sweeping Langmuir probe, along with data from the electric field probe is used to measure the temperature of the atmosphere as shown in figure 4.4.

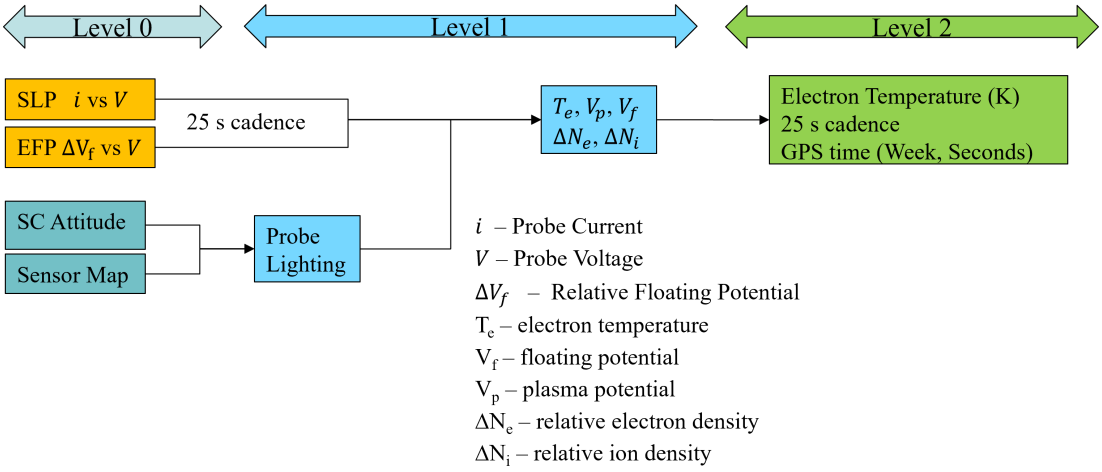

Fig. 4.4: Temperature Data Product

Sheath Potential Estimate

The Langmuir probe compares the potential applied to the plasma by the probe to the current collected. Space Weather Probes uses data collected by the floating potential

probes of the Electric Field Probe to estimate the sheath potential. Figure 4.5 shows how SPORT SWP potentials interact with each other.

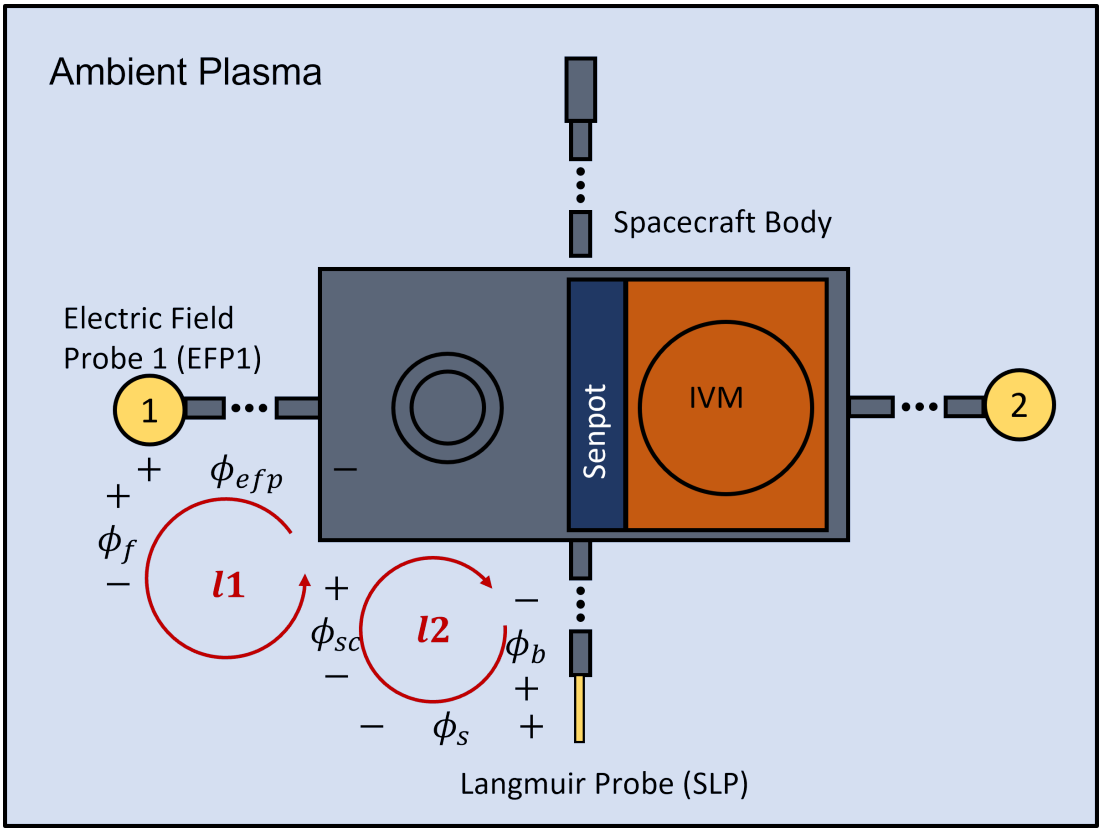

Fig. 4.5: SPORT Current Loops

Kirchhoff's Voltage Law is used to calculate the sheath potential, ϕ_s, of the spacecraft by defining two current loops, $l1$, and $l2$, as shown in figure 4.5, and solving for ϕ_s as shown in equations 4.1-4.5.

$$l1 : -\phi_{efp} + \phi_f - \phi_{sc} = 0 \tag{4.1}$$

$$\phi_{sc} = \phi_f - \phi_{efp} \tag{4.2}$$

$$l2 : -\phi_b + +\phi_s - \phi_{sc} = 0 \tag{4.3}$$

$$\phi_s = \phi_b + \phi_{sc} \tag{4.4}$$

$$\phi_s = \phi_b + \phi_f - \phi_{efp} \tag{4.5}$$

The Electric Field Floating Potential, ϕ_f, is unknown, and must be solved for along with parameters for temperature and density.

4.2.3 Wave and Electric Field Data Products

The electric field and electric field wave probe are directly interpreted from measurement data from the electric field probe, and electric field wave probe measurements as shown in figure 4.6.

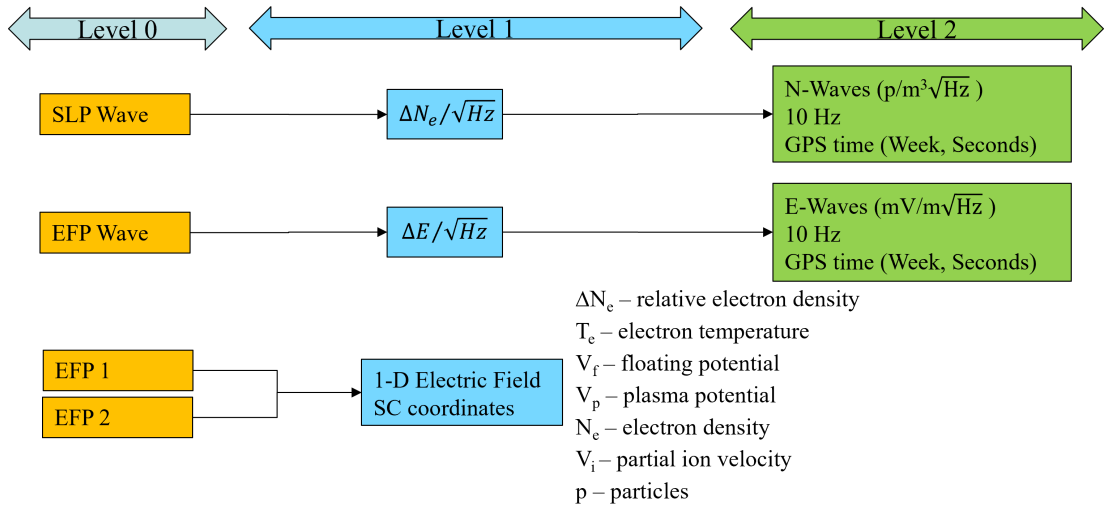

Fig. 4.6: Wave and E-field Data Products

CHAPTER 5

Conclusions

This thesis presents the instrumentation techniques used by Space Weather Probes on the SPORT spacecraft. The theory behind Langmuir probes is also introduced, along with an understanding of what special considerations that are needed to interpret Langmuir probe data on a small spacecraft.

The methods used to test and calibrate the Space Weather Probes instrument, long with the results of such calibration efforts are presented to demonstrate the process of interpreting Space Weather Probe measurements as physical units.

The interaction of the in-situ plasma environment, and the SPORT spacecraft is modeled using two simulation programs. LTspice presented a simple, but less accurate method for gaining a quick understanding of how probe potentials will interact with the space environment. Nascap-2k presents a more in depth simulation with more rigorous results.

The efforts made to prepare to receive and processes Space Weather Probe data received from the SPORT spacecraft are discussed. Although at the time of this thesis, no data was received from the SPORT spacecraft. Utah State University is prepared to receive and process SWP data.

5.1 Lessons Learned and Future Work

Utah State University is currently developing a second revision of Space Weather Probes, SWP2. The intention of the board is to develop the same set of instruments as SWP, but take advantage of the many lessons learned from the development of SWP. This section describes some of the lessons learned, and progress in developing an updated SWP2 board.

5.1.1 Langmuir Probe Analog Design

The SPORT Space Weather Probes Langmuir probe makes high precision current measurements. The functionality of the Langmuir probe depends on how accurately the instrument can make these instruments. While the low gain channel of the Langmuir probe met system requirements, the Langmuir probe is redesigned to be more sensitive. The instrument is improved by: increasing the dynamic range, redesigning the high gain channel, and increasing instrument sensitivity. The improvements to the analog design are shown in figure 5.1.

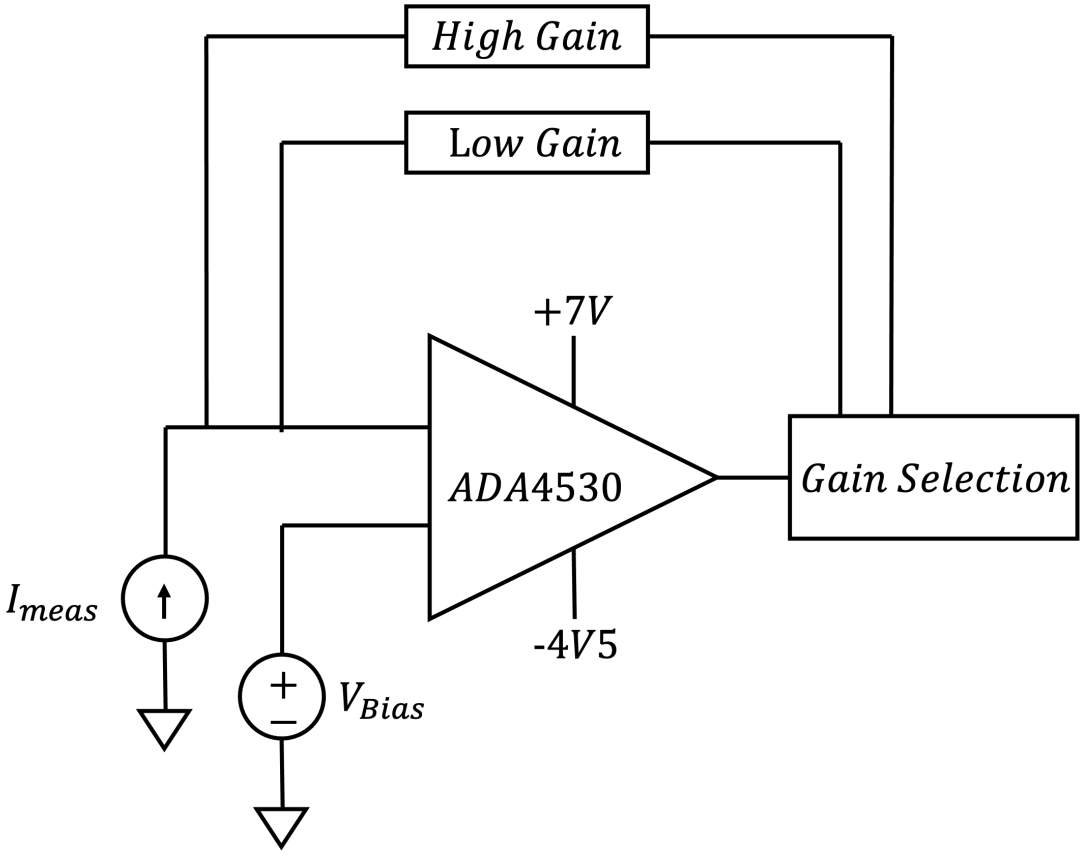

Fig. 5.1: SWP2 Langmuir Probe Analog Design

Dynamic Range

The Langmuir probe in the original Space Weather Probes board had a non-linear response at higher current levels. The non-linear response is a result of voltage railing in

the analog system chain. The redesigned Space Weather Probes is corrected by increasing the supply rails of the input operational amplifier to $+7V$.

High Gain Channel

As shown previously, the Langmuir probe high gain channel did not function as expected for SPORT. This is because the high gain channel attempted to apply a signal gain after the transimpedance amplifier. The result was all the noise introduced by the initial transimpedance amplifier was included in the high gain signal. SWP2 resolves this issue by designing a programmable gain trans-impedance amplifier based on Luis Orzoco's Design [15]. The design uses switches to control the TIA gain as shown in figure 5.2.

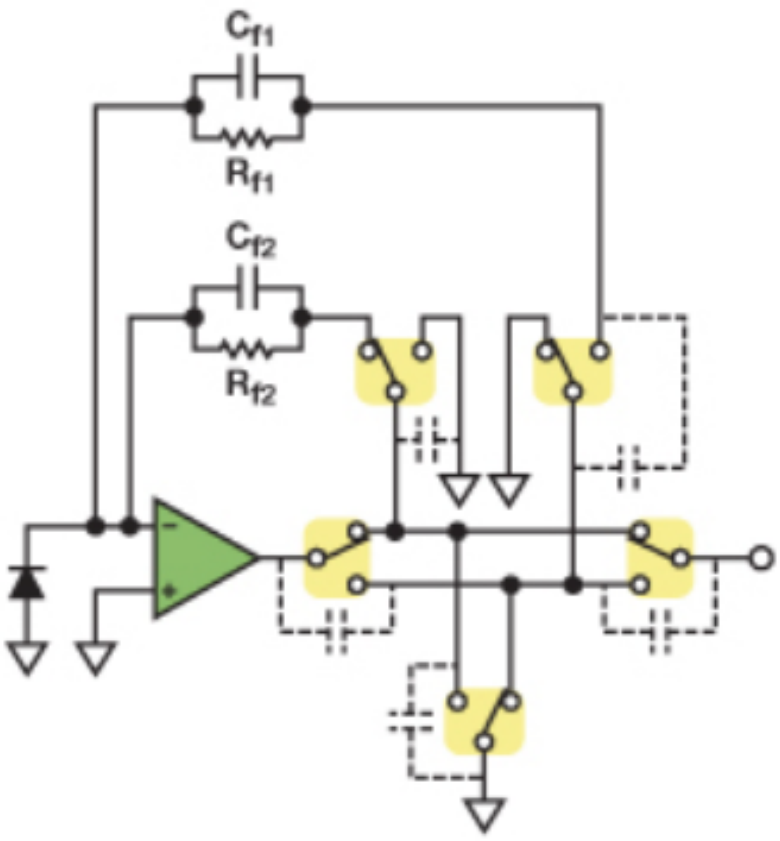

Fig. 5.2: Programmable Gain Transimpedance Amplifier Design

Instrument Sensitivity

Space Weather Probes increases instrument sensitivity by using a new transimpedance Amplifier, ADA4530-1. The ADA4530-1 is a femtoampere (10−15 A) level input bias current operational amplifier suitable for use as an electrometer that also includes an integrated guard buffer. It provides ultralow input bias currents that are production tested at $25°C$ and at $125°C$ to ensure the device meets its performance goals in user systems. The integrated guard buffer isolates the input pins from leakage in the printed circuit board (PCB), minimizes board component count, and enables easy system design. [16]. Figure 5.3 shows the input bias sensitivity of the ADA4530-1 over the specified temperature range.

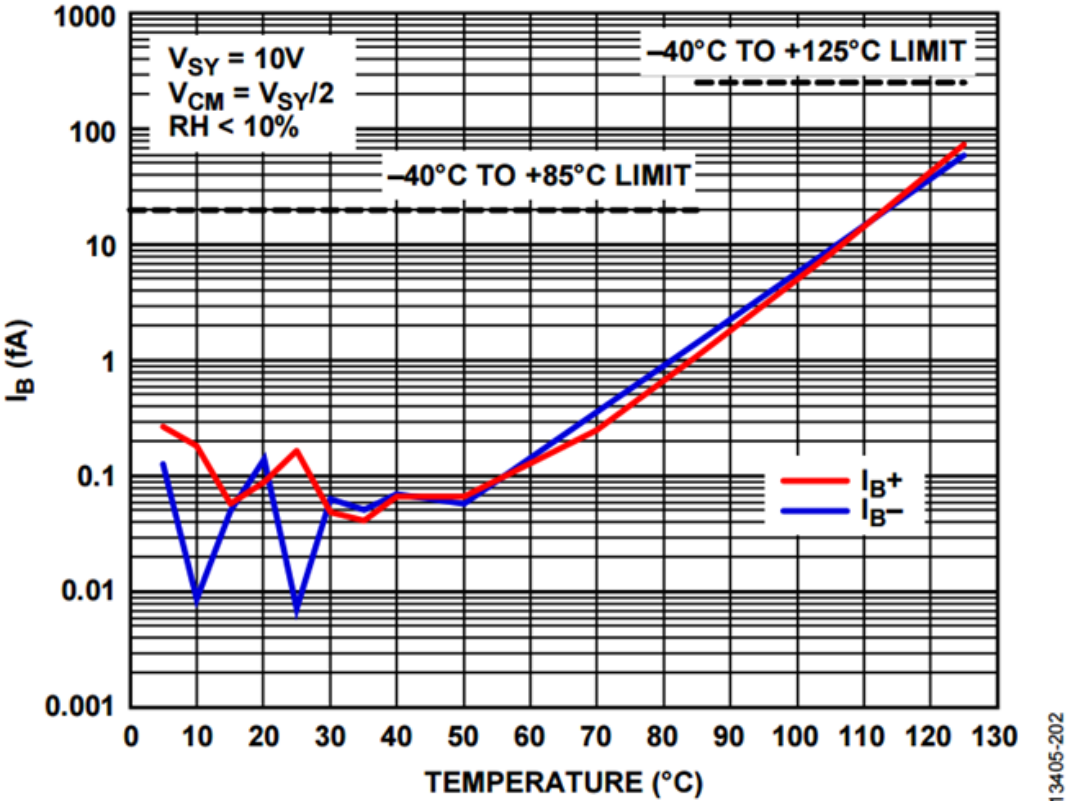

Fig. 5.3: Input Bias Current (I_B) vs. Temperature for ADA4530-1

5.1.2 Additional Testing Procedures

Space Weather Probes test procedures incorrectly assumed instrument measurements

made at different sampling rates would respond the same. Additional SWP projects should carefully revise calibration and testing procedures to include measurements of all instruments at the expected sampling rates. Additionally, SWP test procedures should verify the timing and alignment of measurements made simultaneously, such as the langmuir probe electric field probe, and current measurements.

REFERENCES

[1] R. W. Schunk and A. F. Nagy, *Ionospheres - Physics, Plasma Physics, and Chemistry*. Cambridge, 2000, ch. 9, p. 242.

[2] N. P. Tipton, "Design of miniaturized sweeping langmuir probe and electric field probe for the sport mission," Master's thesis, Utah State University, Logan, UT, 2021.

[3] C. W. Young, "Design of a sweeping impedance probe for the sport mission," Master's thesis, Utah State University, Logan, UT, 2020.

[4] J. Haws, "Command, control, and telemetry for utah state univeristy's scintillation prediction observation research task (sport) mission," Master's thesis, Utah State University, Logan, UT, 2020.

[5] R. L. Merlino, "Understanding langmuir probe current-voltage characteristics," *American Journal of Physics*, vol. 75, pp. 1078–1085, 2007.

[6] H. M. Mott-Smith and I. Langmuir, "The theory of collectors in gaseous discharges," *Physical Review*, vol. 28, pp. 728–763, 1926.

[7] W. R. Hoegy and L. E. Wharton, "Current to a moving cylindrical electrostatic probe," *Journal of Applied Physics*, vol. 44, no. 12, pp. 5365–5371, 1973. [Online]. Available: https://doi.org/10.1063/1.1662157

[8] L. H. Brace, *Measurment Techniques in Space Plasmas: Particles*. American Geophysical Union, 1998, ch. Langmuir Probe Measurements in the ionosphere, pp. 22–35.

[9] A. J. Auman, "The adaptability of langmuir probes to the pico-satellite regime," Master's thesis, Utah State University, Logan, UT, 2008.

[10] T. A. Bekkeng, E. S. Helgeby, A. Pedersen, E. Trondsen, T. Lindem, and J. I. Moen, "Multi-needle langmuir probe system for electron density measurements and active spacecraft potential control on cubesats," *IEEE Transactions on Aerospace and Electronic Systems*, vol. 55, no. 6, pp. 2951–2964, 2019.

[11] R. N. A. S.-V. C. W. T. Quarles, D. Pederson. The spice page. [Online]. Available: http://bwrcs.eecs.berkeley.edu/Classes/IcBook/SPICE/

[12] A. Barjatya, "Langmuir probe measurements in the ionosphere," Ph.D. dissertation, Utah State University, Logan, UT, 2007. [Online]. Available: https://digitalcommons.usu.edu/etd/274

[13] V. Davis. (2016) Nascap-2k version 4.3 user's manual.

[14] lsqcurvefit. [Online]. Available: https://www.mathworks.com/help/optim/ug/lsqcurvefit.html

[15] L. Orozco. Programmable-gain tansimpedance amplifiers maximize dynamic range in spectroscopy systems. [Online]. Available: https://www.analog.com/en/analog-dialogue/articles/programmable-gain-transimpedance-amplifiers.html

[16] Ada4530-1 femtoampere input bias current electrometer amplifier. [Online]. Available: https://www.analog.com/media/en/technical-documentation/data-sheets/ADA4530-1.pdf

APPENDICES

APPENDIX A

Software Data Package

Included with this thesis work is a software data package. This package includes all of the codes and models presented in this thesis work.

A.1 SPORT Data Processing Code

SPORT data processing code is managed in a GitHub repository. A copy of the SPORT data processing code is included with this thesis. The code is organized into directories as shown in table A.1. Additional information for running SPORT data processing code can be found in the readme files, included with the code.

Table A.1: SPORT Data Processing Code Directory

Directory Name	**Function**
Calibration	The calibration directory contains code for computing calibrations based on test data. Note: the calibration is not applied to SPORT data here, just the computation of calibration
Function Library	The function library contains utilities not specific to an activity of data processing.
L0-L1 Data Processing	The L0-L1 data processing directory contains all the functions neccessary for the top-level MATLAB routines to produce Level 1 data from Level 0 data.
L1-L2 Data Processing	The L1-L2 data processing directory contains all the functions neccessary for the top-level MATLAB routines to produce Level 2 data from Level 1 data.
Routines	The routines directory contains top level MATLAB scripts to elevate SWP data from one level to another
Verification Tests	The verification tests directory is for reviewing data from specific SPORT campaigns that are done to verify that SWP is functioning properly.

A.2 LTspice Simulation Files

The LTspice `Langmuir` directory contains the LTspice SPORT circuit model. Several different configurations are included. This thesis work presents the results from the LT-

spice model as configured in `SPORTmodelV5`. Additional MATLAB scripts are included for reviewing and plotting LTspice data.

A.3 Nascap-2k Simulation Files

The `Nascap-2k` directory contains the Nascap-2k SPORT circuit model. The `SPORT` directory contains the SPORT object model, SPORT grid model, and driver files. Custom scripts for setting the spacecraft environment are included in the top level directory.

A.4 Auxiliary Files

The SPORT command and telemetry dictionary is included in the excel document `Command and Telemetry Dictionary.xlsx`. The SPORT USU Space Weather Probes test and calibration plan is also included in powerpoint `SPORT USU Space Weather Probes Test and Calibration.pptx`. A presentation version of this thesis is included as `Thesis Presentation.pptx`.

APPENDIX B

LTspice Simulation Figures

LTspice Simulations for Different Spacecraft Area Ratios

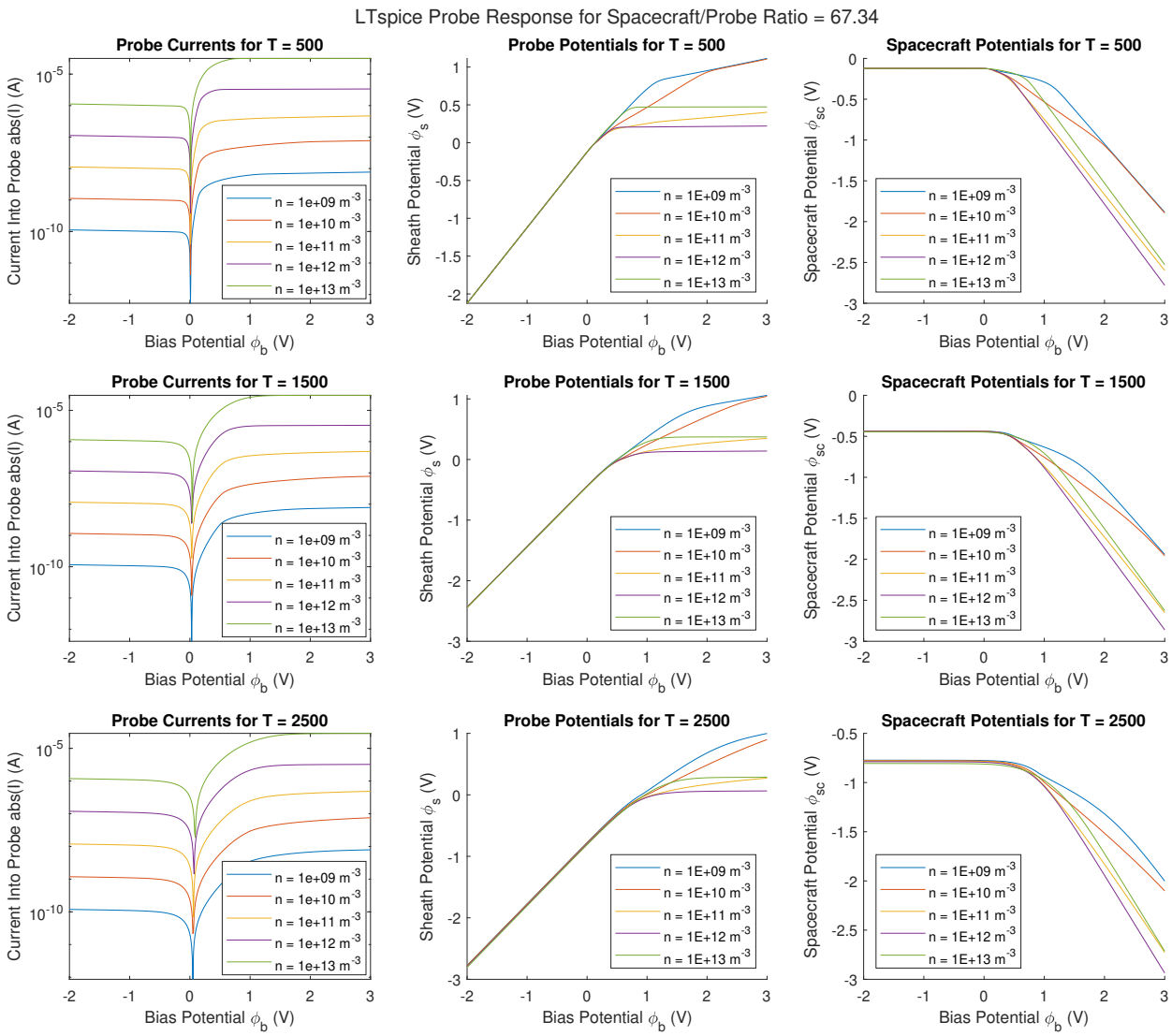

Fig. B.1: LTspice Simulation Results Small Area

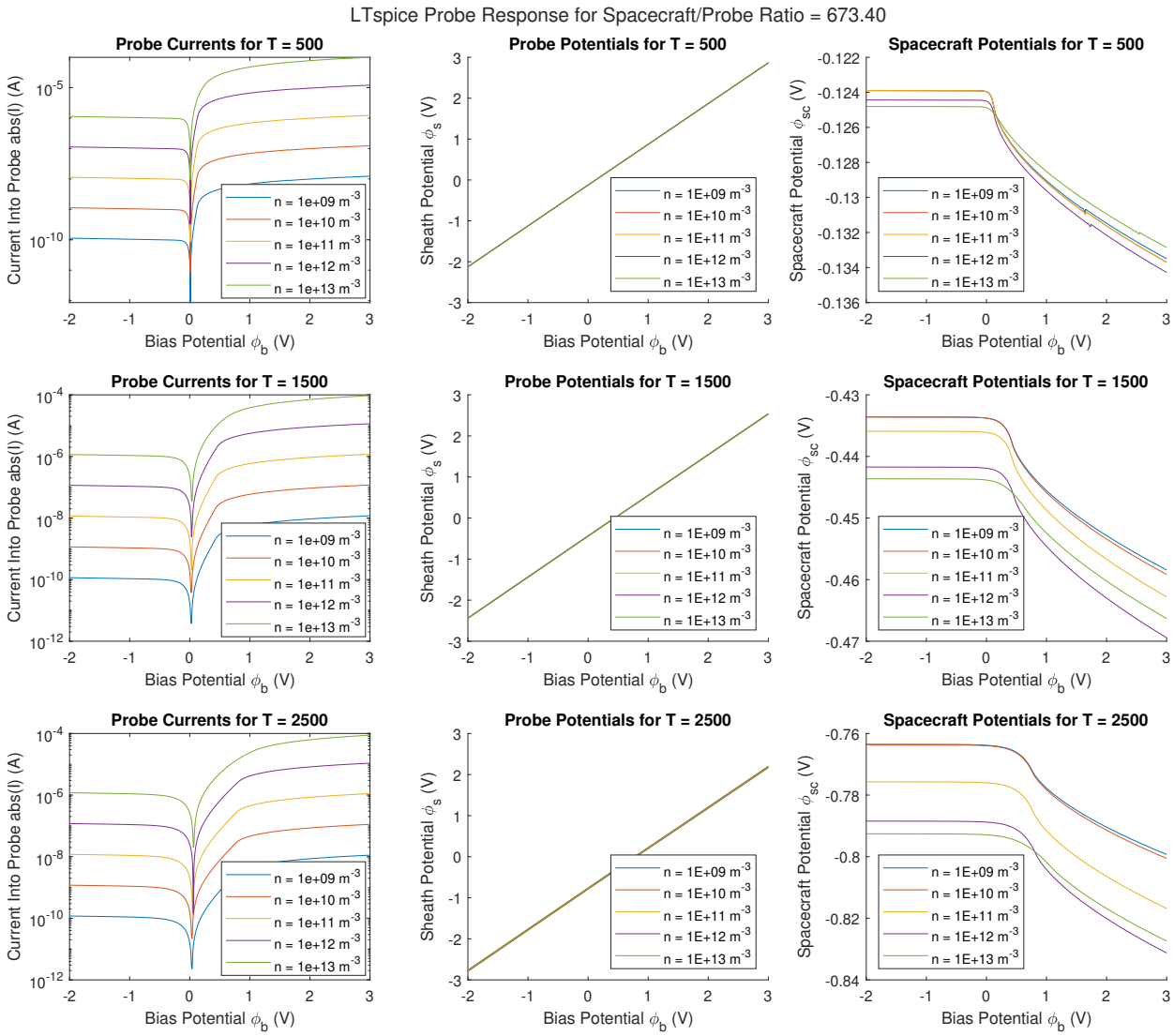

Fig. B.2: LTspice Simulation Results Large Area